Specific Applications of Satellite Remote Sensing to the Benguela Ecosystem

Scarla Jeanne Weeks
Dipl. Ther. Rad., B.Sc. (Med), B.Sc. (Hons), M.Sc.

Thesis Presented for the Degree of
DOCTOR OF PHILOSOPHY
In the
Department of Oceanography
UNIVERSITY OF CAPE TOWN
August 2004

TABLE OF CONTENTS

DECLARATION

PhD Thesis Title:

Specific Applications of Satellite Remote Sensing to the Benguela Ecosystem

I, Scarla Jeanne Weeks, hereby declare that:

The above thesis is my own original work, both in concept and execution, and that apart from the normal guidance and advice from my supervisors, I have received no assistance except as stated below:

Chapter 2. The SeaWiFS Project, NASA, collaborated in determining the optimal parameters for processing of HRPT SeaWiFS data for Benguela regional waters.

Chapter 3. Ms. Bronwen Currie and Ms. Kathleen R. Peard of the Ministry of Fisheries, Namibia, undertook *in situ* sampling and measurements. Dr. Volker Brüchert of the Max-Planck Institute, Germany, developed the HPLC methodology to determine the presence of elemental sulphur in water samples. Prof. Andrew Bakun, RSMAS, University of Miami, provided guidance and input toward understanding causes of the hydrogen sulphide eruptions and triggering mechanisms.

Chapter 4. Dr. Grant Pitcher, M&CM, Cape Town, undertook the collection, processing and analysing of *in situ* samples. Mr. Stewart Bernard, University of Cape Town, undertook processing and analysing of the *in situ* radiance data. The MODIS Rapid Response Team provided requested MODIS data.

Neither the substance nor any part of the above thesis has been submitted in the past, or is being, or is to be submitted for a degree at this University or at any other university.

Signed Signed by candidate

Date: 30 January 2005

ACKNOWLEDGEMENTS

I wish to thank my supervisors, Prof. Frank Shillington, University of Cape Town (UCT), Dr. Ray Barlow, Marine and Coastal Management (MCM), Cape Town, and Dr Claude Roy, Institut de recherche pour le developpement (IRD), France, for guidance, support and helpful comments throughout this work. Special thanks go to Dr. Gene Feldman and members of the SeaWiFS Project, NASA, for making this PhD possible; Wayne Robinson, Norman Kuring, John Wilding, Bryan Franz, Jeremy Werdell, Sean Bailey, Mark Ruebens, and other members of the SeaWiFS "family", with whom I collaborated extensively in determining the optimal SeaWiFS processing parameters for Benguela waters. Thank you. Very special thanks go to Prof. Andy Bakun, of RSMAS, University of Miami, whose belief in my work never wavered, for input toward understanding the causes of the hydrogen sulphide eruptions and the triggering mechanisms, and for keeping my spirits up! I wish to acknowledge the contributions of all the members of the Namibian Ministry of Fisheries "Sulphide Team", especially Bronwen Currie and Kathi Peard. We all had fun unraveling the hydrogen sulphide puzzle! Thanks to Dr. Volker Brüchert of the Max-Planck Institute, Germany, for developing the HPLC methodology to determine the presence of elemental sulphur in water samples. Thanks to Dr. Grant Pitcher, MCM, for collecting, processing and analysing the *in situ* coccolithophore samples, and to Stewart Bernard, UCT, for processing and analysing the *in situ* radiance data. Thanks to the MODIS Rapid Response Team for so willingly providing the requested MODIS data. Thanks to Prof. Geoff Brundrit, UCT, always there to advise. Thanks to Dr. Pierre Freon, IRD, for unswerving support. I thank my OceanSpace "right-hand man", Christo Whittle, for assistance in image processing and sharing the load. Thanks also to Dr. Richard Lord, UCT, for many tireless hours of assisting with IDL code! Sincere thanks go to the French Ministry of Foreign Affairs (FSP) for its generous support, and the German GTZ BENEFIT Programme for financial support.

Special thanks go to my very dear friends whose encouragement and love supported me through this endeavour, David Kantey, Lynn and Shirley Gillis, Aliki Romano, my family, and many others close to my heart. Last, but most importantly, my daughter, Sian, who allowed me the "time out", whose love and pride in me gave me the strength to complete this task. Radha Soami.

Abstract

The objective of this thesis was to utilise high resolution satellite data, from the NOAA AVHRR and OrbView-2 SeaWiFS sensors, to investigate the upper layer dynamics of the Benguela ecosystem in more detailed space and time scales than previously undertaken. The standard SeaWiFS bio-optical algorithms and processing parameters are not ideal for the highly productive Benguela waters. Hence, a detailed investigation was undertaken, and the processing parameters modified for more optimal application to Benguela waters. Examination of the individual radiances used in the bio-optical algorithm revealed that constituents, other than chlorophyll, were at times contributing significantly to the in-water light field. The approach adopted in this thesis was that the application of satellite data to Benguela waters should be considered either as qualitative, for event scale phenomena, or quantitative, for the longterm study.

Two specific event scale qualitative applications of satellite data were identified, examined in detail and documented. The capability to identify and monitor hydrogen sulphide eruptions in the northern Benguela, using ocean colour satellite data, was recognized. This new discovery appears to have altered the conventional view. The new view of their very large extent and high frequency of occurrence has made clear their potential ecological importance to the northern Benguela ecosystem. The pattern of occurrences implies a new, very different mechanism as being primarily responsible for widespread anoxic conditions over the continental shelf, and for extreme anoxic episodes. The first extensive coccolithophore bloom in the southern Benguela region was identified by satellite, and the evolution thereof monitored and documented. The bloom was dominated by a species not previously known to form such intense concentrations. A close match-up of SeaWiFS-derived and *in situ* normalized-water leaving radiances provided validation of the processing parameters selected for Benguela coastal waters. The SeaWiFS bio-optical algorithm was shown to yield depressed estimates of chlorophyll *a* in the presence of coccoliths, or precipitated sulphur.

A consistent time series of high quality daily sea surface temperature and chlorophyll *a* concentration images, for the period July 1998 to June 2003, was generated, and a quantitative analysis undertaken. The extent and frequency of upwelling in the southern Benguela, and the consequent phytoplankton response, was identified. Sea surface temperature, upwelling and phytoplankton indices were derived for selected locations, and the relationship between these parameters determined. The results suggest that SST indices may be used to determine the development of upwelling cells, and chlorophyll indices to determine the development of a phytoplankton bloom. The evident relationships may be used to elucidate the response of phytoplankton biomass in relation to thermal changes due to upwelling. These indices should be developed further to serve as a routine time series of updateable ecosystem indicators, as input into the management of the ecosystem.

Chapter 1

1. General Introduction

The Benguela Current flows equatorward along the western coast of southern Africa forming the eastern boundary current segment of the subtropical gyre of the South Atlantic Ocean. From near the southern extremity of the African Continent, it bathes the coasts of South Africa, Namibia, and the southern part of Angola. It leaves the coast and veers northwestward at about 18°S latitude to eventually merge with the westward-flowing South Equatorial Current. The Benguela Current is a direct analog to the other major subtropical eastern boundary currents of the Atlantic and Pacific Oceans: the Canary Current, the California Current and the Peru-Humboldt Current systems (Wooster and Reid, 1963, Parrish et al., 1982). As for the other systems, wind-driven offshore-directed transport of surface waters and resulting coastal upwelling is a dominant aspect of its dynamics and its ecology. However, the Benguela is unique in the extreme strength of this offshore transport and of the resulting upwelling near the coast of waters originating at depth (Bakun, 1996).

The large marine ecosystem of the Benguela Current (Sherman, 1999) is usually considered to represent a combination of two somewhat autonomous regional ecosystems, the northern Benguela and the southern Benguela, respectively. The division between the two is usually placed in the vicinity of Lüderitz (26.6^{0}S), which is located on the Namibian coast approximately 200 km north of the border with South Africa. It is the northern Benguela that features by far the more intense upwelling, its highest intensity core located near Lüderitz. This high rate of upwelling is reflected in very high primary productivity.

Our present understanding of the functioning of the Benguela ecosystem is based on data collected mostly from research cruises and the use of low resolution (4 - 18 km) satellite data. Although *in situ* data may be of very high quality, synoptic coverage of the ecosystem is not achieved. Conversely, low resolution satellite data may provide broad synoptic coverage, but exclude the detailed temporal and spatial variability of upwelling and of phytoplankton response that occurs in the Benguela. Higher resolution (1 km) data from satellites that provide daily synoptic coverage of the ocean have been acquired locally over the past number of years. Exploitation of such data, in particular from the NOAA AVHRR and the OrbView-2 SeaWiFS sensors, offers the opportunity of investigating the upper layer dynamics of the Benguela ecosystem in more detailed space and time scales than has

previously been undertaken. In particular, a study of the mesoscale upwelling events and consequent phytoplankton response in the Benguela using the higher resolution data would improve our knowledge of the key processes that drive the Benguela ecosystem.

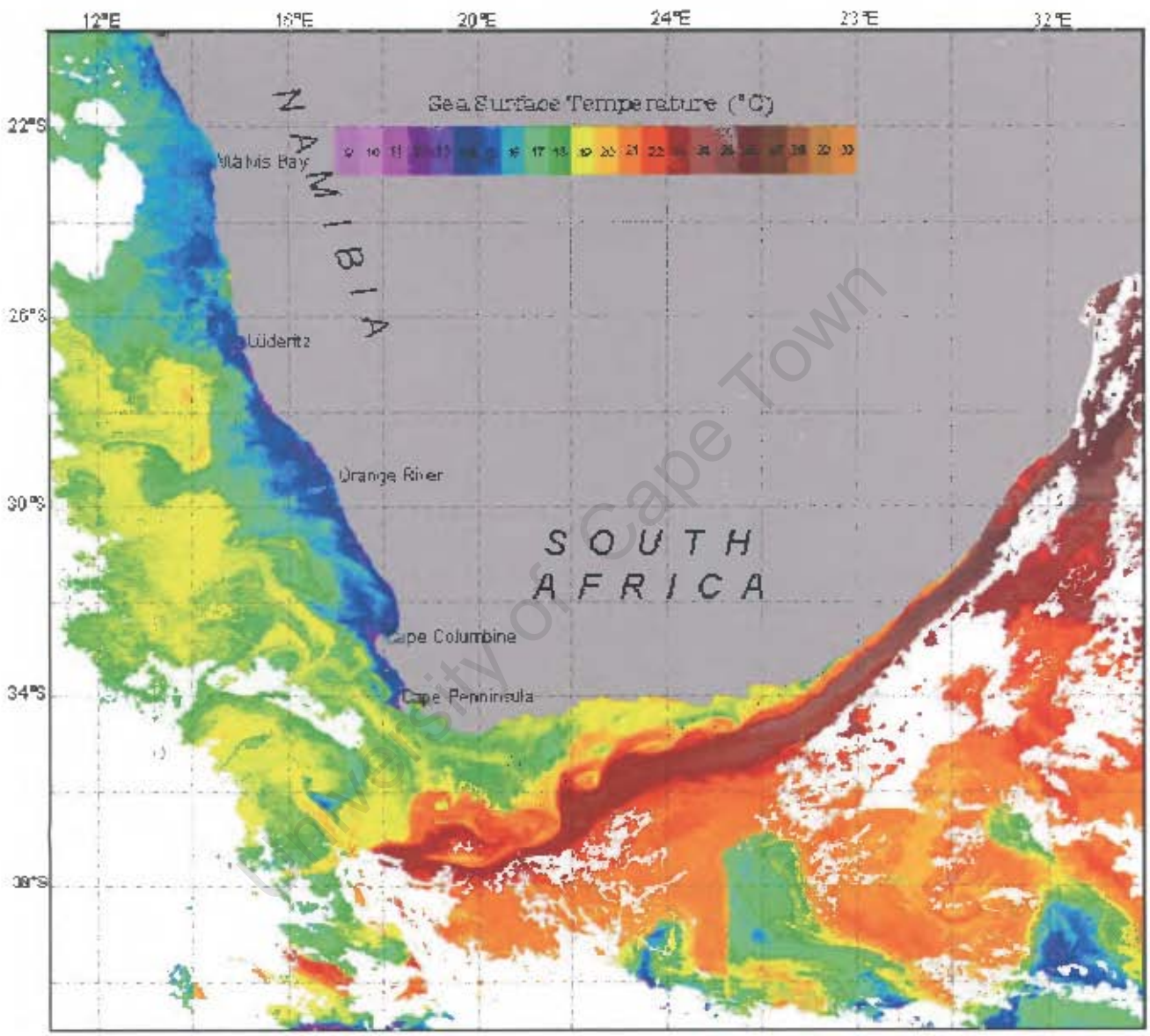

Figure 1.1. NOAA AVHRR sea surface temperature image for 15 May 2003 showing the Benguela Current system extending along the western coast of southern Africa, with the warm Agulhas Current flowing down the south-eastern coast. The Benguela Current forms the eastern boundary current of the South Atlantic and is bounded at both the equatorward and poleward ends by warm water regimes, the Angola-Benguela frontal zone in the north (not shown) and the Agulhas retroflection area in the south.

A study of the dynamic variations in upwelling intensity and phytoplankton biomass requires a consistent time series of sea surface temperature (SST) and chlorophyll *a* concentration images from NOAA AVHRR and SeaWiFS ocean colour data, respectively. The generation of high quality images was considered the primary initial task for this study. However, in processing the one kilometre resolution SeaWiFS data, it soon became apparent that the standard bio-optical algorithms and processing parameters are not ideal for the high productivity waters of the Benguela. These parameters had been determined by the SeaWiFS Project, based at the NASA Goddard Space Flight Centre (GSFC), for application to the global dataset and generally open water conditions. Hence, they could not be expected to be optimal for specific coastal waters. Therefore, a detailed investigation of the bio-optical algorithms and processing parameters was first required. It was necessary to modify and refine the processing parameters for more optimal application to Benguela regional waters. This work, which was undertaken in close collaboration with the SeaWiFS Project at NASA, is outlined in Chapter 2 of this thesis.

The detailed investigation of processing parameters and regional one kilometre resolution SeaWiFS data soon revealed that constituents other than chlorophyll were at times contributing significantly to the in-water light field. This was unexpected. Subsequent examination of the individual radiances used in the bio-optical algorithms led to the recognition of specific event scale phenomena occurring in the Benguela ecosystem, in particular, hydrogen sulphide eruptions in northern Benguela waters. It was realised therefore that no one set of processing parameters is perfect for every individual day's data within a longterm time series and that a simple direct approach to this work could not be followed. Moreover, it was recognized that within the African situation, the lack of scientific facilities and resources limited opportunities for quantitative calibration of event scale signals. Hence, the approach adopted in this thesis is to consider the application of satellite data to Benguela waters either as qualitative, for event scale phenomena, or quantitative, for a longterm time series study. The processing of SeaWiFS ocean colour data should be adjusted accordingly, as is outlined in Chapter 2. Chapters 3 and 4 therefore document specific event scale qualitative applications of satellite data, namely hydrogen sulphide eruptions in northern Benguela waters and an unusual coccolithophore bloom in the southern Benguela. Chapters 5 and 6 focus on a quantitative analysis of one kilometre resolution NOAA AVHRR and SeaWiFS ocean colour data for the southern Benguela, and the development of operational indices towards their application in the management of the ecosystem.

2. Qualitative applications

Based on analysis of low resolution (4.5km) SeaWiFS satellite data, Carr (2002) estimates that the annual primary production in the Benguela Current region as a whole is greater than in any of the other classical eastern ocean upwelling regions, being nearly twice that of the Peru-Humboldt region and nine times that of the California Current region. Of the two Benguela regions, the northern Benguela appears to be much more productive (Carr, 2002), as might be expected from the strength of its upwelling of cold, nutrient-rich waters into the euphotic zone. However, the associated very rapid offshore transport of the ocean surface layer, along with organisms that might be passively entrained in it, has major consequences for the ecology of this system. For example, planktonic grazing organisms (herbivorous copepods, etc.) may have difficulty maintaining substantial populations near the upwelling zone. Grazing by zooplankton may therefore be inhibited. This, together with the high rate of downstream primary production, produces a situation along the Namibian central coast where enormous numbers of phytoplankton cells apparently sink unutilized to the sea floor. This situation may be intermittently augmented by the development of harmful algal blooms (Pitcher, 1998) that at times produce massive "red tide" accumulations.

The net result of the accumulation of large amounts of unoxidized organic matter on the continental shelf is the production of extensive areas of sea floor hypoxia (<0.5 ml O_2 l^{-1}), and even total anoxia. Beneath this, poisonous hydrogen sulphide and methane gas are generated within the diatom sludge (Emeis et al., 2002). The largest known bacteria in the world, *Thiomargarita namibiensis*, which may be up to three-quarters of a millimeter across, occur at and near the surface of this layer. Here they sustain themselves, together with other species of sulphide-oxidizing bacteria, by oxidizing sulphide with nitrate from the water column above (Schulz et al., 1999; Wuethrich, 1999).

Nearshore hydrogen sulphide eruptions are familiar experiences along the central coast of Namibia. Local inhabitants have become inured to the disagreeable smells and corrosive effects of the sulphurous gases released from the sea into the coastal atmosphere. Mortalities of nearshore animals occur annually with varying intensity, with a variety of fish and invertebrates being victims. This results in a fortuitous feast for seabirds, which converge on the milky turquoise-coloured patches of sulphide-infused waters to feed on floating casualties. Local people also harvest rock lobsters fleeing ashore from the noxious conditions in the water. However effects have sometimes been far less innocuous. For example, a catastrophic loss of two billion young Cape hake, *Merluccius capensis*, during austral summer of 1992-93 has been blamed on an anoxic outbreak (Woodhead et al., 1998).

In addition to its direct toxic impact, hydrogen sulphide has the secondary effect of depleting oxygen from the water, so that extensive surrounding areas suffer from severe hypoxia and anoxia . In this case, about half of the recruit population of Namibian Cape hake was estimated to have died as a result of being trapped by widespread anoxia in shelf bottom waters. Even the surviving hake that escaped offshore apparently suffered greatly increased mortality from predation during the following year because of exclusion from their favored near-coastal habitat by lingering anoxia (Hamukuaya and O'Toole, 1994).

In spite of such major effects ascribed to anoxic episodes, the conventional view had been that the sulphide-laden eruptions that are observed from the shore in this region are very local features and thus must have only rather limited ecosystem-scale consequences. This is because observations have been land bound and without broad coastwise coverage. But, as is documented in Chapter 3 of this thesis, it is now possible to identify and monitor such anoxic phenomena using higher resolution (1km) ocean colour satellite data (Weeks et al., 2002, Weeks et al., 2004a). This recently-recognised capability appears to have altered the conventional view. The sulphide eruptions occurring locally on the continental shelf are now seen to be far more spatially extensive, much longer lasting, and much more frequent than previously realised.

Ocean colour satellite observations also introduce another interesting issue. Hydrogen sulphide features separated from the coast, particularly after having existed at the sea surface for some time, tend to appear quite similar to satellite observations of very large coccolithophore blooms. Coccolithophorids are a phytoplankton species that are able to synthesize external calcium carbonate platelets, or coccoliths, that cover the outer surface of the cell. They are widespread (Brown and Yoder, 1994) and known to form near mono-specific blooms that can extend over large areas of ocean surface (Holligan et al., 1983, 1993). Little consideration has been given to the contribution of coccolithophorids to the phytoplankton communities in upwelling systems (Cushing, 1989). In particular, very little has been documented as to the extant of coccolithophores in the Benguela upwelling system.

A study of coccolithophore dynamics in the southern Benguela was undertaken by Giraudeau and Bailey (1995). They found high coccolithophorid species diversity and low concentrations during active upwelling, whereas stratified water following relaxation of upwelling showed low coccolithophorid species diversity, occasionally associated with blooms. At such times, coccolithophores appear to thrive preferentially at the seaward edge of the upwelling centre

(Shannon and Pillar, 1986; Wefer and Fischer, 1993). A previous study in the southern Benguela undertaken by Mitchell-Innes and Winter (1987) suggested that coccolithophores prefer mature, warmer water. These authors reported high concentrations of coccolithophores (2.34×10^6 cells l^{-1}) in aged upwelled waters, dominated by the coccolithophorid, *Emiliania huxleyi*. In the northern Benguela region, high coccolithophore concentrations (6.80×10^6 cells l^{-1}) were recorded off Namibia during an anomalous warm event (Kruger, unpublished data, SA Marine & Coastal Management).

The number of coccolithophorid cells in a bloom frequently accounts for 80 percent or more of the total phytoplankton cells in the water. Coccolithophorid cells may be accompanied by even larger numbers of coccoliths, either attached to the cells or floating in the water. Such blooms provide a milky turquoise colour to the ocean, primarily due to light scatter from the coccoliths [Balch et al., 1996a, Tyrrell et al., 1999). The consequent high reflectances are visible from satellite, allowing the extent of a coccolithophore bloom to be distinguished (Ackleson, Balch & Holligan, 1994). The evolution of such blooms can therefore be monitored using derived quasi-true colour satellite imagery as an alternative to the traditional phytoplankton biomass proxy of chlorophyll *a* concentration. The evolution of a recent, unusual coccolithophore bloom in southern Benguela waters, the first such extensive bloom monitored by satellite in the Benguela upwelling region (Weeks et al., 2004b), is documented in Chapter 4 of this thesis. In that Chapter, ocean colour data from the Moderate-Resolution Imaging Spectroradiometer (MODIS) onboard the NASA Terra and Aqua satellites are also used.

3. Quantitative applications

The oceanography of the Benguela region is dominated by coastal upwelling, the extent and intensity of which is primarily determined by the wind and pressure field (Nelson and Hutchings, 1983). This, together with the topography and orientation of the coast, results in the formation of a number of upwelling cells (Hutchings, 1992, Shannon and Nelson, 1996). The largest upwelling cell off Luderitz is perennial in nature and effectively divides the Benguela into two regional ecosystems, the northern Benguela and the southern Benguela, respectively (Sherman, 1999).

Upwelling in the southern Benguela tends to be short-lived and seasonal. A frontal zone is usually well defined and, although variable, generally coincides with the shelf edge (Shannon and Nelson, 1996). Upwelling filaments may occur with a life span of days to several weeks. These are generally

orientated perpendicular to the coast and cause the front to become highly convoluted (Shannon and Nelson, 1996). The southern boundary of the Benguela is considered to be the Agulhas retroflection generally between 36°S and 37°S (Shannon 1985, Shannon and Nelson, 1996). Warm sub-tropical Agulhas water "leaks" into the south Atlantic, mostly in the form of Agulhas rings, eddies or filaments shed from the Agulhas Current as it retroflects to the east (Duncombe Rae, 1991, Nelson et al., 1998, Garzoli et al., 1999). The Benguela system therefore displays substantial short-term, seasonal and inter-annual variability that impacts significantly on its biological resources.

The high rate of upwelling in the Benguela is reflected in very high primary production. As the upwelled water moves offshore, it warms up and with a rich supply of nutrients in the surface layer, phytoplankton growth commences and blooms occur. Phytoplankton abundance is however highly variable with low values around 27-28°S at the base of the Luderitz cell and high values downstream of upwelling cells. In the southern Benguela, maximum phytoplankton concentrations are considered to occur 20-80 km from the coast, although blooms following periods of active upwelling can extend 100 km or more offshore (Brown et al., 1991). Chlorophyll *a* concentrations in recently upwelled water, maturing upwelled water and aged water are documented as <1, 1-20 and 5-30 mg m^{-3}, respectively (Barlow, 1982). Average primary production estimates for the northern Benguela are 1.2 g C m^{-2} d^{-1} and 2.0 g C m^{-2} d^{-1} for the southern Benguela (Brown et al., 1991).

Results of shipboard studies in the Benguela have suggested a varying response of phytoplankton to upwelling, but such investigations have been confined to microscale areas (Barlow, *pers comm.*). With the availability of one kilometre resolution SeaWiFS data it is now possible to extend these investigations to greater spatial and temporal scales. Daily one kilometre resolution NOAA images display the temporal and spatial variability in Sea Surface Temperature (SST) thus allowing identification of the locality and emergence of upwelling cells whereas daily SeaWiFS images show the distribution patterns of chlorophyll *a* concentration across the Benguela.

Chapters 5 and 6 of this thesis focus on the quantitative analysis of one kilometre resolution NOAA SST and SeaWiFS chlorophyll data within the southern Benguela ecosystem. Chapter 5 concentrates on examining the extent and frequency of upwelling during the period July 1998 through June 2003 and the response of the phytoplankton community to this physical forcing. The specific focus is on the spatial and temporal variability in SST, upwelling and chlorophyll a concentration on intra-seasonal time scales. In addition to examining the dynamic variations in upwelling and phytoplankton abundance in the southern Benguela, appropriate indices are developed to quantify

these variations. In Chapter 6, indices of SST variability, upwelling intensity and chlorophyll variability are derived for selected latitudinal lines, to enable the intra-seasonal variations to be more comprehensively quantified and compared.

The indices are developed specifically for a current regional programme, the BENEFIT (Benefit Environmental Fisheries Interaction and Training) Programme, and selected in consultation with Marine and Coastal Management, the University of Cape Town, and representatives of the French-South African IDYLE (Interactions and Spatial Dynamics of renewable resources in upwelling Ecosystems) Project. A primary goal of the BENEFIT Project, "Application of Remote Sensing in the Benguela System", is to utilise one kilometre resolution NOAA AVHRR and SeaWiFS ocean colour satellite data to study the mesoscale upwelling events and consequent phytoplankton response in the Benguela. Investigation of these dynamic variations offers the opportunity to derive quantitative indexes to serve as a measure of ecosystem function for comparison with fluctuations in recruitment of the exploited marine resources. Additionally, the Benguela Current Large Marine Ecosystem (BCLME) Programme, a regional initiative by Angola, Namibia and South Africa, aims to facilitate the integrated management, sustainable development and protection of the Benguela Ecosystem. An objective of the BCLME Programme is to develop State of Environment (SOE) indices from satellite data for application in the operational management of sustainable resources. The development of appropriate remotely-sensed SOE indices is to include SST, wind, sea state, chlorophyll and primary production. Chapters 5 and 6 serve as an initial exploration for the development of the SOE indices.

Finally, in Chapter 7, a synthesis of both the qualitative and quantitative applications of NOAA and ocean colour satellite data in the Benguela is provided. This work strives to improve our knowledge of the key processes that operate in the Benguela ecosystem over greater time and space scales than has previously been undertaken and in so doing, to provide input into an ecosystem management approach of marine resources in the region.

Chapter 2

Optimal parameters for processing of HRPT data for Benguela regional waters.

1. Introduction

A study of the dynamic variations in upwelling and phytoplankton biomass requires a consistent time series of sea surface temperature (SST) and chlorophyll *a* concentration images from NOAA AVHRR (Advanced Very High Resolution) and OrbView-2 SeaWiFS (Sea-viewing Wide Field-of-view Sensor) data, respectively. HRPT (High Resolution Picture Transmission, 1km resolution) data from these satellites are acquired locally by the CSIR Satellite Application Centre located close to Pretoria, South Africa. Processing of the data is undertaken by the respective users. For the purpose of this thesis, HRPT NOAA AVHRR and SeaWiFS 1-kilometre data are referred to as "high resolution" data although, with the advent of even higher resolution commercial satellite imagery, the data may well be more correctly referred to as being of moderate resolution.

Processing of NOAA AVHRR data is considered fairly standard and hence is only briefly discussed in the section below. However, in processing the high resolution SeaWiFS data, it soon became apparent that the standard bio-optical algorithms and processing parameters are not ideal for the high productivity waters of the Benguela. Parameters for processing the SeaWiFS ocean colour global dataset are determined by the SeaWiFS Project, based at the NASA Goddard Space Flight Centre (GSFC). These parameters generally form the default parameters for SeaDAS, the SeaWiFS Data Analysis System, also used for processing of high resolution SeaWiFS data. Since initial SeaWiFS data was acquired in September 1997, the NASA SeaWiFS Project has worked consistently at improving and refining the processing parameters. At this time, four global reprocessings of SeaWiFS GAC (global area coverage, 4.5 km resolution) data have been undertaken.

The ongoing improvement and refinement of SeaWiFS processing parameters and the immediate incorporation into local processing of subsequent releases of improved versions of SeaDAS have resulted in an inconsistent regional HRPT SeaWiFS time series. Additionally, in investigating the various algorithms developed for generating ocean colour products, it became apparent that the parameters applied in the processing of global GAC SeaWiFS data, the SeaDAS operational parameters, are not optimal for Benguela waters. Following frequent communication with the

SeaWiFS Project, it was decided to work together to determine the optimal parameters for processing of HRPT SeaWiFS data in Benguela regional waters. A period of intense collaboration ensued, including time based at the NASA GSFC. Working with specific members of the SeaWiFS Project, a number of issues and concerns were addressed of which only the primary are detailed herein.

This chapter provides the fundamental methodology required for determining optimal processing parameters for HRPT satellite data for application to Benguela regional waters, be it qualitative, for event scale phenomena, or quantitative, for a longterm time series study. The processing of SeaWiFS ocean colour data in particular needs to be adjusted accordingly.

2. Methodology

2a. NOAA AVHRR data

The NOAA AVHRR sensor measures radiances primarily in the infrared part of the wave spectrum. The spectral bands of the five AVHRR channels are listed below.

AVHRR Channel	Wavelength	Spectrum
1	0.6-0.7μm	Visible
2	0.7-1.1μm	Near IR
3	3.5-3.9μm	Near IR
4	10.3-11.3μm	Thermal IR
5	11.5-12.5μm	Thermal IR

Daytime NOAA AVHRR (1 km) sea surface temperature images for the Benguela region were generated locally using the standard MultiChannel Sea Surface Temperature (MCSST) algorithm (McClain et al., 1985). Consistent parameters were applied although a manual manipulation of channels 2 and 4 was required for optimal cloud removal each day. The optimal albedo (brightness) threshold for cloud was determined by manipulating the maximum reflectance threshold value for channels 2. The pixel-to-pixel delta-temperature values for channels 2 and 4 were also manipulated daily. Since the temperatures of cold upwelled waters in this region are at times similar to temperatures of overlying cloud or fog, careful manipulation of the channel 4 minimum threshold was also required.

Further, a minimum solar reflection angle was determined in order to best avoid sunglint in regional waters. A maximum satellite zenith angle was also selected so as to remove data towards the swath edge.

2b. OrbView-2 SeaWiFS

The SeaWiFS sensor measures radiances primarily in the visible part of the wave spectrum. The eight spectral bands are listed below. Bands 1 to 6 have a 20nm bandwidth while bands 7 and 8 have 40nm bandwidth.

SeaWiFS Channel	Centre Wavelength	Spectrum
1	412nm	violet
2	443nm	blue
3	490nm	blue-green
4	510nm	blue-green
5	555nm	green
6	670nm	red
7	765nm	near IR
8	865nm	near IR

Processing of SeaWiFS data may broadly be divided into levels one, two and three. It is not within the scope of this thesis to detail the various processing steps. However, a very brief summary of SeaWiFS data products is provided in Appendix 2.1 (http://seawifs.gsfc.nasa.gov/SEAWIFS/SOFTWARE/ DATA_PRODUCTS.html). A multi-sensor code, MSl12, is used in processing SeaWiFS data from level-1 to level-2 with numerous parameters to control the processing and provide user-specified output. MSl12 performs the atmospheric correction of top-of-atmosphere (TOA) radiances, and derives the atmospheric and bio-optical properties. Input parameters are through a series of keywords that may be manipulated or modified to achieve a desired output. A list of the most recent MSl12 (version 3) input parameter keywords, along with the operational defaults, is tabulated in Appendix 2.2 (MSl12 Version 3.0 User's Guide, SeaDAS online documentation).

Additionally, during level-2 and level-3 processing, specific data may be flagged, noting a condition, or masked, denoting the data as unacceptable due to a condition. Table (2.1) lists the flag and masks used in the most recent (fourth) global reprocessing, including changes from the third reprocessing (Robinson *et al.*, 2003). For many flags, the underlying algorithm that generates the flag was

changed. In these cases, the new algorithm is an improvement over the old, in that it characterises the flag condition better, and in some cases, allows for a greater number of retrievals to be made. Using these most recent operational parameters (algorithms, flags and masks) as a baseline for application to Benguela waters, this section describes the numerous conditions tested, and control parameters and thresholds manipulated to determine optimal SeaWiFS data quality and data retrieval for Benguela regional waters.

The OC4V4 (ocean colour four band, fourth revision) bio-optical algorithm (O Reilly et al., 2000) is currently used to determine chlorophyll concentration. This fourth order polynomial equation uses a maximum band ratio such that chlorophyll *a* concentration (C_a):

$$C_a = 10.0 \exp (0.366 - 3.067R_{4S} + 1.930R_{4S}^{\ 2} + 0.649R_{4S}^{\ 3} - 1.532R_{4S}^{\ 4})$$

where the band ratio, $R_{4S} = \log_{10} (R^{443}_{555} > R^{490}_{555} > R^{510}_{555})$. In R_{4S}, the numerical part denotes the number of bands used and S, the SeaWiFS sensor. The argument of the logarithm represents the maximum of the three values, each being a ratio of SeaWiFS normalized water-leaving radiances at the specified wavelengths. (Normalized water-leaving radiance is a measure of the satellite signal after atmospheric correction, representing light leaving the sea normalised to incoming extraterrestrial values.)

Table 2.1. Flags for the fourth reprocessing (Robinson *et al.*, 2003).

The *Mask in* columns indicate that no geophysical data is created in the level-2 (L2) or level-3 (L3) dataset if the flag conditions marked *Y* exist for that observation. The changes from the third reprocessing fall under one or more of the following categories: a) New (a new flag for the fourth reprocessing); b) Change (a direct change in the algorithm or threshold was made); and c) *Mask in L2* or *Mask in L3* indicates that in the fourth reprocessing, data are now excluded from the L2 or L3 product and *Flag in L2* or in *Flag in L3* indicates that data which were previously excluded are now included.

No.	Flag Name	Mask in L2	Mask in L3	Description	Change from 3rd reprocessing
1	ATMFAIL	Y	Y	Atmospheric algorithm failure	-
2	LAND	Y	Y	Land	-
3	BADANC			Missing ancillary data	-
4	HIGLINT			Sun glint contamination	Flag in L2 & L3
5	HILT	Y	Y	Total radiance above the knee	Change
6	HISATZEN		Y	Satellite zenith angle above the limit	Change
7	COASTZ			Shallow water	Change
8	NEGLW			Negative water-leaving radiance in bands 7 and 8	-
9	STRAYLIGHT	Y	Y	Stray light contamination	Change, mask in L2
10	CLDICE	Y	Y	Clouds or ice	Change
11	COCCOLITH		Y	Coccolithophore bloom	-
12	TURBIDW			Turbid, Case-2 water	Change
13	HISOLZEN		Y	Solar zenith angle above the limit	-
14	HITAU			High aerosol concentration	-
15	LOWLW		Y	Low water-leaving radiance at 555 nm	-
16	CHLFAIL	*	Y	Chlorophyll not calculable	Change
17	NAVWARN		Y	Questionable navigation (tilt change)	-
18	ABSAER		Y	Absorbing aerosol index above the Threshold	Change
19	TRICHO			Trichodesmium bloom condition	-
20	MAXAERITER		Y	Maximum number of iterations in the NIR algorithm	-
21	MODGLINT			Glint corrected measurement	-
22	CHLWARN		Y	Chlorophyll is out of range	Mask in L3
23	ATMWARN		Y	Epsilon value outside of reasonable range or Lw at 490, 510 or 555 nm is less than zero	-
24	DARKPIXEL			Rayleigh corrected radiance is less than zero for any band	-
25	SEAICE			Sea ice present based on climatology	New
26	NAVFAIL	Y	Y	Navigation of the line is bad	New
27	FILTER		Y	Insufficient surrounding pixels for aerosol model filter **	New
28	- 31			Spare for future use	N/A
32	OCEAN			Ocean data	New

* The chlorophyll value is not computed, but *first guess* Lwn values are computed

** The filter algorithm is only applied to HRPT and LAC data

A primary concern in the application of the most recent operational parameters to Benguela waters is the large impact of the stray light correction. Stray light contamination occurs as a result of light from bright sources - cloud, land, desert - contaminating measurements of adjacent ocean pixels both up-scan and down-scan from the bright source. To correct for this, HRPT pixels located 3 pixels or closer to a bright source are masked (Table 2.1) and a stray light correction is applied to pixels up to 14 pixels away from the bright target. However, application of the stray light correction to Benguela high productivity waters results both in enhanced chlorophyll concentration in inshore waters, and masking of freshly upwelled and coastal waters.

By way of illustration, Figure (2.1) represents HRPT data for the southern Benguela region on 15 October 2002. This data was processed using the SeaWiFS operational parameters and simply manipulating the stray light correction and masking parameter. Only pixels flagged as land (grey), cloud (white offshore) or stray light-contaminated (white inshore) have been masked. The associated flag statistics are presented in Table (2.2).

Case A: 15 October 2002: sl_pixl = 0, maskstr=0
Case B: 15 October 2002: sl_pixl = 1, maskstr=1
Case C: 15 October 2002: sl_pixl = 3, maskstr=1

To start, when the stray light correction is switched off (*sl_pixl* = 0, Case A, Fig. 2.1a), no correction for stray light is done at all. So, all pixels up to about 14 pixels away from the bright target will be affected by stray light with the pixels closest to the target being affected the most. With *sl_pixl* > 0 (Cases B and C, Figs. 2.1b and 2.1c), the stray light correction is applied except to the first three pixels away from the target. No correction is even attempted for these pixels. The standard practice is to mask those out (*maskstr*=1). The value of *sl_pixl* determines the number of pixels from the bright target that are assigned the stray light mask. Hence, the change from Cases (A) to (B) and (C) is the combination of two changes: the switching on of the stray light correction and a reduction in the un-corrected pixels getting into the statistics.

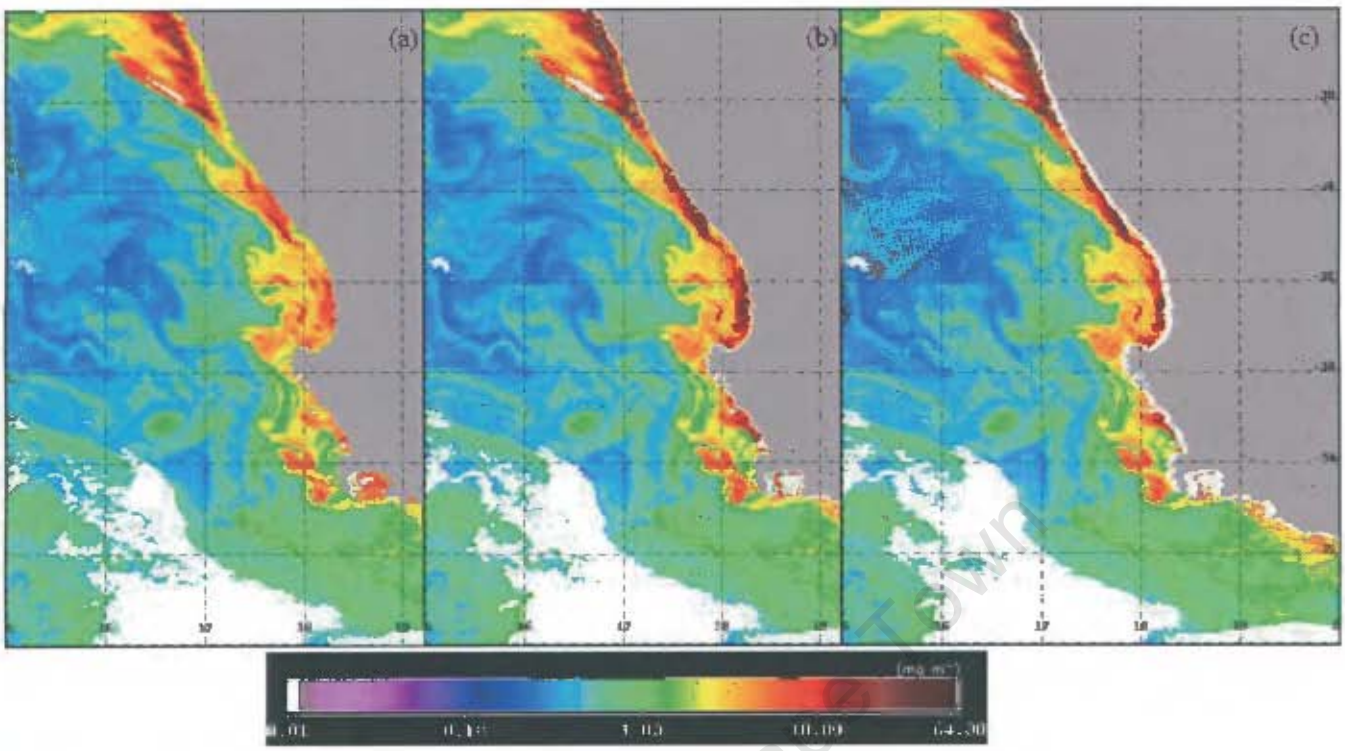

Figure 2.1. SeaWiFS chlorophyll a concentration for the southern Benguela region on the 15 October 2002. White masking along the coast is due to manipulation of the stray light correction and the masking parameters: (a) sl_pixl = 0, maskstr=0; (b) sl_pixl = 1, maskstr=1; and (c) sl_pixl = 3, maskstr=1. Offshore, white represents cloud.

Application of the stray light correction results in a notable increase in chlorophyll *a* concentration in the affected areas (Fig. 2.1). Considering only the inner continental shelf (0-100m) from 29.00°S to 34.35°S (tip of the Cape Peninsula), the mean chlorophyll *a* concentrations (Fig. 2.2) are 13.22 $mg.m^{-3}$ and 13.53 $mg.m^{-3}$ for Cases (B) and (C) respectively, relative to 4.82 $mg.m^{-3}$ for Case (A). Hence, for this example, an almost three-fold increase in mean chlorophyll *a* occurs over the first 16 coastal pixels (average width of the inner shelf) when the stray light correction is switched on. In this scenario, masking of the first three coastal pixels results in only 59 percent of the inner shelf pixels being included in the statistics (Fig. 2.2, Case C), while 82 percent are included when the first coastal pixel is masked (Fig. 2.2, Case B), relative to 97 percent pixel inclusion when the stray light correction is off (Fig. 2.2, Case A).

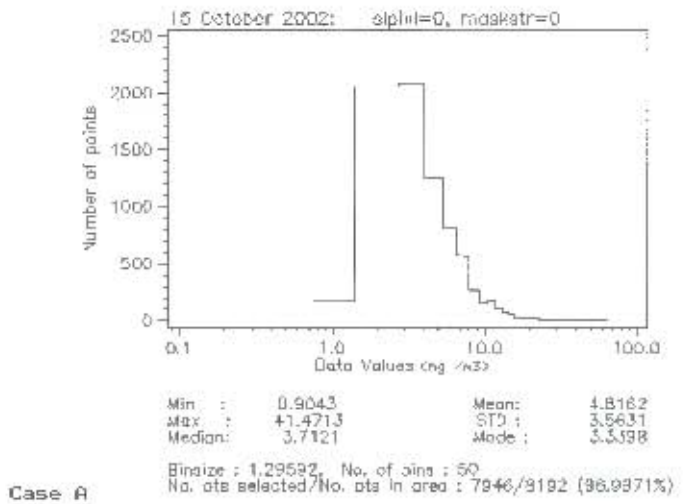

Case A

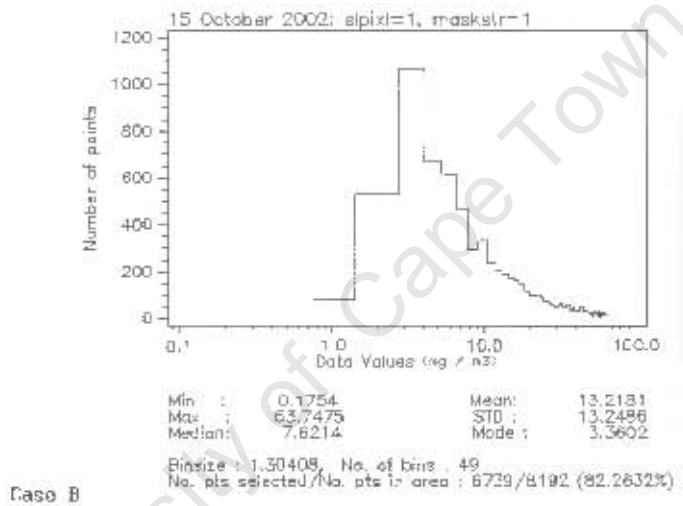

Case B

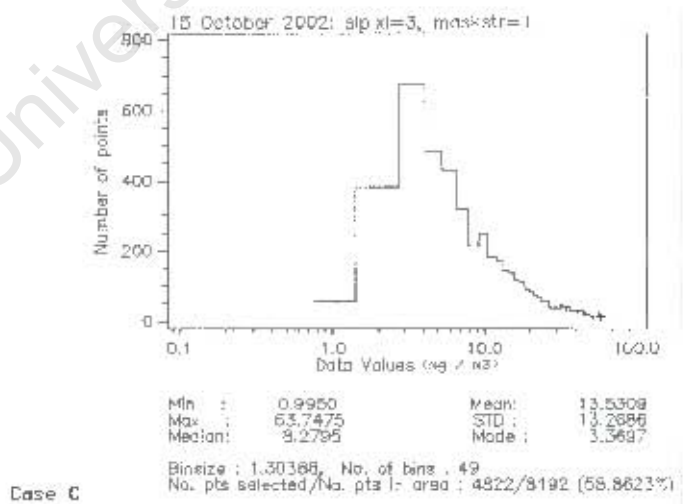

Case C

Figure 2.2. Output statistics for the southern Benguela inner shelf on 15 October 2002, processed with differing stray light parameters (reference Fig.2.1).

Table 2.2. Flag statistics for southern Benguela data of 15 October 2002, processed with differing stray light parameters (reference Fig.2.1).

Flag No.	Flag Name	Case A Pixels	Case A Pixels %	Case B Pixels	Case B Pixels %	Case C Pixels	Case C Pixels %
Flag # 1:	ATMFAIL	235	0.097	3	0.0012	2	0.0008
Flag # 2:	LAND	75324	31.0886	75324	31.0886	75324	31.0886
Flag # 3:	BADANC	0	0	0	0	0	0
Flag # 4:	HIGLINT	0	0	0	0	0	0
Flag # 5:	HILT	93818	38.7217	93818	38.7217	93818	38.7217
Flag # 6:	HISATZEN	19533	8.0619	19533	8.0619	19533	8.0619
Flag # 7:	COASTZ	1361	0.5617	1361	0.5617	1361	0.5617
Flag # 8:	NEGLW	3193	1.3179	6066	2.5036	5005	2.0657
Flag # 9:	STRAYLIGHT	0	0	104720	43.2213	109305	45.1137
Flag #10:	CLDICE	25611	10.5705	25496	10.523	25496	10.523
Flag #11:	COCCOLITH	69	0.0285	6	0.0025	1	0.0004
Flag #12:	TURBIDW	3291	1.3583	1424	0.5877	831	0.343
Flag #13:	HISOLZEN	0	0	0	0	0	0
Flag #14:	HITAU	912	0.3764	381	0.1573	314	0.1296
Flag #15:	LOWLW	297	0.1226	506	0.2088	232	0.0958
Flag #16:	CHLFAIL	357	0.1473	599	0.2472	325	0.1341
Flag #17:	NAVWARN	0	0	0	0	0	0
Flag #18:	ABSAER	225	0.0929	219	0.0904	219	0.0904
Flag #19:	TRICHO	7	0.0029	0	0	0	0
Flag #20:	MAXAERITER	66	0.0272	260	0.1073	192	0.0792
Flag #21:	MODGLINT	0	0	0	0	0	0
Flag #22:	CHLWARN	3	0.0012	32	0.0132	29	0.012
Flag #23:	ATMWARN	594	0.2452	909	0.3752	351	0.1449
Flag #24:	DARKPIXEL	324	0.1337	486	0.2006	486	0.2006
Flag #25:	SEAICE	0	0	0	0	0	0
Flag #26:	NAVFAIL	0	0	0	0	0	0
Flag #27:	FILTER	0	0	0	0	0	0
Flag #28:	SPARE	0	0	0	0	0	0
Flag #29:	SPARE	0	0	0	0	0	0
Flag #30:	SPARE	0	0	0	0	0	0
Flag #31:	SPARE	0	0	0	0	0	0
Flag #32:	OCEAN	141353	58.3409	141468	58.3884	141468	58.3884

There are many considerations as to how the stray light affects the chlorophyll determination. In these high productivity waters, it would appear that an overcorrection has been applied to the normalized water-leaving radiances of the individual bands, and hence a ratio of the two bands used in the OC4V4 bio-optical algorithm (O Reilly et al., 2000) results in enhanced chlorophyll *a* concentrations. This increase in chlorophyll is noted immediately on application of the stray light correction, whether masking one (Fig. 2.1b) or more (Fig. 2.1c) contaminated coastal pixels.

Further differences are noted in the flag statistics (Table 2.2), with manipulation of the stray light parameter, primarily Flags 1, 8, 12, 14, 15, 16, 20, 23 and 24. It is not easy to determine exactly all the effects that make for the flag changes but interaction with members of the NASA SeaWiFS Project led to the following clarification:

Stray light is an excess of radiance over the correct amount of radiance. One would therefore expect the aerosol optical thickness at 865nm, or tau_865, to be higher, since there is nothing else in SeaWiFS Band 8 except Rayleigh and aerosol radiance (SeaWiFS Project, *pers comm.*). This could explain the increase in Flag 14 – HITAU (Table 2.2) in Case (A), where no correction has been applied, relative to Cases (B) and (C), above. Due to the violation of the black pixel assumption[1] in high chlorophyll waters, there is a possibility that some of this radiance may get considered to be water-leaving radiance. The chlorophyll-related correction used for SeaWiFS is described in Siegel et al., 2000. It is to be noted, however, that substances other than chlorophyll in the water may also lead to non-zero radiance in the near-infrared bands and hence affect the atmospheric correction.

The effect of stray light is not consistent throughout all the bands (W. Robinson, SeaWiFS Project, *pers comm.*). Due to the geometry of the detectors in the SeaWiFS instrument, the even bands have more stray light on the leading edge while the odd bands have more on the trailing edge. This will add some error to any computation that uses even and odd bands, such as Bands 7 and 8 in the aerosol estimation and Bands 2 and 5 or 4 and 5 in the chlorophyll estimation. Hence, this may affect the ability to perform an aerosol correction, triggering Flags 1-ATMFAIL and 23-ATMWARN. In Table 2.2, Flag 23- ATMWARN is in fact seen to flag the highest number of pixels with application of the stray light correction in Case (B), but not in Case (C). This is because the majority of the ATMWARN-flagged pixels are located one to three pixels from shore and hence are masked increasingly from Figure (1b) to Figure (1c).

Switching the stray light correction off (Case A) appears to raise the individual normalized water-leaving radiances, leading to lower chlorophyll determination (Fig. 2.1a). So in going from Cases (A) to (B), the numbers of pixels flagged by Flags 8-LOWLW, 15-NEGLW and 24-DARKPIXEL are increased. This probably means that the SeaDAS MSH12 software code is using an aerosol model that removes more aerosol radiance, leaving less water-leaving radiance, perhaps even removing

[1]The black pixel assumption refers to the assumption that the water-leaving radiance is zero for the near-infrared bands, Bands 7 and 8 for SeaWiFS (and Band 6 to a degree). In the presence of chlorophyll over 2 mg m^3, this assumption causes problems in estimation of the aerosol radiance (Siegel et al., 2000).

some water-leaving radiance. From Cases (B) to (C), the numbers of pixels flagged by Flags 8-LOWLW and 15-NEGLW decrease, inferring that some of these flagged pixels are coastal pixels and hence also included in the stray light masked pixels.

Enhanced chlorophyll concentration, associated with the application of the stray light correction (Figs. 2.1b and 2.1c), results in an increase in the number of pixels both where chlorophyll is not calculable (Flag 16-CHLFAIL) and where at least 10 iterations are undertaken in the NIR (near-infrared) algorithm in trying to calculate the chlorophyll concentration (Flag 20-MAXAERITER). The final flag considered in this example is Flag 12-TURBIDW. The flag statistics (Table 2.2) decrease notably from Cases A to B to C as the number of coastal TURBIDW-flagged pixels are increasingly masked by the stray light mask. Subsequent tests showed this flag to be triggered in Benguela high productivity waters by both coastal sediment and also by high chlorophyll concentrations.

Investigation showed that the SeaWiFS stray light correction was derived under laboratory conditions – an on-orbit analysis has not been performed. Also, operational processing parameters are generally determined in the lower end of the chlorophyll range, as is more applicable to the global dataset. Hence, a minor error in the correction of individual water-leaving radiances in low chlorophyll waters may manifest as a large over-correction in high chlorophyll water radiances, resulting in significantly enhanced chlorophyll concentrations. Using such in any analysis of the Benguela ecosystem could lead to erroneous results. After running a number of tests together with the SeaWiFS Project, it was agreed that more accurate chlorophyll concentrations are obtained in Benguela waters with the stray light correction switched off[2].

A downside to this approach is an increase in cloud edge contamination: cloud edges have stray light, but not always a coastal influence. Extensive testing and manipulation of flag thresholds and masks was undertaken to determine the primary changes related to cloud edge when the stray light correction was switched off. These showed that, in Benguela waters, the primary differences related to cloud edge manifest in Flags 14 – HITAU, 15-NEGLW, and 23- ATMWARN (Table 2.1). Further work followed and improved thresholds were determined for triggering these flags, while minimally impacting good data. Additionally, masking of data triggered by the HITAU flag – the maximum

[2] There is a suspicion that switching the stray light correction off compensates for another problem in making coastal retrievals in high productivity Benguela waters. However, for the global dataset, the operational stray light correction is presently the best available correction for the real effect of stray light and is still optimal for global open ocean waters (Wayne Robinson, SeaWiFS Project, NASA, *pers comm.*).

aerosol optical depth at 865nm – was activated. (This mask is not generally activated in operational processing - reference Table 1.)

A number of further operational parameters were similarly tested and manipulated for optimal application to Benguela waters, the detail of which is not included in this thesis but listed as: Total radiance above the knee in Bands 7 and 8 (Flag 5, Table 2.1), low water-leaving radiance at 555nm (Flag 15, Table 2.1), the application of filter kernels (Flag 27, Table 2.1), the dilation of the cloud mask, the application of the absorbing aerosol index (Flag 18, Table 2.1), the maximum number of iterations in the NIR (near infrared) algorithm (Flag 20, Table 2.1), application of the coccolithophore flag (Flag 10, Table 2.1; Chapter 4), and the values for application of the Epsilon flag (Flag 23, Table 2.1).

Also, to date meteorological and ozone climatology had been used during local processing for the atmospheric correction (due to problems of transfer of near-realtime ancillary data). However, analysis showed that this frequently led to erroneous and contaminated products. This was particularly notable in the Namibian region coincident with offshore wind at which times dust plumes may extend considerable distances offshore causing severe atmospheric contamination. Additionally, it was determined that ozone concentrations can vary considerably day-by-day during particular seasons at these regional latitudes. Hence, the operational default application of the closest EPTOMS (Earth Probe Total Ozone Mapping Spectrometer) satellite data for short-term EPTOMS outages may result in chlorophyll concentration increases by up to a factor of two at certain locations. This is illustrated by Figure (2.3) showing global TOVS (TIROS Operational Vertical Sounder) ozone concentration for 11 to 13 August 2002 and EPTOMS ozone for 13 August 2002. The day-to-day variation of ozone is particularly noticeable in the TOVS data, just to the south of the African continent. A short-term EPTOMS outage occurred during this time and by default, the EPTOMS data of the 13 August was applied to the atmospheric correction for 11 August 2002 resulting in substantially enhanced chlorophyll concentrations (not shown). It was subsequently determined that, at these regional latitudes, a much-improved result is achieved by using the TOVS satellite data of the day rather than the closest EPTOMS data, during short-term EPTOMS outages. (This would not be the case for equatorial regions, SeaWiFS Project, *pers comm.*)

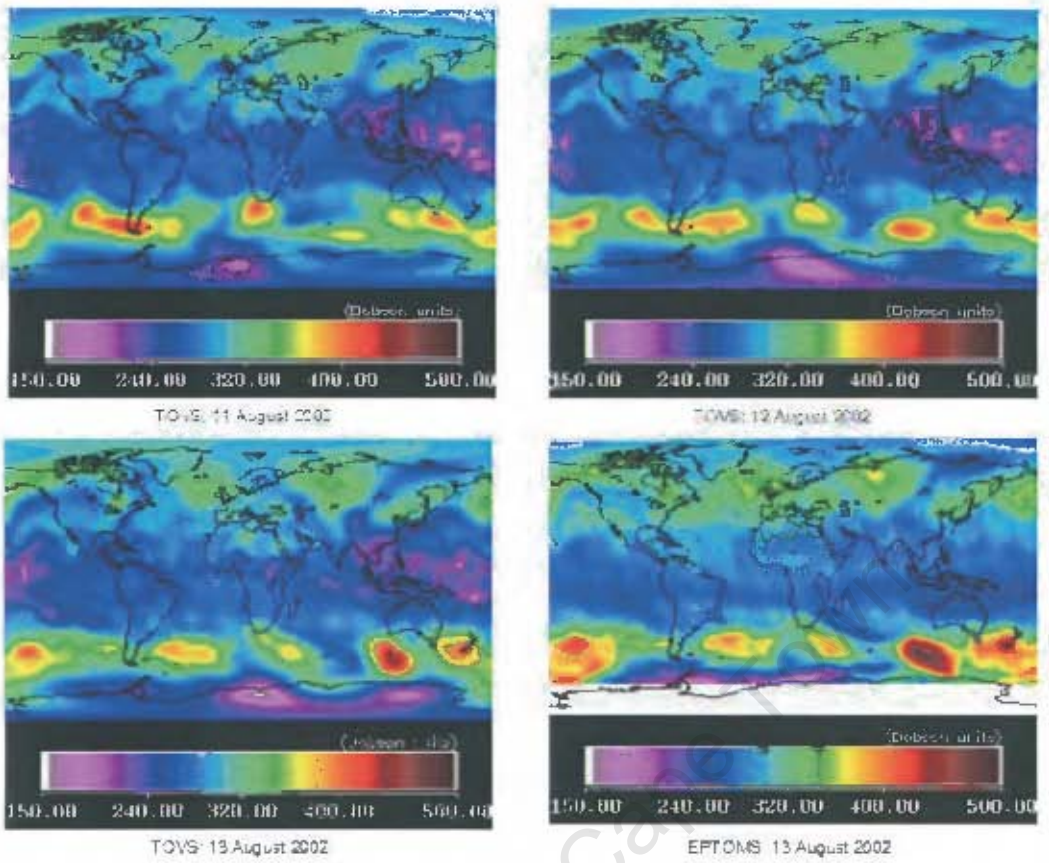

Figure 2.3. Global TOVS ozone concentration for 11 to 13 August 2002 and EPTOMS ozone for 13 August 2002.

3. Results and summary

The optimal SeaWiFS processing parameters for Benguela waters (hereafter referred to as Benguela parameters) were thus determined, and tested locally. The selected parameters for level-1 to level-2 (MSl12) processing are tabulated in Table 2.3, being an excerpt of Appendix 2.2, and including only specific parameters relevant to processing of SeaWiFS data for Benguela waters. Additionally, the selection of ancillary data for the atmospheric correction was set such that, should EPTOMS data be unavailable for any one day, TOVS data for that day will be used rather than the closest EPTOMS data.

Table 2.3. MSI12 control parameters for Benguela waters. Departures from the SeaWiFS standard operational parameters are in bold text.

Keyword	Definition	Benguela waters
l2prod1	Level-2 products to be generated	**chlor_a; K_490; l2_flags; nLw_412; nLw_443; nLw_490; nLw_510; nLw_555; nLw_670**
spixl	start pixel number	**101**
epixl	End pixel number	**1185**
dpixl	pixel subsampling interval	1
dline	Line subsampling interval	1
ctl_pt_incr	control-point pixel increment for lon/lat arrays	**8**
Proc_ocean	turn-on/off all ocean-specific processing (1=on)	1
atmocor	turn-on/off atmospheric correction processing (1=on)	1
aer_opt	aerosol mode option -3: Multi-scattering with 765/865 Gordon-Wang model selection and NIR iterative NIR correction.	**-3**
aer_iter_max	Maximum number of aerosol iterations	**10**
glint_opt	correct for residual glint radiance (1: On)	1
foq_opt	perform f/Q correction (0: Off)	0
outband_opt	Out-of-band corrections 2: full correction (nLw, Lw, La, Lr)	2
oxaband_opt	SeaWiFS 765nm band Oxygen correction (1: On)	1
filter_opt	filtering input data option (1: On)	**1**
met1	1st meteorological ancillary data file	**Syyyyddd06_NCEP.MET (06h00)**
met2	2nd meteorological ancillary data file	**Syyyyddd12_NCEP.MET (12h00)**
met3	3rd meteorological ancillary data file	**Syyyyddd12_NCEP.MET (12h00)**
ozone1	1st ozone ancillary data file	**Syyyyddd12_EPTOMS.OZONE of day -1**
ozone2	2nd ozone ancillary data file	**Syyyyddd12_EPTOMS.OZONE of day**
ozone3	3rd ozone ancillary data file	**Syyyyddd12_EPTOMS.OZONE of day**
vcal_opt	Vicarious calibration option controls 0=defaults	0
offset	calibration offset adjustment	[0.0,0.0,0.0,0.0,0.0,0.0, 0.0,0.0]
gain	calibration gain multiplier	[1.0,1.0,1.0,1.0,1.0,1.0,1.0, 1.0]
albedo cloud_thresh	cloud reflectance threshold	0.027
glint glint_thresh	Sun glint threshold	0.005
absaer	Absorbing aerosol threshold on aerosol index.	**0.5**
sunzen	sun zenith angle threshold (deg)	75.0
satzen	satellite zenith angle threshold (deg)	**58.0**
epsmin	minimum epsilon to trigger atmospheric correction failure flag.	**0.70**
epsmax	maximum epsilon to trigger atmospheric correction failure flag.	1.35

Keyword	Definition	Benguela waters
tauamax	maximum 865 aerosol optical depth to trigger hitau flag	**0.25**
nlwmin	Minimum nLw(555) to trigger low Lw flag.	**0.16**
wsmax	windspeed limit on white-cap correction.	8.0 m/s
maskland	land masking (1: On)	**1**
maskbath	shallow water masking (0: Off)	0
maskcloud	cloud masking (1: On)	1
maskglint	glint masking (1: On, 0: Off)	0
masksunzen	large sun zenith angle mask option (1: On)	**1**
masksatzen	large satellite zenith angle mask option (1: On)	**1**
maskhilt	high Lt masking (1: On, 0: Off)	**0**
maskstlight	stray light masking (1: On, 0: Off)	**0**
st_frac	Lt 865 threshold for stray-light correction	0.25
st_pixl	number of pixels over which stray-light correction is applied.	**0**

Further, in the generation of the daily level-2 to level-3 product (Appendix 2.1), the flags selected for masking are tabulated in Table 2.4. Both the standard operational masking and that selected for Benguela waters are listed. In the masking parameter, departures from the standard operational processing are listed as:

1. STRAYLIGHT mask off.
2. COCCOLITH mask off - include the "coccolithophore" flagged data.
3. HITAU mask on - to improve removal of cloud edge contamination. Note the flag threshold was changed from 0.3 to 0.25 (Table 2.3).
4. NAVWARN mask off - keep the sensor "change of tilt" data range.
5. ABSAER mask off - generally keep the absorbing aerosol-like data. However, this mask is activated at times of strong atmospheric dust contamination.
6. MAXAERITER mask off - keep data that does not converge to a final chlorophyll value.

Also,

7. the ATMWARN mask is on, as for the standard processing, but data with epsilon values down to 0.7 will be included, instead of the default minimum value 0.85 (Table 2.3).
8. the LOWLW mask is on, as for the standard processing, but data with nLw_555 values above 0.16 will be included, instead of the default 0.15 (Table 2.3).

Table 2.4. Masks selected for Benguela level-2 to level-3 processing relative to masks for the current operational SeaWiFS level-2 to level-3 processing. The mask in columns indicate that no geophysical data is created in the level-3 (L3) data product for the particular flag conditions marked ON for that observation. The mask changes from the operational processing are marked as OFF.

Flag no	Flag Name	Standard Mask in L3	Description	Benguela Mask in L3
1	ATMFAIL	ON	Atmospheric algorithm failure	ON
2	LAND	ON	Land	ON
3	BADANC		Missing ancillary data	
4	HIGLINT		Sun glint contamination	
5	HILT	ON	Total radiance above the knee	ON
6	HISATZEN	ON	Satellite zenith angle above the limit	ON
7	COASTZ		Shallow water	
8	NEGLW		Negative water-leaving radiance in Bands 7 and 8	
9	STRAYLIGHT	ON	Stray light contamination	OFF
10	CLDICE	ON	Clouds or ice	ON
11	COCCOLITH	ON	Coccolithophore bloom	OFF
12	TURBIDW		Turbid, Case-2 water	
13	HISOLZEN	ON	Solar zenith angle above the limit	ON
14	HITAU	OFF	High aerosol concentration	ON
15	LOWLW	ON	Low water-leaving radiance at 555nm	ON
16	CHLFAIL	ON	Chlorophyll not calculable	ON
17	NAVWARN	ON	Questionable navigation (tilt change)	OFF
18	ABSAER	ON	Absorbing aerosol index above the threshold	OFF *
19	TRICHO		Trichodesmium bloom condition	
20	MAXAERITER	ON	Maximum number of iterations in the NIR algorithm	OFF
21	MODGLINT		Glint corrected measurement	
22	CHLWARN	ON	Chlorophyll is out of range	ON
23	ATMWARN	ON	Epsilon value outside of reasonable range or Lw at 490, 510 or 555nm is less than zero	ON
24	DARKPIXEL		Rayleigh corrected radiance is less than zero for any band	
25	SEAICE		Sea ice present based on climatology	
26	NAVFAIL	ON	Navigation of the line is bad	ON
27	FILTER	ON	Insufficient surrounding pixels for aerosol model filter	ON
28-31		N/A	Spare for future use	N/A
32	OCEAN		Ocean data	

OFF *: When atmospheric contamination due to offshore dust is marked, the ABSAER mask is activated.

3a. Satellite Validation

In situ chlorophyll data from cruises undertaken in Benguela waters was compiled for the purpose of validating the Benguela processing parameters relative to the standard default processing. Data from the following cruises was included:

The *Atlantic Meridional Transect Cruise* from 15 – 25 May 1998
The *Meteor Cruise* from 26 – 28 October 2000
The *Benefit Cruise* from 16 – 21 February 2002
The *BenCal Cruise* from 24 – 27 October 2002

All potential match-up data was sorted. Since no *in situ* radiance data was available, total *in situ* chlorophyll was integrated over the top 10 metres. The 10 metre depth was selected as the average upper mixed layer in Benguela waters, on the basis of *in situ* temperature and chlorophyll profiles (R. Barlow, M&CM, Cape Town, *pers comm.*). The corresponding satellite data was located, extracted and processed using both the standard default parameters and the Benguela parameters. Where HRPT SeaWiFS data was not available, lower resolution (GAC, 4.5km) data was substituted instead. Working with the SeaWiFS Project, the following constraints were applied: For the *in situ* data, sampling must have occurred (1) +/- five hours of the SeaWiFS overpass, and (2) between 9am and 3pm local time. For the SeaWiFS data, a 3x3 pixel box was centred over the *in situ* location and the following constraints applied: (a) 50% of the ocean pixels needed to be valid, and (b) the median and absolute coefficients of variance of the water leaving radiances at 412nm, 443nm, 490nm, 510nm and 555nm needed to be less than 0.15. Having applied these exclusion criteria, only a total of 24 records remained, the detail of which is included in Appendix (2.3). Lower resolution SeaWiFS data (GAC) was required to validate four of these cruise records (*AMT cruise*, 1998). SeaWiFS derived chlorophyll was correlated with *in situ* integrated chlorophyll for both the standard default processing and the Benguela processing, as is shown in Figure (2.4). The associated statistics are provided in Table (2.5). No statistically significant difference is apparent although the results from the Benguela processing appear to be marginally better. In particular, a difference is noted in the 'bias', which provides a general tendency, a bias of zero indicating a perfect correlation. For this correlation,

bias = sum (SeaWiFS chlor [i] - *in situ* chlor [i]) / 24 records.

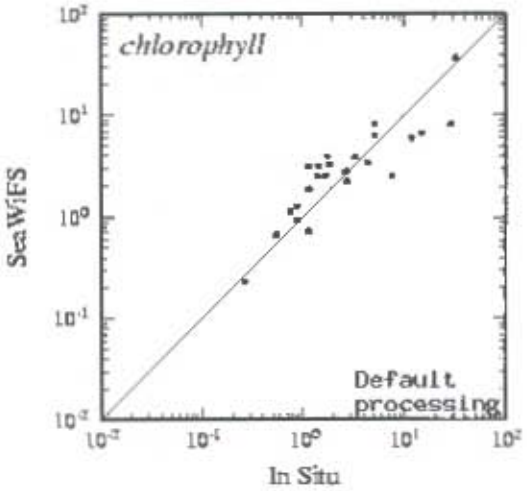

Figure 2.4a.

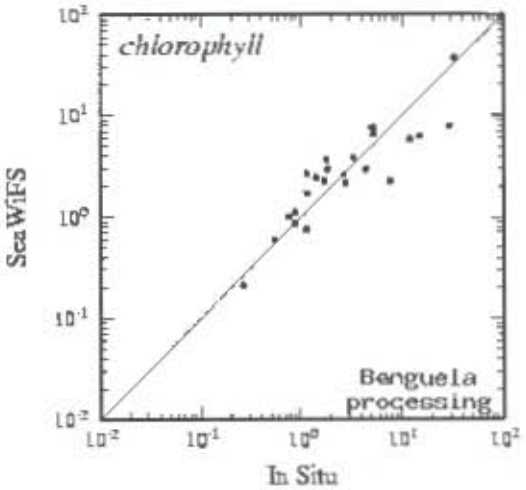

Figure 2.4b.

Figure 2.4. Correlation of SeaWiFS derived chlorophyll with *in situ* integrated chlorophyll for (a) the standard default processing and (b) Benguela processing.

Table 2.5. Correlation statistics for Figure (2.4).

(a) Default processing

Band	Median Ratio	Median %Diff	%Diff StDev	N	In Situ Range	Satellite Range
chlorophyll	1.2063	49.2515	41.8862	24	[0.26200 32.18050]	[0.22914 36.59005]

Slope statistics for chlorophyll

Slope	intercept	r^2	bias	RMsq
0.8354	0.2329	0.7999	0.0823	0.5258

(b) Benguela processing

Band	Median Ratio	Median %Diff	%Diff StDev	N	In Situ Range	Satellite Range
chlorophyll	1.1623	34.8500	32.8540	24	[0.26200 32.18050]	[0.20937 36.68364]

Slope statistics for chlorophyll

Slope	intercept	r^2	bias	RMsq
0.8686	0.1307	0.8148	0.0036	0.5217

Hence, a bias of 0.0036 for the Benguela processing relative to a bias of 0.0823 for the standard default processing suggests that chlorophyll derived from the former tends to be more closely correlated with the *in situ* integrated chlorophyll. Nonetheless, the number of records available for the statistical analysis was extremely limited and disparate, the 24 records having been sampled at various locations throughout the northern and southern Benguela over an almost five year period. Amongst these, less than half were located close inshore where more notable improvements would be expected using the Benguela parameters. It is hoped that in time, more extensive *in situ* sampling will be undertaken in these regional waters for the purpose of improved validation and calibration of regional ocean colour products. An initial limited validation was in fact possible in April 2003 when both *in situ* and SeaWiFS chlorophyll as well as individual normalized water-leaving radiances were sampled during an unusual event in southern Benguela waters. This is discussed in detail in Chapter 4.

3b. Generation of time series

During the ensuing many months, a full reprocessing of local SeaWiFS HRPT data was undertaken. The following daily products were generated: normalised water-leaving radiances at 443nm, 490nm, 510nm, 555nm, the attenuation coefficient (K_490), chlorophyll *a* concentration. Chlorophyll *a* concentration was output as byte format, calibrated according to the log scale:

chlor = 10 ^ (0.015 * byte value -2.000).

Additionally, 24-bit, quasi-true colour composites were generated from the SeaWiFS calibrated and Rayleigh-corrected radiances at 670, 555, and 412 nm (Bands 6, 5 and 1, respectively)[3]. Finally, consistent HRPT time series of both SeaWiFS chlorophyll *a* concentration and NOAA AVHRR sea surface temperature were generated for the period July 1998 through June 2003. The products were projected to a cylindrical equirectangular projection such that each pixel represents 0.0104° of latitude and longitude.

In closing, it is recognized that no one set of parameters is perfect for each individual day's data within a longterm time series. However, optimal parameters for regional waters were selected such that the gain in good data would far outweigh limited contamination that might result due to relaxation of specific parameters, or further changes implemented. Similarly, a conscious decision

[3] The code used to produce the quasi-true colour images was provided by Norman Kuring and the SeaWiFS Project.

was taken to include data where constituents other than chlorophyll at times contribute significantly to the in-water light field. Two examples of such, namely precipitated sulphur and coccolithophore blooms, are discussed in detail in Chapters 3 and 4. Depressed satellite-derived chlorophyll estimates result in both these cases. However, it was felt that it would nonetheless be a better reflection of the true scenario than to remove all affected data, and hence perhaps result with artificially enhanced mean chlorophyll concentrations. Caution should therefore be exercised in using time series data for the event scale phenomenon. For this reason, the associated quasi-true colour images were generated for each day within the five year time series, such that they may be used in the interpretation of such. For the event scale, SeaWiFS data should be processed with modification of specific parameters should any unusual feature or constituent be visible in a quasi-true colour image.

In the chapters to follow, Chapters 3 and 4 document specific event scale qualitative applications of satellite data, namely hydrogen sulphide eruptions in northern Benguela waters and an unusual coccolithophore bloom in the southern Benguela, while Chapters 5 and 6 focus on a quantitative analysis of the NOAA AVHRR and SeaWiFS time series data for the southern Benguela. In documenting the evolution of the coccolithophore bloom in Chapter 4, quasi-true colour imagery from the more recently-launched Moderate-Resolution Imaging Spectroradiometer (MODIS) onboard NASA Terra and Aqua satellites was also used[4]. These quasi-true colour images were generated from MODIS Bands 1, 4 and 3 (centred at 645nn, 555nm and 469nm, respectively). With a resolution of 250m (Band 1) and 500m (Bands 4 and 3), the higher resolution allowed for a more detailed analysis of the event.

[4] Provided by the Modis Rapid Response Team

Chapter 3

Hydrogen sulphide eruptions in the Benguela ecosystem: Implications of a new view based on SeaWiFS satellite imagery

1. Introduction

Within the Benguela ecosystem, it is the northern Benguela that features by far the more intense upwelling, its highest intensity core located near Lüderitz. The associated very rapid offshore transport of the ocean surface layer has major consequences to the ecology of this system. Planktonic grazing organisms may have difficulty maintaining significant populations near the upwelling zone. This, together with the high rate of downstream primary production, produces a situation along the Namibian central coast where vast numbers of phytoplankton cells appear to sink unutilized to the sea floor. The net result of the accumulation of large amounts of unoxidized organic matter on the continental shelf is the existence of extensive areas of sea floor hypoxia (<0.5 ml O_2 l^{-1}), and even total anoxia, beneath which poisonous hydrogen sulphide and methane gas are generated within the diatom sludge (Emeis et al., 2002).

Nearshore hydrogen sulphide eruptions are familiar occurrences along the central coast of Namibia. In addition to its direct toxic impact, hydrogen sulphide has the secondary effect of depleting oxygen from the water, so that extensive surrounding areas suffer from severe hypoxia and anoxia. Yet, in spite of major effects ascribed to anoxic episodes, the conventional view has been that the sulphide-laden eruptions that are observed from the shore in this region are very local features and thus must have only rather limited ecosystem-scale consequences. This is because observations until recently have been land bound and without broad coastwise coverage. But, as is documented in this chapter, it is now possible to identify and monitor such anoxic phenomena using high resolution (1km) ocean colour satellite data. This newly-discovered capability appears to have altered the conventional view. Furthermore, the pattern of occurrences seems to imply a new, very different mechanism to be added to those earlier suggested (e.g., Bubnov, 1972; Chapman and Shannon, 1987) as being primarily responsible for widespread anoxic conditions over the continental shelf (Bailey et al., 1985), and for such extreme anoxic episodes as those thought to have decimated the Cape hake population during 1993-94 (Woodhead et al., 1998, Hamukuaya et al., 1998). In this chapter, example sequences of SeaWiFS images are presented to indicate eruption types that are observed and to support discussion

of potential eruption mechanisms. Certain methodological problems in interpreting effects on local productivity are outlined. Connotations of these phenomena to the local ecology are discussed. This chapter comprises work undertaken during 2001-2003 and published in *Nature* and *Deep-Sea Research* (Weeks et al., 2002, Weeks et al., 2004a).

2. Methodology

The remote sensing methodology relies upon the peculiar milky turquoise discolouration of the water that occurs consistently during hydrogen sulphide eruption episodes. This "milky water" is created by a slurry of highly reflective precipitated micro-granules of sulphur resulting from oxidation of sulphide ions near the oxygenated sea surface (B.B. Joergensen, pers. comm.[5]) The discolouration of the sea surface can be identified in quasi-true colour composites (designated by the label "TC" in Figs. 3.1 to 3.4 and in the associated discussions) generated from the Orbview-2 SeaWiFS sensor. The 24-bit, quasi-true colour images are composed of logarithmically-scaled, Rayleigh-corrected, surface reflectances (Vermote and Tanre, 1992) at 670nm, 555nm, and 412 nm (SeaWiFS bands 6, 5 and 1, respectively)[6].

Identification and monitoring of the evolution of these events from the SeaWiFS sensor has been limited, severely at times, by other factors in addition to those generally encountered, such as cloud and fog. For example, (1) coverage is restricted because the closest HRPT (High Resolution Picture Transmission) station is far east of Namibian waters, (2) broad latitudinal "stripes" of data are lost because the SeaWiFS sensor tilt occurs directly over these waters during the austral summer months (the period during which hydrogen sulphide eruptions are traditionally considered to occur more frequently), and (3) acute sunglint, which similarly severely impacts data quality from this region during austral summer, introduces a further complication.

Chlorophyll a concentration was determined with the SeaWiFS Data Analysis System (SeaDAS) and the OC4v4 bio-optical algorithm (O'Reilly et al., 2000). This fourth order polynomial equation uses a maximum band ratio:

$$C_a = 10.0 \exp (0.366 - 3.067R_{4S} + 1.930R_{4S}^{\ 2} + 0.649R_{4S}^{\ 3} - 1.532R_{4S}^{\ 4})$$

[5] B. B. Joergensen, Max Planck Institute for Marine Microbiology, Germany
[6] The code used to produce the quasi-true colour images was provided by Norman Kuring and the SeaWiFS Project. NASA.

where $R_{4S} = \log_{10}(R^{443}_{555} > R^{490}_{555} > R^{510}_{555})$, and in R_{4S}, the numerical part denotes the number of bands used and S, the SeaWiFS sensor. The argument of the logarithm represents the maximum of the three values, each being a ratio of SeaWiFS normalized water-leaving radiances at the specified wavelengths. Sea Surface Temperature (SST) images were generated from the daytime NOAA AVHRR data using the standard multichannel SST algorithm (McClain et al., 1985). Further aspects of both the SeaWiFS and NOAA AVHRR processing are detailed in Chapter 2.

A methodological problem (chlorophyll estimation)

The extreme reflectivity of the sulphur particles at the sea surface interferes with the SeaWiFS chlorophyll estimation. Not only are the radiances used in the bio-optical algorithm affected by the very high reflectivity, but the radiances used in the atmospheric correction process are also likely to be adversely affected by the reflectivity of the sulphur granules. At locations where the sulphur signal is intense (as identified in quasi-true colour composites), the SeaWiFS chlorophyll algorithm is unable to retrieve any chlorophyll value at all, be the location coastal or offshore, because of extreme reflectivity and scattering (SeaDAS Flag 5: "total radiance greater than the knee value" being applicable to these pixels). Where the sulphur signal is less intense, the pixels are flagged in the same way as they would be for coccolithophore blooms (SeaDAS Flag 11), even though *in situ* sampling may have confirmed the water discolouration as being due to precipitated sulphur. Examination of the individual normalized water-leaving radiances (nLw) reveals high values at these locations, with values of nLw 490nm and nLw 510nm approximately equal to or exceeding that of nLw 555nm. Since the algorithm uses band-ratios with the denominator, nLw 555nm, assumed to be relatively stable, the presence of precipitated sulphur, producing a significant contribution at 555nm, will tend to yield erroneous (depressed) estimates of chlorophyll_a. The chlorophyll bio-optical algorithm becomes unreliable in water where precipitated sulphur contributes significantly to the in-water light field.

3. Results

In the following sections, sequences of images assembled during several different hydrogen sulphide eruption episodes of somewhat contrasting types, are examined. These were selected from a recent event history (March 2001 to March 2002). Table (3.1) catalogs the more prominent episodes observed during this period. These examples are used to illustrate the range of characteristics

encountered to date, and to draw inferences as to the causes of the eruptions and the mechanisms that may trigger them.

Example: Mar-Apr'01 - eruption in the upwelling zone, with subsequent advection

At mid-March 2001, moderate upwelling conditions appear to have characterized the situation along the south-central Namibian coast. The composite false-colour sea surface temperature (SST) image for 15-16 March (Fig. 3.1a) shows recently upwelled cold waters, indicated by the blue-coloured zone abutting the coast near Lüderitz. From this zone, a large plume of relatively cool, upwelling-conditioned surface water extends northward and offshore from the zone of strongest upwelling. Shortly thereafter, in the partially cloud-obscured image of 17-18 March (Fig. 3.1b), a rapid intensification of upwelling has clearly commenced. Although the northern part of the SST image for 19-20 March (Fig. 3.1c) is totally obscured, the effect of this intensification in cooling the coastal area and in transporting cooler, upwelling-conditioned waters northwestward is clearly evident. In an SST image four days later (Fig. 3.1d), temperatures over the area had returned to generally the same levels as in panel (a) although those in the warm tongue that appears to be thrusting southward near the coast from the top of the image had diminished considerably.

Table 3.1. Sequence of definitive SeaWiFS-observed hydrogen sulphide events during the period 1 March 2001 to 31 March 2002.

Event #; date first noted; last date of visible remnant; location (maximum area)	**General evolution of event. (If ground-level validating observations are available, cross-reference to information as to their nature presented in Table 2 is indicated in bold type as "VALID. #".)**
1. 12 March 2001 - 8 (20) April 2001 23.2°S–26.6°S (22000 km^2) **(Described: Section 3)**	Precusory localised inshore emissions between Luderitz and Meob Bay (24.5°S – 26.6°S) on 12 and 13 March 2001 coincident with moderate upwelling in the south. Upwelling and emissions dissipated by 16 March as tongue of warm subtropical waters extended southwards of 24°S. Evolved to massive eruption from Luderitz to Conception Bay on 18 March, coincident with intensified upwelling. Upwelling subsided after 21 March. The feature advected northward and offshore to extend over an area ~20000km^2. **VALID. # 1**
2. 2 April 2001 - 20 April 2001 24.6°S–26.7°S (2400 km^2)	Abrupt new inshore eruption between Luderitz and Meob Bay coincident with intensified upwelling, while earlier offshore feature maintained coherent signal. The two features linked by connecting filament on 8 April. Thereafter, appeared to be entrained into offshore filament extending 250km offshore at ~ 25.5°S. **VALID. # 2**
3. 5 May 2001 - 7 May 2001 19.0°S–25.7°S (4200 km^2)	Small localised coastal emissions between Pelgrave Pt and Meob Bay (20.5°S – 24.5°S) on 5 May coincident with initiation of upwelling. Emissions extended alongshore from Mercury Is. to Rocky Pt. (19°S–25.7°S) with intensified upwelling along entire coast on 6 May. Coastal emissions seemed apparent farther southward on 7 May whereafter coastal wind-borne desert dust precluded clarity of the signal.
4. 15 May 2001- 6 June 2001 20.5°S– 25.5°S (11500 km^2) **(Described: Section 4)**	Localised "blob" eruption appeared offshore and to south of Hentjies Bay (~22.4°S) on 15 May, expanding to about 3000 km^2 in days to follow. Event coincident with cessation of upwelling from 15 – 20 May. Puffs of sulphur occurred off Walvis Bay (23.0°S) & Sandwich Harbour (23.3°S) on 22 May coincident with initiation of upwelling. Coastal emissions extended alongshore and appeared to be entrained into offshore "blob". Upwelling subsided 24 and 25 May as did coastal emissions while offshore blob maintained its identity just northward and offshore of inshore cooler waters. Fresh upwelling 26-31 May extended along the entire Namibian coast while inshore sulphide emissions extended from Sylvia Hill to Cape Cross (25.3°S-22.8°S) Interaction between in- and offshore emissions notable by entrainment offshore ~21.5°S, while offshore signal continued to expand southward & seaward of upwelled water boundary. Coastal emissions extended as upwelling continued into early June. Coastal emissions dissipated after 5 June at which time offshore blob covered over 7000 km^2 of ocean surface. Thereafter offshore signal dispersed.
5. 29 June 2001 - 6 July 2001 18.8°S–24.0°S (4200 km^2)	Intense sulphide eruptions extended along coast from Conception Bay to Cape Cross (18.8°S – 20. 0°S) with less intense emissions further north (21.5°S – 24.0°S) on 29 & 30 June following extensive upwelling from 25 June. Atmospheric interference (dust, cloud) on 1 – 4 July precluded SeaWiFS data clarity. Intense clear sulphur signals again evident on 5 and 6 July from Sandwich Harbour to Tascanini (21.3°S – 23.7°S) while signal further north remained obscured. Thereafter, atmospheric interference limited data clarity.
6. 17 August 2001 - 22 August 2001 20.2°S – 23.2°S (3500 km^2)	Intense coastal sulphide eruption from Sandwich Harbour north to Tascanini on 17 August, coincident with upwelling along the full extent of the Namibian coast. Emissions extended both north- and southward in following days but clarity of sulphur signal questionable beyond 22 August due to sediment in the water column.
7. 27 October 2001 - 8 November 2001 24.3°S –25.4°S (8000 km^2) **(Described: Section 5)**	Sulphide eruption seemingly from a point source just offshore of Sylvia Hill (~25.3°S) and just north of cooler 14°C waters. No discolored water inshore on previous 2 days. Signal expanded offshore and northward in sluggish current drift to cover area of ~7200 km^2 on 31 October before being displaced somewhat offshore with initiation of moderate coastal upwelling. Further expansion and dispersion of signal as moderate coastal upwelling continued into early November.
8. 20 November 2001- 22 November 2001 25.0°S –26.4°S (5200 km^2)	Strong offshore sulphur signal on 20 November between 25°S –26.4°S coincident with sudden initiation of coastal upwelling following dense cloud and cessation of upwelling over previous week. Discolored water displaced offshore of freshly upwelled coastal waters and composed of two separate blobs linked by a filament. Signature consistent 20-22 November. No useable SeaWiFS data for week prior to and post these 3 days -dense cloud/sensor tilt/no coverage.

9. 1 December 2001 - 4 December 2001 22.5°S –23.4°S (400 km^2)	No sulphur signal detected in SeaWiFS data of 30 November. SeaWiFS sensor tilt occurred over area of interest on 1 and 2 December. No HRPT SeaWiFS data for this region on 3 December. Signal evident on 4 December close inshore from Sandwich Harbour to north of Walvis Bay – assumed to be remaining emission event. Region was masked by cloud or sensor tilt until 9 December at which time no signal was evident. **VALID. # 9**
10. 8 January 2002 - 9 January 2002 21.8°S –25.3°S (3800 km^2)	Sulphide emissions on 8 January from Sylvia Hill northward to Cape Cross following intensified upwelling on 7 and 8 January (no SeaWiFS coverage on 6 and 7 Jan). Emissions evident between cloud on 9 January. Subsequent data for January severely affected by sensor tilt and sunglint – evolution of event uncertain.
11. 6 February 2002 8 February 2002 23.0°S –25.7°S (4000 km^2) (Described: Section 6)	Moderate upwelling southward of Mercury Is. on 4 – 6 February. Localised sulphide emissions on 6 February northward of Mercury Is. (SeaWiFS data cloudy 4 and 5 February). Intense inshore sulphide emissions on 7 February from Mercury Is. northward to Walvis Bay, coincident with intensified upwelling. Emissions partly masked by thick fog on 8 February Event no longer evident in next clear data on 11 February. **VALID. # 11**
12. 13 February 2002 15 February 2002 21.8°S –25.7°S (3000 km^2) **(Described: Section 6)**	Concurrent with initiation of upwelling, a precursory sulphide emission noted on 13 February ~Mercury Is. (25.7°S), the locale coincident with the boundary of freshly upwelled waters. Strong sulphide emissions extended northward to Walvis Bay on 14 February reaching Cape Cross by 15 February, as upwelling moderated in the south and extended northward along the coastal boundary beyond Walvis Bay. **VALID. # 12**
13. 3 March 2002 8 March 2002 23.5°S –27.3°S (3000 km^2)	Strong inshore sulphide emissions from Mercury Is. northward on 3 and 4 March (no data on 2 March), coincident with initiation of moderate upwelling in vicinity and to the south of Mercury Is. Sulphide emissions extended southward of Luderitz to ~ 27.2°S by 7 and 8 March following subsidence of moderate upwelling and considerable cloud cover. **VALID. # 13**
14. 15 March 2002 16 March 2002 24.1°S –25.9°S (2600 km^2)	Moderate upwelling again on 13-15 March southward of 26°S with sulphide emission on 15 & 16 March to the north of 26°S (no data on 14 March).
15. 19 March 2002 22 March 2002 23.0°S –24.4°S (2600 km^2)	Following subsidence of both upwelling and sulphide emissions 17 – 18 March, sulphide emissions resurged on 19 and 20 March (no data on 21 March) coincident with strong upwelling on 19 – 21 March. Sulphur signal dissipated after 22 March as did upwelling. **VALID. # 15**
16. 26 March 2002 29 March 2002 22.9°S –26.7°S (2500 km^2)	Strong upwelling from 22°S –29°S on 27 – 30 March. Precursory sulphide eruption north of Mercury Is. on 26 March, extended northward to Walvis Bay on 27 March. Less intense emissions between Walvis Bay and Luderitz by 29 March (no data on 28 March) whereafter sulphur signal dissipated. **VALID. # 16**

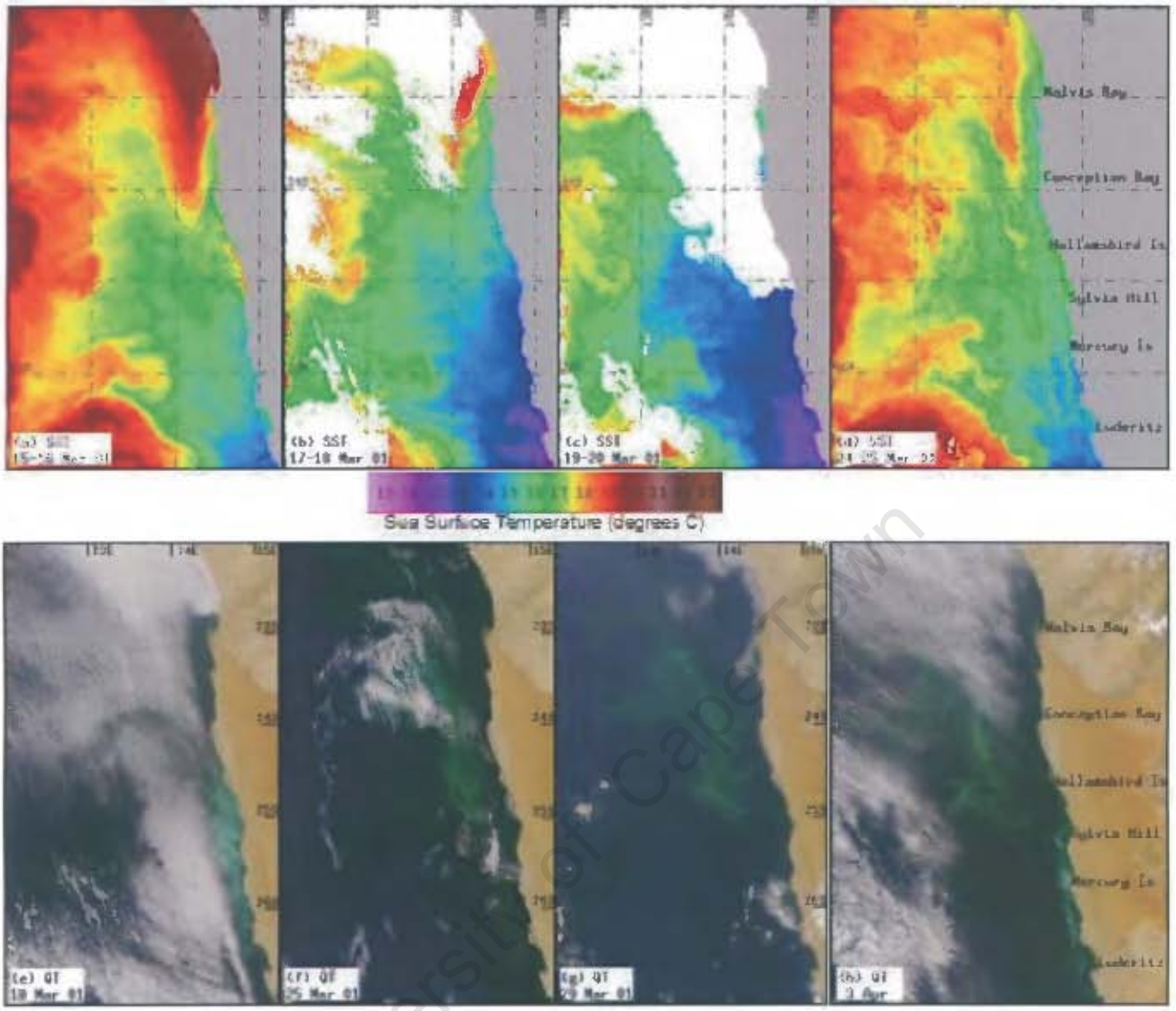

Figure 3.1. NOAA AVHRR false-colour SST and SeaWiFS quasi-true colour (TC) images for the region long 12°E-16°E; lat 22°S-27°S during the period March-April 2001. (a) SST 15-16 March; (b) SST 17-18 March; (c) SST 19-20 March; (d) SST 24-25 March; (e) TC 18 March; (f) TC 25 March; (g) TC 29 March; (h) TC 3 April. The area of milky turquoise colouration in panels (e)-(h) indicates high concentrations of suspended sulphur granules in surface waters. (Note that the dates of each of the images shown in the lower row of panels do not necessarily correspond to those of the image directly above.)

In a TC SeaWiFS image for 18 March (Fig. 3.1e), i.e. during the upwelling intensification episode, a massive hydrogen sulphide eruption is evident in the turquoise-coloured patch that stretches more than 200 km along the Namib Desert coast from Lüderitz more than half way to Walvis Bay (Weeks et al., 2002). No such large sulphide outbreak feature had been evident in an image taken two days earlier on 16 March (in that image there had been only small isolated spots of milky colouration localized against the coast; earlier images indicate that these much more minor precursory eruptions seem to have commenced at least as early as 12 March). During the major outbreak, personnel from the Namibian Ministry of Fisheries were able to demonstrate the presence of intense hydrogen sulphide emissions in that zone and to confirm that the peculiar milky turquoise colouration of the

water occurred simultaneously as viewed from the satellite. Dissolved oxygen concentration, even in the surface "milky" water, was found to be very low (0.9 ml l^{-1}), very high values of dissolved hydrogen sulphide were measured in the water column (up to 49.5umol.l^{-1}), and significant values were found even at the sea surface (Table 3.2); the local lobster stock appeared consequently to be forced to occupy an extremely narrow, shallow, inshore zone of distribution.[7]

In the days to follow (Fig. 3.1, panels f & g), the feature is seen to be advected northward and offshore, as well as exhibiting some spreading due to turbulent diffusion. This is as expected in the equatorward geostrophic current flow and offshore-directed surface wind drift fields implied in the evolution of the SST patterns (Fig. 3.1, panels a-c), generally characteristic of such eastern ocean coastal upwelling systems. The zone of rather intense discolouration ultimately extends over an area of ocean surface exceeding 20,000 km^2. Finally, in the TC image of 3 April (Fig 3.1h), even while the earlier feature continues to maintain a coherent identity offshore, another totally new hydrogen sulphide emission event is observed to have abruptly commenced within the coastal upwelling zone north of Lüderitz, coincident with newly intensified upwelling inferred from the SST distribution (not shown).

Example: May-Jun'01: offshore "puff" appearing in a warm interval (upwelling relaxed)

While the example discussed in the preceding paragraphs clearly coincided with an upwelling pulse and exhibited an initial spatial pattern (elongated directly against the coast) typical of upwelling-conditioned surface waters, the next example to be examined - the fourth event in the sequence listed in Table (3.1) - is very different. It appeared not during an upwelling pulse but on the contrary during an interval of cessation of upwelling as indicated by the warm SST distribution shown in Figure 3.2a. Furthermore, the initial indication of a sulphide eruption, the "puff" of discoloured surface water that appears off the coastal bight just north of Walvis Bay (Fig. 3.2e), is well separated from the coast in a position that does not at all match any normally observed or expected upwelling location. Several days later, when upwelling recommenced (Fig. 3.2b) the "puff" feature remained roughly in place (Fig. 3.2f), although appearing to intensify somewhat. The location of the feature does not appear to be under any significant influence of coastal upwelling at this time, although two incipient sulphur plumes (Fig. 3.2f) do appear in local upwelling foci (Fig. 3.2b) located off two headlands immediately to the south of Walvis Bay.

[7] C.A.F. Grobler, Ministry of Fisheries Marine Research Station, Lüderitz, Namibia (pers. comm.)

Table 3.2. Ground-level validation data from opportunistic sampling.

Event # (as per Table 3.1)	Date	Locality	Sample depth [b]	H_2S µmol.l^{-1}	Dissolved Oxygen ml.l^{-1}	Chl a µg.l^{-1}	Elemental Sulphur nM [c]	Observations
1.	17 March 2001	Ichaboe Island 26.29°S 14.94°E	*10m (B)*	<1	1.7	-	-	Milky water surrounding the island from 17-18 March 2001.
		as above[a]	37m (B)	49.5	0	-	-	Very low surface dissolved oxygen values.
		as above[a]	28m (B)	27.9	0	-	-	
			Surface	<1	1.5	-	-	
	18 March 2001	as above[a]	42m (B)	-	0.6	-	-	
		as above[a]	52m (B)	-	0.2	-	-	
		as above[a]	Surface	-	0.9	-	-	
	26 March 2001	Mercury Island 25.7°S 14.83°E	Surface	1.8	-	-	-	Milky water smelling of H_2S.
2.	2 April 2001	as above[a]	10m (B)	4.7	-	-	-	Discoloured water noted on 1 April, extreme milky water conditions persisted for
		as above[a]	Surface	2.4	-	-	-	12 days until 13 April, when H_2S odour was still prominent.
	4 April 2001	as above[a]	Surface	1.3	-	-	-	
		as above[a]	Surface	2.5	-	-	-	
9.	30 November 2001	Swakopmund 22.67°S 14.51°E	Surface	-	6.5	-	-	Preceding day – no odour or discolouration.
	1 December 2001	as above[a]	13m (B)	99.6	0	-	-	Strong smell of H_2S & milky water.
			7m (M)	95.7	0	-	-	Copious H_2S at surface: oxidation
			Surface	17.9	2.2	-	-	not keeping apace with emission
	2 December 2001	as above[a]	15m (B)	88.16	-	-	-	Sample from milky brown water
	2 December 2001	as above[a]	16m (B)	75.3	0	-	-	Strong smell of H_2S; intensely white milky water. Dead small fish at surface
			8m (M)	-	0	-	-	
			Surface	0.6	1.0	-	-	
11.	2 February 2002	Easter Cliffs 25.27°S 14.8°E	9m (B)	2.5	3.3	-	-	Preceding event – no odour or discolouration.
	7 February 2002	Mercury Island 25.7°S 14.83°E	Surface	1.4	-	-	-	*Seabird flocks feeding on dead / dying fish at surface in milky water.*
	8 February 2002	as above[a]	Surface	0.9	-	-	-	Strong smell of H_2S, milky water.
	8 February 2002	Hottentot Point 26.13°S 14.9°E	20m (B)	1.1	-	-	-	
			Surface	2.1	-	-	-	
	9 February 2002	Ichaboe Island 26.29°S 14.94°E	Surface	1.3	-	-	-	
12.	14 February 2002	Swakopmund 22.67°S 14.51°E	15m (B)	63.5	0	--	-	H_2S smell, discoloured milky water.
			Surface	-	0.7	1.4	773	
	14 February 2002	as above[a]	16m (B)	61.2	0	-	-	
			Surface	-	0.8	1.1	874	
	15 February 2002	as above[a]	12m (B)	28.4	0	-	-	Intensely milky water
			5m (M)	1.8	0.6	-	-	
			Surface	0.6	0.4	1.6	1802	
	15 February 2002	as above[a]	(B)	49.1	0	-	-	Intensely milky water
			7m (M)	49.5	0	-	-	
			Surface	-	0.6	1.1	1524	
	15 February 2002	as above[a]	28m (B)	2.4	0	-	-	No noticeable discolouration in surface water at this station.
			14m (M)	<1	0.07	-	-	
			Surface	<1	1.5	3.3	127	
13.	3 March 2002	Mercury Island 25.7°S 14.83°E	Surface	1.4	-	-	-	H_2S smell, discoloured milky water, dying fish
	4 March 2002	as above[a]	Surface	3.4	-	-	-	As above
	4 March 2002	as above[a]	Surface	2.3	-	-	-	As above
	4 March 2002	as above[a]	Surface	3.2	-	-	-	As above
15.	21 March 2002	Ichaboe Island 26.29°S 14.94°E	Surface	<1	33	-	-	Discoloured water, no smell
	21 March 2002	Marshall Rocks 26.35°S 14.97°E	19m (B)	5.7	0	-		Milky water
			Surface	<1	0.4	-	-	
	21 March 2002	as above[a]	22m (B) Surface	-	0	-	-	Flocks of seabirds feeding above discoloured water
				-	1.4		-	
16.	28 March 2002	*Bird Island, 2km north of Walvis Bay*	16m(B)	18.5	0	-	-	Milky water
			8m (M)	1.5	0.09	-	-	
			Surface	<1	0.3	-	-	
	28 March 2002	*Langstrand, 15km north of Walvis Bay*	18m(B)	26.6	0	-	-	Milky water
			9m(M)	1	0.1	-	-	
			Surface	<1	0.3	-	-	

a indicates a new sampling locality, within a 2 km radius of the position given above.

b (B) indicates a sample close to the sediment, (M) a mid-water sample and Surface to samples taken within the first meter of the water column.

c Although limited analyses of milky waters for their elemental sulphur content has indeed demonstrated that they contain polysulphide or elemental sulphur granules, the signal has not yet been calibrated. Toward this end, collaboration with the Max-Planck Institute for Marine Microbiology, Germany, is under discussion.

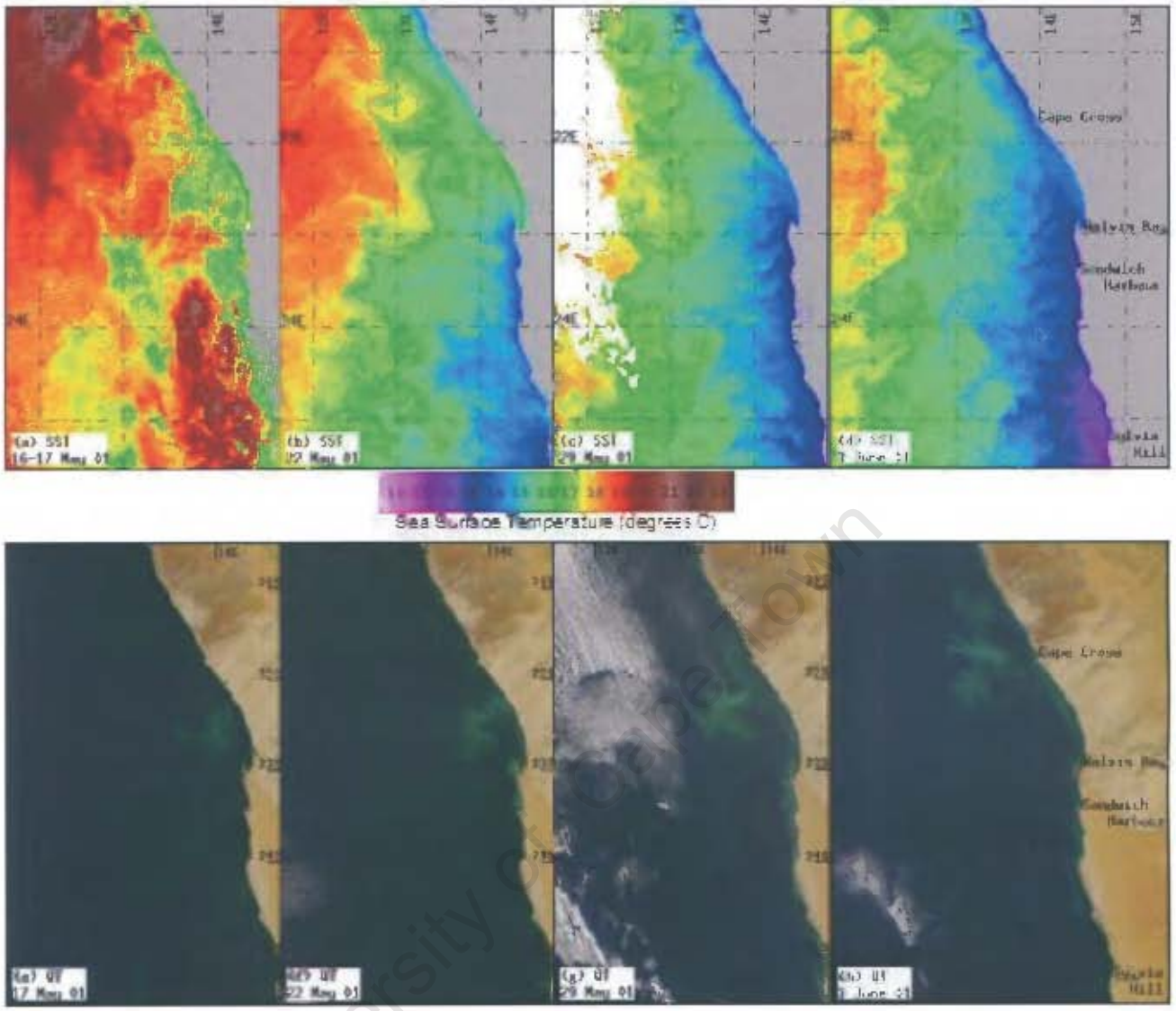

Figure 3.2. NOAA AVHRR false-colour SST and SeaWiFS quasi-true colour (TC) images for the region long 11.5°E-15.5°E; lat 20.5°S-25.5°S during the period May-June 2001. (a) SST 16-17 May, (b) SST 22 May, (c) SST 29 May, (d) SST 3 June; (e) TC 17 May; (f) TC 22 May; (g) TC 29 May; (h) TC 3 June. The area of milky turquoise colouration in panels (e)-(h) indicates high concentrations of suspended sulphur granules in surface waters.

By the period 29 May to 3 June coastal upwelling has spread northward along the coast (Fig. 3.2, c and d) and the sulphur feature is displaced slightly offshore and northward (Fig. 3.2, g & h), and seems to have further intensified. This is the expected advective tendency in an upwelling-associated surface flow pattern. The feature maintained a clear identity, although spreading and diffusing somewhat, at least until 5 June. In summary, this appears to be a clear example of an eruption that cannot be ascribed to a mechanism of simple upward transport in the upwelling circulation of hypoxic sulphide-laden subsurface waters.

Example: Late Oct'01 – Offshore "blob" appears upon a shift from "cold" to "warm"

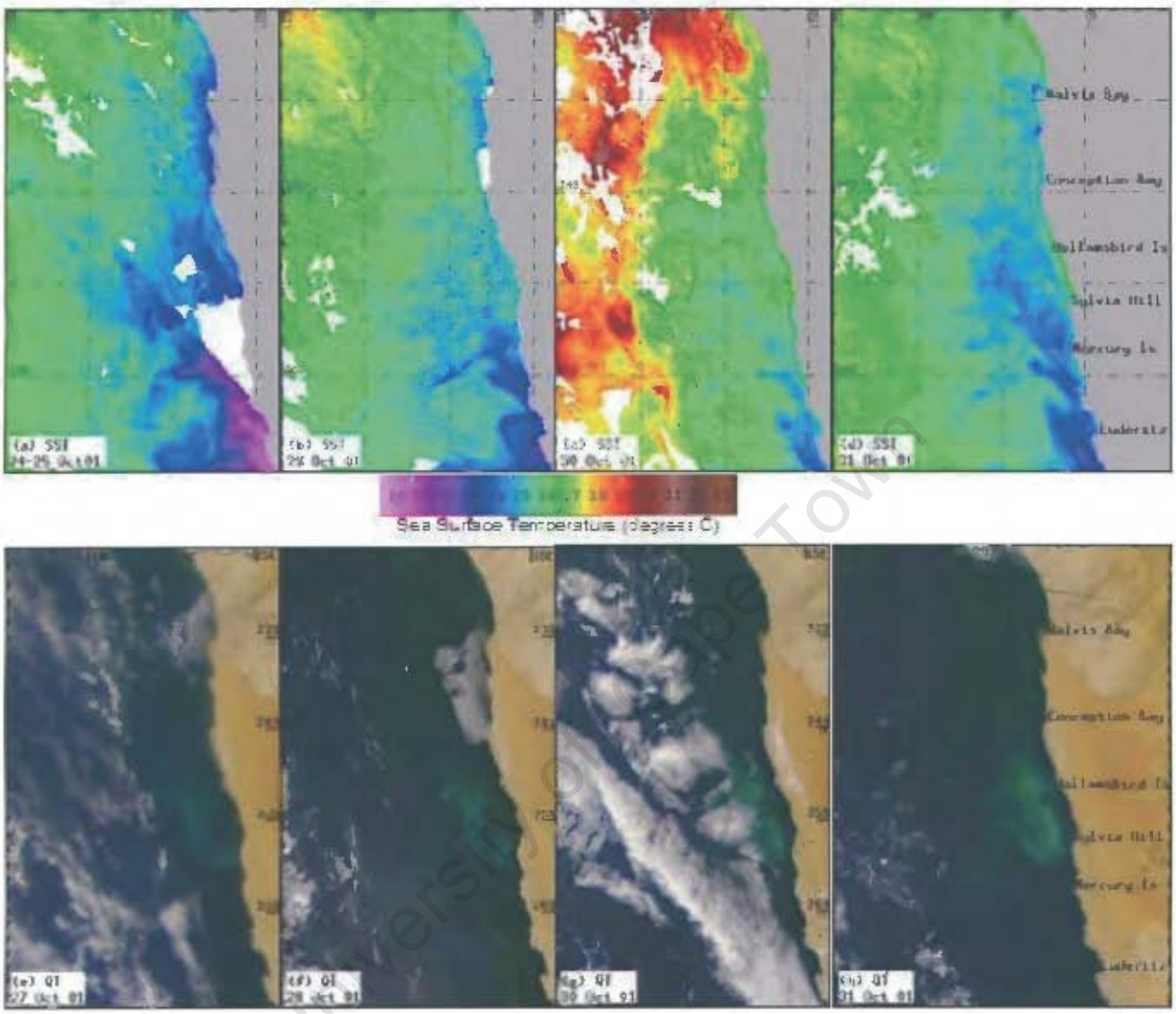

Figure 3.3. NOAA AVHRR false-colour SST and SeaWiFS quasi-true colour (TC) images for the region long 12°E-16°E, lat 22°S-27°S during the period October 2001. (a) SST 24-25 October; (b) SST 28 October; (c) SST 30 October; (d) SST 31 October; (e) TC 27 October; (f) TC 28 October; (g) TC 30 October; (h) TC 31 October. The area of milky turquoise colouration in panels (e)-(h) indicates high concentrations of suspended sulphur granules in surface waters.

At the opposite season of the year (austral spring) another striking episode clearly reinforced the pattern of non-conformance to a mechanism involving simple upward entrainment in a coastal upwelling circulation. In this case, the event was initiated during a sudden relaxation of wind-driven upwelling that was apparently due to a wind reversal associated with the passage of a low pressure weather cell. The passage of such a cell would produce a reversal in wind direction to northerly, downwelling-favourable winds, in direct contrast to the usual strong southerly (equatorward) winds that are responsible for the persistent intense upwelling characteristic of the area. In the sequence of SST images in panels (a), (b), and (c) of Figure (3.3), one can clearly follow the progressive

southward withdrawal toward Lüderitz of the coastal cool strip which is characteristic of active coastal upwelling, as well as the progressive general warming of the entire area shown. On 31 October (Fig. 3.3d), upwelling conditions are seen to be recommencing, as indicated by the coastal cooling spreading northward from the zone near Lüderitz.

Immediately upon initiation of the warming trend, a "blob" of discoloured water, indicating a sulphide eruption having a quite localized source area, is evident offshore of Sylvia Hill (Fig. 3.3e). No discoloured water was visible inshore in clear images for the previous two days. The feature was observed over the next several days (Fig. 3.3, f, g & h) to remain roughly in place in the sluggish advective circulation of the relaxed upwelling situation, while intensifying and spreading somewhat and casting off filaments in the local eddy field. An extended period of cloud cover then interrupted observation of this feature.

Example:* Feb'02: *evident effects on biological production

The situation on 6 February 2002 was characterized by fairly vigorous upwelling south of Mercury Island (Fig. 3.4a). On 7 February upwelling strongly intensified and appeared to spread northward along the coast (Fig. 3.4b). That same day an extended coastwise "milky water" sulphur signature appeared (Fig. 3.4c), reaching from Mercury Island all the way north to Walvis Bay. Significant hydrogen sulphide was measured in the surface at a number of locations within this feature (Table 3.2). By 8 February the feature was obscured by thick fog (Fig. 3.4d) and had disappeared in the next clear image on 11 February.

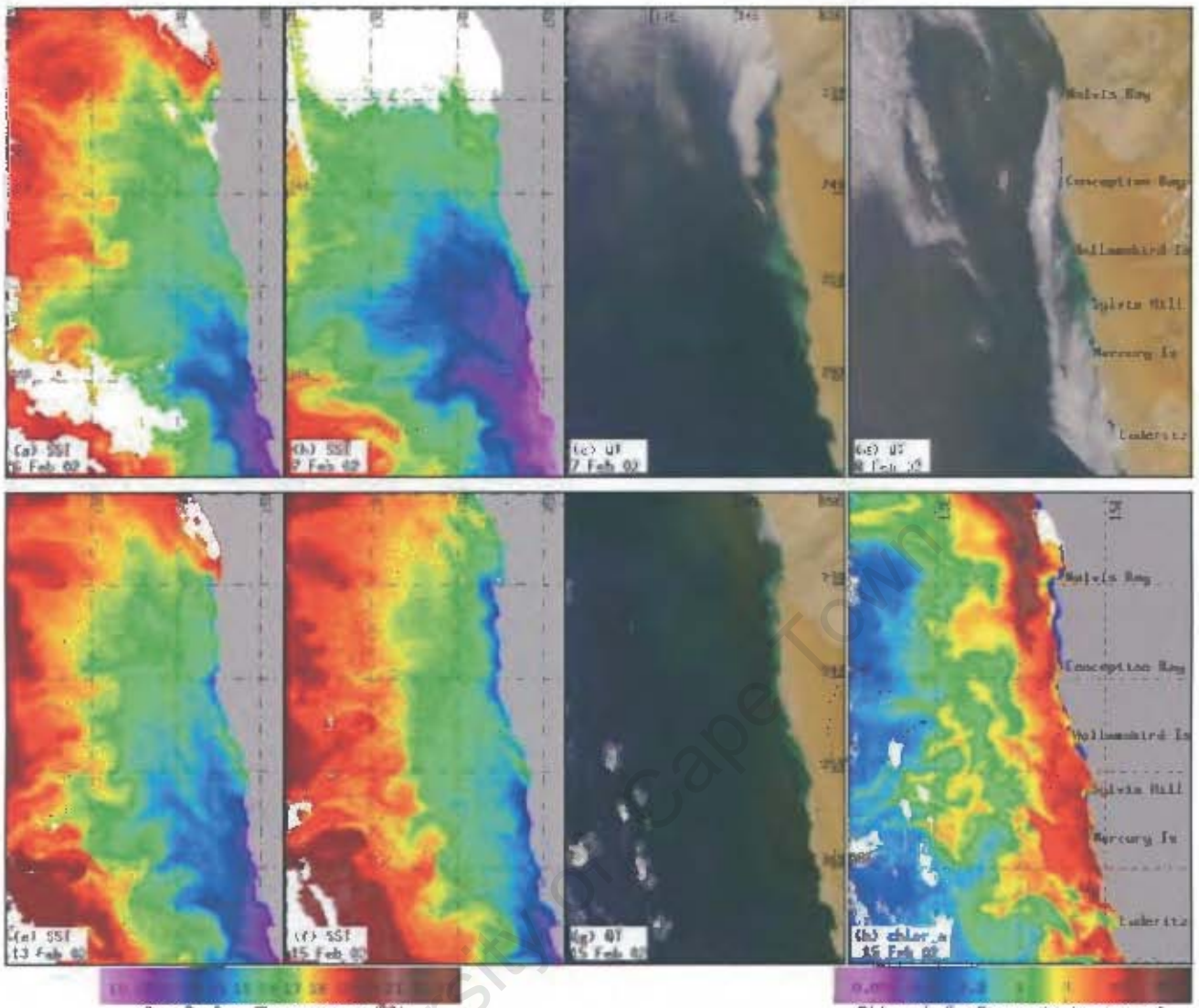

Figure 3.4. NOAA AVHRR SST, SeaWiFS quasi-true colour (TC) and SeaWiFS chlorophyll *a* concentration (chlor *a*) images for the region long 12°E-16°E, lat 22°S-27°S during the period February 2002. (a) SST 6 February; (b) SST 7 February; (c) TC 7 February; (d) TC 8 February; (e) SST 13 February; (f) SST 15 February; (g) TC 15 February; (h) chlor *a* 15 February. The blue mask along the inshore zone in panel (h) denotes pixels flagged due to extreme reflectivity and scattering. The SeaWiFS chlorophyll algorithm was unable to retrieve any chlorophyll values for these pixels.

On 13 February (Fig. 3.4e), an extensive upwelling-associated cool zone stretched northward from the Lüderitz upwelling centre. However, northward of Sylvia Hill coastal cooling appears only off the change in coastline south of Conception Bay and near local upwelling foci (adjacent to headlands, etc.). Two days later, although the offshore extent of upwelling-conditioned waters has lessened southward of Sylvia Hill, the cold coastal strip indicative of active upwelling has spread northward to occupy the stretch of coast from Conception Bay to Walvis Bay (Fig 3.4f). Simultaneously, a line of milky sulphur-laden surface water (Fig. 3.4g) appeared in the near-coastal zone all along the stretch of coast where upwelling appears to be rather newly initiated. This correspondence of sulphide eruptions in the coastal upwelling zone to newly intensified upwelling is

the most common pattern for the appearance of surface evidence of hydrogen sulphide emissions during the study period (Table 3.1).

The corresponding chlorophyll image (Fig. 3.4h) shows two important coincident changes. The first is an indication of general increase in surface chlorophyll compared to two days earlier (not shown), particularly in the northern part of the area shown (interestingly in the area off Walvis Bay, Figure (3.4h) exhibits some of the highest surface chlorophyll concentrations observed in the SeaWiFS imagery for this area). The second change is the sharply reduced chlorophyll indication in the same narrow zone along the coast where the sulphur signature is newly visible in Figure (3.4f). In view of this suppression of the chlorophyll signal, a question naturally arises as to the effect of the sulphide eruptions in these cases. Is the toxic effect of the hydrogen sulphide destroying the chlorophyll-bearing phytoplankton cells in the zone near the coast? Or might the suppression be simply an effect of the strong surface flow divergence and replacement by waters from depth? Unfortunately, two interfering issues act to complicate appraisal of the effect of toxicity on phytoplankton survival and on subsequent primary production.

The first is the methodological problem, outlined in the Methodology Section, whereby the extreme reflectivity of the sulphur particles at the sea surface interferes with the SeaWiFS chlorophyll estimation. Generally, the chlorophyll bio-optical algorithm becomes untrustworthy in any water where constituents other than chlorophyll contribute significantly to the in-water light field. Hence, alternative algorithms need to be explored for estimates of chlorophyll concentration from these "Case 2" waters.

The second issue is the effect of the nutrients that may be brought into the surface photic layer by upward water motion associated with the effervescence of gases held in solution near the sea floor by high ambient hydrostatic pressure. Once the toxic sulphide has dissipated or been oxidized (first to the sulphur particles that produce the "milky water" signature, and later to more highly oxidized sulphate forms), whatever phytoplankton cells have survived or been diffused into the zone from less-affected adjacent areas are then situated in an environment that has been more or less depleted of oxygen. This may pose great difficulty to heterotrophic grazing organisms but less difficulty to the autotrophic phytoplankton. Also, this environment would tend to have been enriched in dissolved plant nutrients (nitrate, ammonia, phosphate, silicate, iron, etc.) that had been generated by remineralization of organic compounds contained in the decomposing cells in the sediments on the sea floor and transported upward in the eruption process. Thus there may be a tendency for rapid

blooming of phytoplankton near the sea surface in the very zone where toxic effects had perhaps, a short time earlier, destroyed most of the pre-existing phytoplankton cells. (Note panels 'g' and 'h' in Fig. 3.4 where, although the chlorophyll algorithm was unable to accurately determine chlorophyll concentration in the narrow band where the milky water signature was particularly strong, the general level of surface chlorophyll outside of that band is very high, and in fact markedly higher than observed in images immediately prior to this eruption event.)

4. Discussion

Previous observations in this region had shown an association of low oxygen conditions with cessation of upwelling (Boyer, 1996). Local observers had also noticed a tendency for coastal sulphide eruptions to often correspond to occasional periods of rainfall in the coastal hinterland (which would also indicate the passage of an atmospheric low pressure cell). However, in the study period (March 2001 to March 2002), this particular pattern, while observed, has not been the dominant one. More often, the initial surface sulphur signature that emerges appears to directly overlie the upwelling zone along the coast, often appearing to directly coincide with an episode of accelerating upwelling (Figs. 3.1 and 3.4). Furthermore, in examining the TC SeaWiFS images, one often notes small milky spots or incipient plumes precisely at the locations adjacent to the coast where upwelling-associated "cold spots" are noted in satellite SST imagery.

The resulting surface "milky water" patterns frequently resemble what one would expect if the sulphide were merely carried to the surface in the upwelling of water from depth. However, while it is certainly possible that some amount of upwelled water, if brought up from depths near the sea floor, might be bearing some entrained sulphide and sulphur particles, it seems hard to accept that the major emission events such as depicted in Figures (3.1) to (3.4) represent the simple upward advection of sulphide in the same way that much more conservative tracers such as water temperature and dissolved nutrients may be carried to the surface. Clearly, the offshore "puffs" and "blobs", such as shown in Figures (3.2) and (3.3), appear not to have direct connections to the near-coastal band where coastal upwelling predominates. For example, eruptions arise out of warm (relaxed upwelling) conditions (Fig. 3.2) or during a relaxing phase from cooler to warmer conditions (Fig. 3.3). Thus there seems to be more to the phenomena than mere upward advection of low oxygen sulphide-bearing water in the coastal upwelling process.

The Namib Desert coast is one of the driest places on earth. Consequently, the major expanse of coast is largely uninhabited. This, combined with the lack of major established scientific and technological facilities in southern African developing countries, greatly limits opportunities for *in situ* validation of the sulphide eruption phenomena. However, although the ground verification of these events by qualified well-trained observers is far from complete (i.e. available for only about half of the eruption events occurring within the one-year period summarized in Table 3.1), the results are consistent. Whenever trained scientific personnel on the ground have managed to be at the scene simultaneously with the identification in a TC SeaWiFS image of the "milky water" surface signature of an eruption, the identification has been confirmed to be associated with hydrogen sulphide emissions. The strong "rotten egg" odour is always clearly evident. Floating dead organisms are invariably seen attracting flocks of seabirds. When appropriate sampling and measurement equipment has been available (Table 3.2), the dissolved oxygen concentrations in the water clearly have indicated depletion of oxygen from the water column, and significant concentrations of dissolved hydrogen sulphide or elemental sulphur are detected (Table 3.2).

More recently parasounding of the inner shelf sediments along the Namibian coast during the R.V. Meteor M48/2 cruise indicated substantial gas pockets lying centimetres to metres below the sediment surface (Emeis et al., 2002). It thus appears that the gaseous pressure that exists within these sediments is held in check only by the ambient hydrostatic pressure and is ready to burst out of solution when that pressure is released. Gases produced by bacterial action are continually building up in solution within the upper sediment layers and adjacent to the sediment surface. At some point, the partial pressure of the gases in solution may exceed the opposing hydrostatic pressure whereupon incipient microscopic gas bubbles will begin to emerge. Eventually, growth and coalescence of these bubbles will generate sufficient buoyancy to break loose from surface tension effects and initiate upward motion. The rapidly lowering hydrostatic pressure in the upward moving water parcel would cause more effervescing gas to progressively burst explosively from solution, accelerating the motion upward.

Upwardly accelerating motion of water has the dynamical effect of lowering the fluid pressure in the water column below it. And since pressure is a continuous variable that cannot support discontinuities, the ambient pressure in closely adjacent zones of the sea floor will also experience a lowering. Thus an incipient upward motion initiated near the sea floor, may trigger effervescence in the adjacent areas, initiating concomitant upward motions there. Thus there may be an outward radiating "domino effect", propagating the effect of the initial release over large areas where the

buildup of gaseous pressure within and adjacent to sediment surface has made them ripe for eruption. This could account for the large scale and the distinctive shapes of observed patterns in large eruption episodes (e.g., extended integrally-connected coastwise bands which terminate rather abruptly at each end, or isolated puffs and large blobs which when emerging roughly concurrently often appear as being interlinked by a connecting narrower, more linear pattern of milky water).

This view of the process concurs with the observed pattern that the eruptions seem to be triggered under several different circumstances, either during the initiation of an episode of stronger upwelling, during an interruption of the upwelling process by wind relaxations or reversals, concurrent with incidence of rainfall in the normally dry desert coastlands. Each of these circumstances would contribute to a lowering of hydrostatic pressure at the continental shelf/slope surface. The hydrostatic pressure at the sea floor is a combination of two factors, the weight of the overlying water column and the atmospheric pressure bearing down on the sea surface. Intensified coastal upwelling involves an increase in the onshore-offshore slope of the sea surface, thus lowering the actual sea level near the coast. Consequently, the hydrostatic pressure at the sea floor near the coast is lowered, increasing the likelihood of an effervescent outbreak. On the other hand, the events that are initiated during the passage of an atmospheric low pressure weather cell may be triggered by the drop in atmospheric pressure acting on the sea surface, which in turn is reflected as a transient drop in hydrostatic pressure at depth. Coincidence with periodic tidal height minima would be an additional supporting factor in both these cases.

It is worth emphasizing here that hydrostatic pressure drops are not suggested as being a primary forcing mechanism for an eruption. The primary mechanism envisioned is the buoyancy force released by the effervescence, coalescence and expansion of bubbles of trapped gas. The hydrostatic pressure changes favoring initiation of effervescence would merely constitute a triggering process that would affect (i.e., advance) the timing of an eruption that already had been building on its own toward a point of spontaneous initiation. The effervescing gas is initially a mixture of methane and carbon dioxide (Emeis et al., 2004); hydrogen sulphide, which reaches concentrations of up to 22 mM/L in sediment pore waters, diffuses into the effervesced gaseous bubbles. Hence, the hydrogen sulphide is carried upward rather passively in the eruption process, being oxidized to elemental sulphur as it mixes with oxygenated waters higher in the water column or at the wave-mixed sea surface.

This brings up another interesting issue. Hydrogen sulphide features separated from the coast, particularly after having existed at the sea surface for some time (e.g., Fig. 3.1, panels f, g, and h), tend to appear quite similar to satellite observations of very large coccolithophore blooms (Tyrrell et al., 1999; Chapter 4). However, the continuity of the features in the available satellite images and the oceanographic context as inferred from SST, generally make it rather clear that the offshore features are the same features that had been earlier observed as episodes of sulphide emission nearer the coast. Unfortunately, the only ground verification that has been possible has been in connection with the milky zones near the coast. The possibility of some degree of involvement of coccolithophores in the offshore signatures cannot be discounted at this point[8]. If so, such a relationship of coccolithophore blooms to sulphide/anoxia is previously unreported and in itself would be of ecological significance. In any case, sea-truth data are urgently needed to accurately calibrate the satellite sulphur signal. Attempts to resolve this problem would seem to require some significant supporting at-sea observational / experimental operations.

The new capability for identifying and monitoring these events by satellite has already revealed much that was previously unsuspected about these sulphide eruption phenomena. It clearly suggests that hydrogen sulphide emissions from the sediment can be held more responsible for hypoxic conditions along the Namibian coast than advected hypoxic water of Angolan origin Certainly, the new view of their very large extent and high frequency of occurrence has made clear their great potential ecological importance to the northern Benguela Current marine ecosystem. The hydrogen sulphide emissions are perhaps also very important to the Benguela marine ecosystem as a whole, in that they may be a major factor in the functional separation into northern and southern subsystems, of what would seem to be a natural integral large marine ecosystem. The ecosystem implications for migrating fish species of this functional separation, are discussed in the Chapter (7) of this thesis.

[8] Additional factors might support the long-enduring (up to several weeks) character of the sea surface sulphur signatures. (1) In waters that have been de-oxygenated, injected with nutrients, and subjected to passage of toxic gas, certain types of autotrophic organisms more resistant to toxic effects and able to thrive under hypoxic conditions might bloom in the opportune "free space" created by the eruption. If such microalgal blooms have highly scattering optical properties (Tyrrell et al., 1999), they could conceivably reinforce the offshore-advected satellite sulphur signatures. (2) Also possible, although likewise not documented at this time, is that sulphur granules encased and protected within the bodies of sulphide-oxidizing *Thiomargarita* bacteria might be carried upward in the eruption process and remain suspended at the surface.

Chapter 4

Monitoring the evolution of a coccolithophorid bloom in the southern Benguela upwelling system

1. Introduction

Coccolithophorids are a phytoplankton species that synthesize external calcium carbonate platelets, or coccoliths, which cover the outer surface of the cell. They are widespread (Brown and Yoder, 1994) and known to form near mono-specific blooms that can extend over large areas of ocean surface (Holligan et al., 1983, 1993). The number of coccolithophorid cells in a bloom frequently accounts for 80% or more of the total phytoplankton cells in the water. Coccolithophorid cells may be accompanied by even larger numbers of coccoliths, either attached to the cells or floating in the water. Such blooms provide a milky turquoise colour to the ocean, primarily due to light scatter from the coccoliths (Balch et al., 1996a). These small inorganic platelets are extremely effective scatterers of light, particularly when detached from the host cells. It is largely the influence of high concentrations of these detached coccoliths that cause coccolithophorid blooms to differ optically from other blooms of non-calcifying marine phytoplankton (Ackleson et al., 1994; Balch et al., 1996a).

Absorption and backscattering are the two processes primarily responsible for the quality of light returned to the sea surface. Absorption by chlorophyll is generally the dominant optical process for phytoplankton with a volume reflectance in the order of two to three percent. However, in the midst of a coccolithophore bloom, surface irradiance reflectance values (the ratio of upwelling to incoming irradiance measured above the sea surface) of over 20 percent have been reported (Groom and Holligan, 1987). An increase in backscattering relative to absorption, induced by the presence of coccoliths, is responsible for the increased reflectance values. These high reflectance values are visible from satellite, allowing coccolithophore blooms to be distinguished. The evolution of such blooms can therefore be analysed using satellite-derived quasi-true colour imagery as an alternative to the traditional phytoplankton biomass proxy of chlorophyll a concentration.

Little consideration has been given to the contribution of coccolithophorids to the phytoplankton communities in upwelling systems (Cushing, 1989). In particular, very little has been documented as to the of extant of coccolithophorids in the Benguela upwelling system. In this chapter, the evolution of an unusual coccolithophore bloom in the southern Benguela during the autumn of 2003 is

documented, using satellite ocean colour and sea surface temperature imagery. This chapter comprises work undertaken in 2004 and recently published in *Oceanography* (Weeks et al., 2004b).

2. Methodology

Satellite imagery

The coccolithophore signal was initially identified on the 26 March 2003 in 24-bit, quasi-true colour composites generated from SeaWiFS calibrated and Rayleigh-corrected radiances at 670, 555, and 412 nm (bands 6, 5 and 1, respectively)[9]. The one kilometre resolution SeaWiFS data were acquired and processed locally and the signal thus monitored throughout the event. Quasi-true colour imagery generated from MODIS onboard the NASA Terra and Aqua satellites using bands 1, 4 and 3 (at 645nn, 555nm and 469nm, respectively), was additionally acquired[10]. With a resolution of 250m (band 1) and 500m (bands 4 and 3), the higher resolution allowed for a more detailed analysis of the event.

Daytime NOAA AVHRR (1 km resolution) sea surface temperature images were generated locally using the standard McClain et al., (1985) algorithm. These provided information on the physical environment important in determining the evolution of the bloom. Chlorophyll *a* concentration, representing phytoplankton biomass, was determined using the SeaWiFS Data Analysis System (SeaDAS) and the OC4v4 algorithm (O'Reilly et al., 2000). Further detail with regard to the processing of SeaWiFS and NOAA AVHRR data is provided in Chapter 2.

In situ and spectroradiometric measurements

In situ bottle sampling (NIO) was undertaken from a ski boat off Lambert's Bay on the 15 April 2003 (Fig. 4.3: Stn 1). Further bottle samples were collected from surface waters in St Helena Bay on the 24 April 2003 (Fig. 4.3: Stns 2, 3, 4 and 5) using a rosette sampler from a research vessel. Surface spectroradiometric measurements were also made on the 15 April 2003. A Satlantic HyperTSRB (Satlantic Inc., Halifax, Canada) was used to obtain near surface upwelling radiance (upwardly directed light flux per solid angle just beneath the sea surface) and above surface

[9] The code used to produce the quasi-true colour images was provided by Norman Kuring and the SeaWiFS Project, NASA.
[10] Provided by the Modis Rapid Response Team

irradiance. Subsurface radiance data were propagated to the surface using diffuse attenuation values (a measure of the attenuation of naturally occurring upward light flux), as determined by the Austin and Petzold (1981) and Morel (1988) models. Normalised water-leaving radiance values were then calculated using the protocols of Mueller et al. (2003).

3. Results and discussion

Bloom evolution

A sequence of satellite images from the 26 March to 5 May 2003 (Figs. 4.1 and 4.2) documents the evolution of the coccolithophore bloom. Dominated by the coccolithophorid *Syrachosphaera pulchra* the bloom was confined to the region between the Namaqua and Cape Columbine upwelling cells, where a broadening of the shelf favours stratification of the water column, conducive to the development of flagellate dominated blooms. This region is thought to be characterised by retentive, near surface circulation patterns dominated by a cyclonic gyre north of St Helena Bay (Holden 1985, Probyn *et al.* 2000), and is an area particularly susceptible to red tide formation and its negative impacts (Pitcher and Calder, 2000).

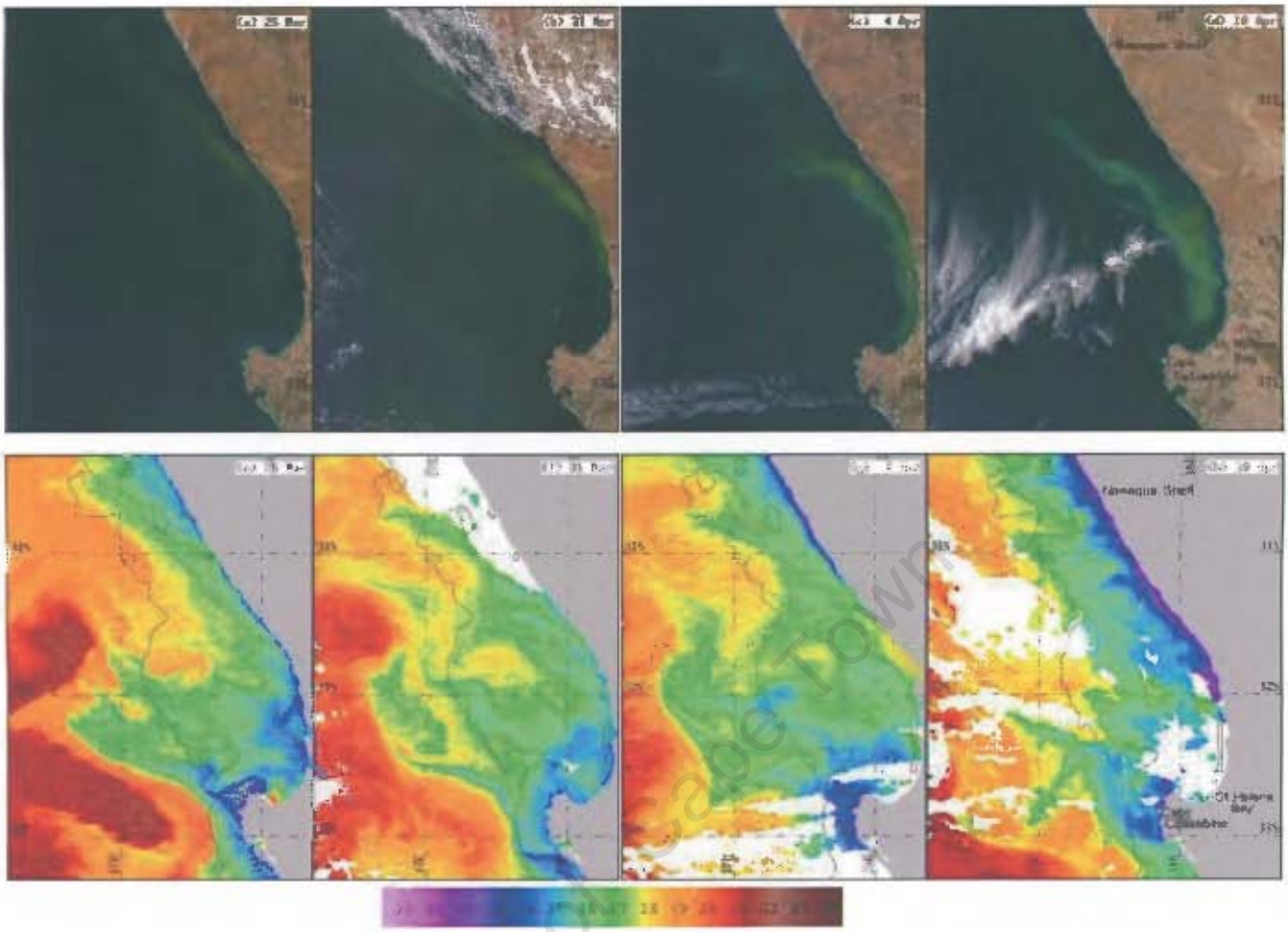

Figure 4.1. Modis quasi-true colour (TC) and NOAA AVHRR false colour SST images for the region lon 18.2°E-18.7°E; lat 30.3°S-33.3°S during the period March-April 2003. (a) TC 26 March, (b) TC 31 March; (c) TC 4 April; (d) TC 10 April; (e) SST 26 March; (f) SST 31 March; (g) SST 4 April; (h) SST 10 April. The area of milky green colouration in panels (a)-(d) indicates high concentrations of the coccolithophorid *Syrachosphaera pulchra* in surface waters. White patches represent cloud. The black contour represents the 200m isobath.

The bloom was first observed towards the end of March (Fig. 4.1a) to the north of St Helena Bay following a period of moderate upwelling. The bloom was associated with warm water (16°C) on the seaward edge of the upwelling front demarcating a narrow band of upwelling inshore (Fig. 4.1c). As upwelling activity diminished and thermal stratification increased (Fig. 4.1f), the bloom intensified (Fig. 4.1b) and was advected into St Helena Bay during the first few days of April (Fig. 4.1c). Under these conditions the frontal system and associated bloom are considered to move shoreward, and the development of an inshore counter current results in the southward progression of the bloom. Although the resumption of upwelling conditions displaced the bloom from the coast during the second week of April (Fig. 4.1d and h), the bloom remained in St Helena Bay and extended a distance of 220 km to the north.

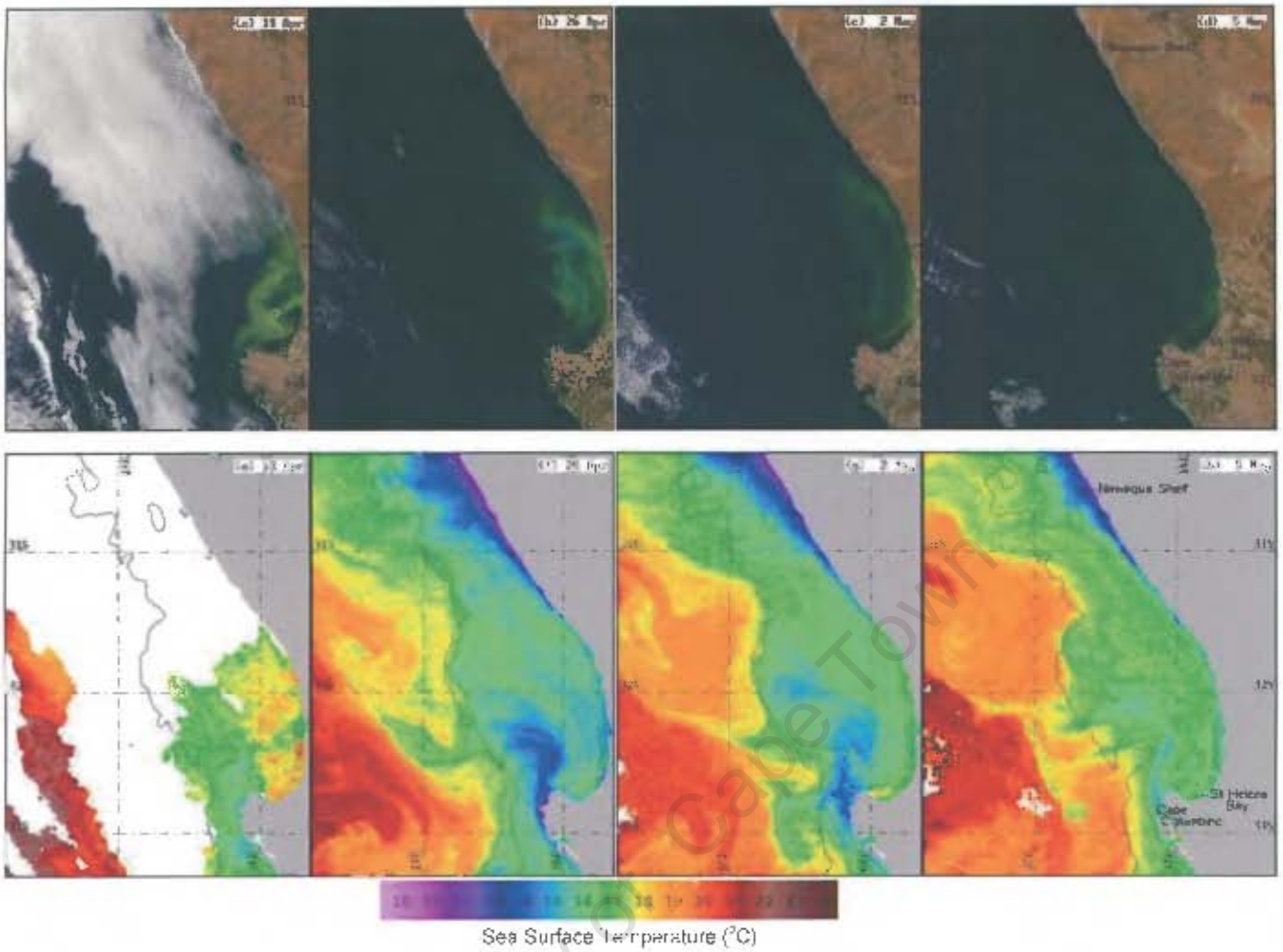

Figure 4.2. Modis quasi-true colour (TC) and NOAA AVHRR false colour SST images for the region lon 18.2°E-18.7°E; lat 30.3°S-33.3°S during the period April-May 2003. (a) TC 19 April; (b) TC 26 April; (c) TC 2 May; (d) TC 5 May; (e) SST 19 April; (f) SST 26 April; (g) SST 2 May; (h) SST 5 May. The area of milky green colouration in panels (a)-(d) indicates high concentrations of the coccolithophorid *Syrachosphaera pulchra* in surface waters. White patches represent cloud. The black contour represents the 200m isobath.

Relaxation of upwelling conditions during mid-April once again favoured southward advection of the bloom and on the 19th April (Fig. 4.2a and e) the bloom was observed rounding Cape Columbine. This southward advection of blooms around Cape Columbine appears to be associated with poleward coastal-trapped wave propagation developed equatorward of the Cape (Lamberth and Nelson 1987; Pitcher et al., 1998; Pitcher et al., in press). The surface manifestation of this current is not continuous but usually appears as a flood event (Probyn et al., 2000). Advection of the bloom around Cape Columbine ceased with the resumption of upwelling towards the end of April (Fig. 4.2b and f). Termination of the bloom was associated with quiescent conditions and extensive warming of St Helena Bay (Fig. 4.2c, g, d and h), 41 days after the bloom was first observed.

Satellite derived and in situ measurements

The coccolithophorid *Syrachosphaera pulchra* and a mixed assemblage of dinoflagellates dominated the phytoplankton assemblage off Lambert's Bay on 15 April 2003 (Fig. 4.3a and b: Station 1; Table 4.1). The coccolithophorid concentration approximated 8.9e5 cells l^{-1} and the dinoflagellate assemblage was dominated by *Prorocentrum triestinum* and *Scripsiella trochoidea*. Surface spectroradiometric measurements made on 15 April 2003 allow an assessment of the SeaWiFS sensor to accurately determine normalised water-leaving radiance under bloom conditions. Normalised water-leaving radiance values corresponding to Station 1 (Fig. 4.3a and b) were therefore extracted from SeaWiFS overpass data for 15 April 2003. The match between *in situ* and satellite derived normalized-water leaving radiance values is extremely good, with the SeaWiFS values within 5 % of surface measured values at all wavelengths (Fig. 4.4). Hence, turning off the straylight correction during processing of SeaWiFS data from level-1 to level-2 (Chapter 2) appears to work well along the coast judging from this close match-up of SeaWiFS-derived and *in situ* normalized-water leaving radiances.

Station	Date	SeaWiFS Chlor a	*In-situ* Chlor a	*S.pulchra*	Dinoflagellates	Diatoms
St 1	4/15/2003	5.6	26.9	8.9E+05	9.0E+05	0
St 1	4/24/2003	43.9	-	-	-	-
St 2	4/24/2003	6.8	9.7	9.1E+05	4.8E+04	0
St 3	4/24/2003	9.7	18.3	6.4E+05	6.1E+04	0
St 4	4/24/2003	14.8	18.7	6.1E+04	2.5E+05	0
St 5	4/24/2003	4.0	6.1	0	2.2E+04	2.8E+05

Table 4.1. SeaWiFS and *in situ* measurements of chlorophyll *a* (mg m^{-3}), and cells counts for *Syracosphaera pulchra*, total dinoflagellates, and total diatoms (cells l^{-1}), for the five sampling stations.

On 24 April 2003, Stations 2 and 3 in St Helena Bay (Fig. 4.3c and d) were both dominated by the coccolithophorid *Syrachosphaera pulchra* at concentrations of 9.1e5 and 6.4e5 cells l^{-1} respectively, while dinoflagellate concentrations approximated 4.8e4 and 6.1e4 cells l^{-1} (Table 4.1). Dinoflagellates (2.5e5 cells l^{-1}) dominated the phytoplankton assemblage at Station 4 with *Ceratium lineatum* the most common species. The concentration of *Syrachosphaera pulchra* was only 6.1e4 cells l^{-1} (Table 4.1). At Station 5 diatoms dominated the assemblage with *Skeletonema costatum* the most abundant species (2.8e5 cells l^{-1}). Normalised water-leaving radiance values corresponding to Stations 1 to 5 were also extracted from SeaWiFS overpass data on the 24 April 2003 (Fig. 4.4).

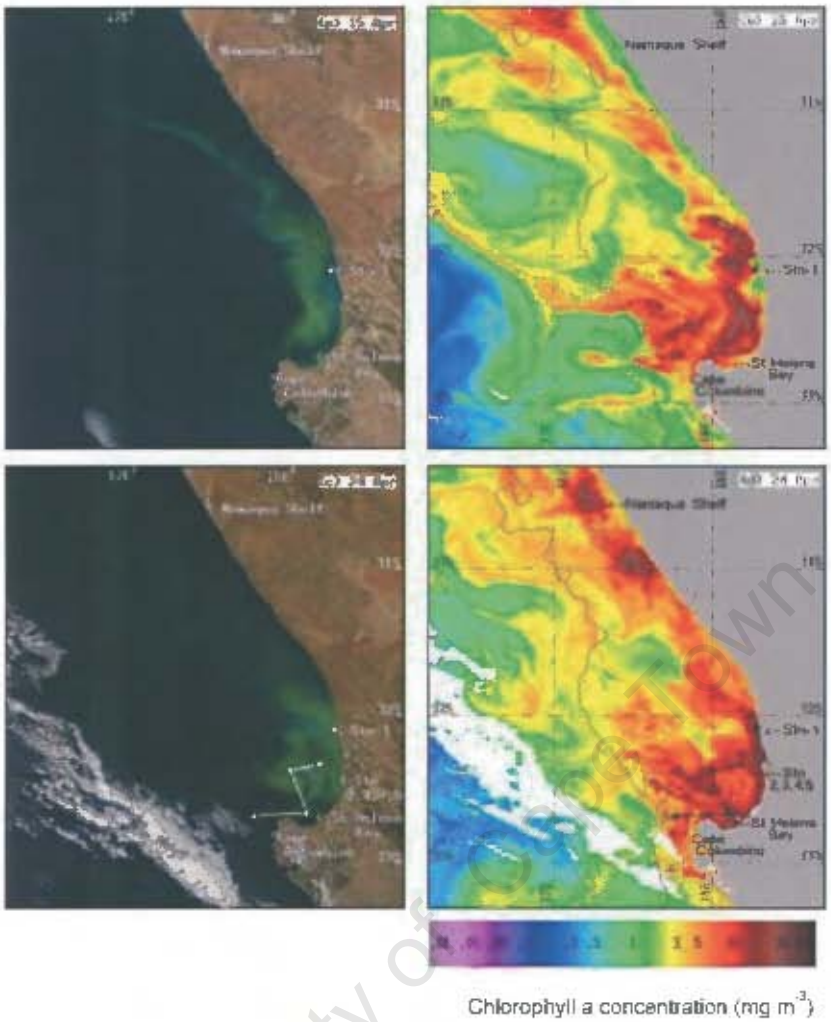

Figure 4 3. Modis quasi-true colour (TC) and SeaWiFS false colour chlorophyll a (CHL) images for the region lon 16.2°E-18.7°E; lat 30.3°S-33.3°S on 15 and 24 April 2003. (a) TC 15 April; (b) CHL 15 April; (c) TC 24 April; (d) CHL 24 April. Locations of in situ sampling, Stations (1) – (5), are shown. The area of milky turquoise colouration in panels (a) and (c) indicates high concentrations of the coccolithophorid *Syrachosphaera pulchra* in surface waters. White patches represent cloud. The black contour represents the 200m isobath.

A comparison of SeaWiFS water-leaving radiance values (Fig. 4.4) and phytoplankton assemblage data (Table 4.1) confirms that stations with high concentrations of *S. pulchra* (Stations 1, 2 and 3) all show elevated normalised water-leaving radiance values, associated with the presence of highly backscattering calcite particles in surface waters. The varying ratio of detached coccoliths to coccolithophorids may be responsible for the imprecise relationship between radiance values and the concentration of *S. pulchra*, owing to the fact that detached coccoliths are more effective backscatterers than the whole plated cells, and are thus the principle source of highly elevated reflectance values (Balch et al., 1996a; Voss et al., 1998). Detachment of coccoliths is typically a function of bloom age: declining or stationary phase blooms having a higher ratio of detached coccoliths (Balch et al., 1993; 1996a). The variable presence of a mixed dinoflagellate community (Table 4.1), on occasion reaching concentrations of ~ 9e5 cells l^{-1}, introduces an additional large

source of absorbing material to the gross optical signal. Thus whilst the *S. pulchra* cell counts demonstrate that the elevated reflectance values can be used as a gross coccolithophorid bloom tracer, the complex admixture of unquantified absorbing and backscattering material precludes a more detailed analysis of the bloom's optical signature.

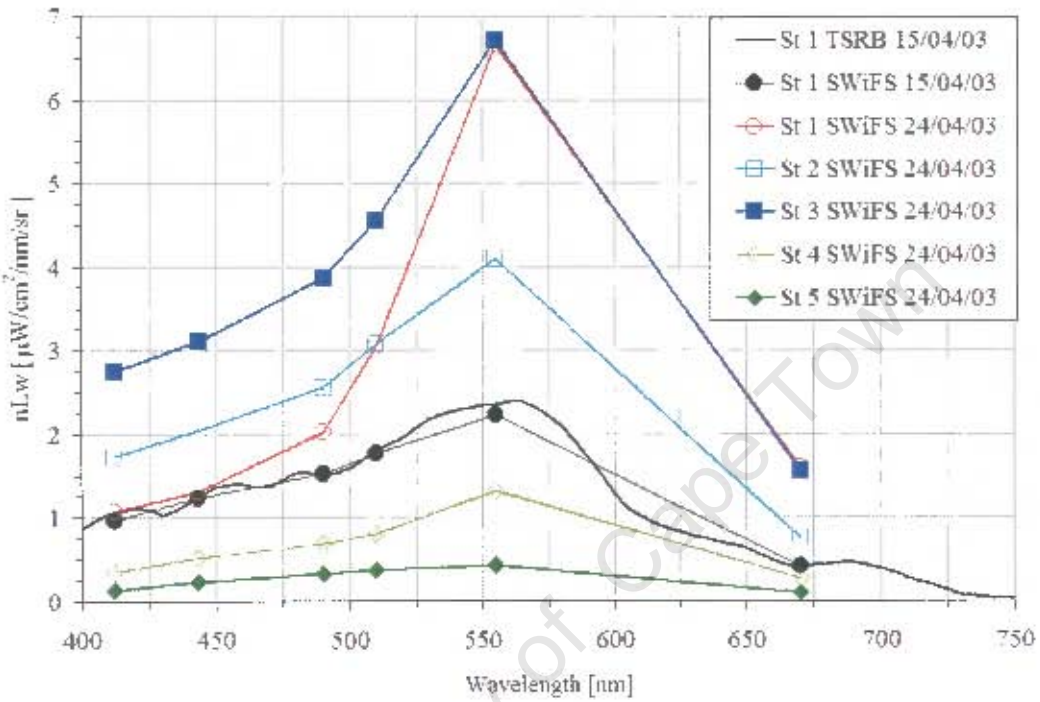

Figure 4.4. SeaWiFS and *in situ* measurements of normalised water-leaving radiance for the five sampling stations.

Furthermore, the high reflectivity of coccolithophorids and associated coccoliths at the sea surface interferes with the SeaWiFS chlorophyll estimation. As for precipitated sulphur in surface waters (Chapter 3), both the radiances used in the bio-optical algorithm and the radiances used in the atmospheric correction process are likely to be adversely affected by the high reflectance. Since the bio-optical algorithm uses band-ratios with the denominator, 555nm, assumed to be relatively stable, the presence of coccolithophorids or coccoliths at any one location, producing a significant contribution at 555nm, will tend to yield erroneous estimates of chlorophyll a. The effect on SeaWiFS normalised water-leaving radiances of a mixed coccolithophorid/dinoflagellate algal community, comprising both coccoliths and absorbing material, is apparent in the reflectance spectra shown in Figure (4.4).

In processing of SeaWiFS data, numerous thresholds are determined and data may be flagged for a specific condition (Chapter 2). The SeaDAS "coccolithophore flag" is determined by several boundary conditions based on thresholds for SeaWiFS normalised water-leaving radiances (nLw) at 443nm and 555nm, the aerosol radiance at 670nm, and specific ratios of nLw_443/nLw_555, nLw_510/nLw_555, and nLw_443/nLw_510 (Brown, 1995). At locations where the reflectance signal is intense, pixels are flagged as coccolithophore dominant (not shown), as the SeaWiFS chlorophyll algorithm is unable to accurately retrieve chlorophyll values due to the high reflectivity and scattering. Examination of the satellite-derived individual normalised water-leaving radiances revealed high values at these locations, with values of nLw 490nm and nLw 510nm approximately equal to or even exceeding that of nLw 555nm; hence the result would be a depressed estimate of chlorophyll. Satellite-derived chlorophyll values for stations with high concentrations of *S. pulchra* (Stations 1, 2 and 3) are on average 52 percent lower than chlorophyll concentrations measured *in situ* (Table 4.1). Generally, the OC4V4 bio-optical algorithm becomes untrustworthy in any "Case 2" waters, where constituents other than chlorophyll contribute significantly to the in-water light field (O'Reilly et al., 2000).

Finally, it is interesting to note that the SeaDAS atmospheric warning flag is triggered at locations where pixels in the quasi-true colour composites are strongly yellow (high reflectance in the 670nm and 555nm bands). This flag represents the ratio of aerosol reflectance in SeaWiFS bands at 765nm and 865nm (bands 7 and 8, near-infrared), used in the atmospheric correction algorithm. Since it is recognized that coccolithophores may produce large quantities of dimethyl sulphide (DMS) that pass into the atmosphere (Brown ands Yoder, 1994), an increase in DMS may trigger the atmospheric warning flag. This scenario was also noted in the study of hydrogen sulphide eruptions in the northern Benguela (Chapter 3) where, when emissions of hydrogen sulphide were considered active, the aerosol warning flag was similarly triggered. It is understood that substances other than chlorophyll can result in a non-zero radiance in the near-infrared bands[11] and hence may affect the atmospheric correction. Nonetheless, *in situ* atmospheric chemistry sampling is worth considering in any potential future calibration of these event-scale signals in Benguela regional waters.

In closing, this chapter documents a recent, unusual coccolithophorid bloom in southern Benguela waters, the first such extensive bloom monitored by satellite in the Benguela upwelling region. The

[11] In SeaWiFS processing, it is assumed that the water-leaving radiance is zero for the near-infrared bands 7 and 8 ("black pixel assumption"). In the presence of chlorophyll over 2 mg m^{-3}, this assumption causes problems in the estimation of aerosol radiance (Siegel et al., 2000).

bloom is also of the first monitored by MODIS satellite ocean colour, the 250m – 500m resolution allowing detailed analysis not possible previously. Although coccolithophorids are typically characteristic of oligotrophic waters, species such as *Emiliania huxleyi* do exhibit unexpectedly good growth in enriched coastal waters at suitable temperatures. As a result *E. huxleyi* and *Gephyrocapsa oceanica* are known to form massive blooms, but blooms of other coccolithophorids including species of the genus *Syrachosphaera* are rarely reported. Here, the detection and monitoring from space of such a bloom in southern Benguela waters is demonstrated, dominated by a species not previously known to form such intense concentrations.

Chapter 5

A quantitative application of satellite data - towards developing operational indices for the Benguela ecosystem. Part 1.

1. Introduction

The generation of consistent time series of daily high resolution (1 km) NOAA AVHRR and SeaWiFS ocean colour data, as described in Chapter 2, is primary to a detailed investigation of the dynamic variations in upwelling and phytoplankton biomass in the Benguela ecosystem. Daily high resolution NOAA images display the temporal and spatial variability in Sea Surface Temperature (SST), allowing identification of the locality and emergence of upwelling cells, whereas daily SeaWiFS imagery shows the distribution patterns of chlorophyll *a* concentration (chlorophyll) across the Benguela.

Chapters 5 and 6 of this thesis focus on the quantitative analysis of high resolution NOAA SST and SeaWiFS chlorophyll data within the southern Benguela ecosystem. This chapter (Part 1) concentrates on examining the extent and frequency of upwelling during the period July 1998 through June 2003 and the response of the phytoplankton community to this physical forcing. Chapter 6 (Part 2) initiates the development of appropriate indices towards their application in operational management of the upwelling system.

Various other studies have been published over many years where either low spatial or temporal resolution indices have been determined (Bakun, 1973; Bakun, 1975; Nykjaer, 1994; Carr and Kearns, 2003). These studies show primarily the long-term mean seasonal cycles. Current research with remote sensing in the regional BENEFIT and IDYLE Programmes focuses on SST and SeaWiFS ocean colour, utilizing both low (4.5 km) and high (1 km) resolution data. Low resolution data has been used to construct a climatology for SST and chlorophyll concentration for the Benguela ecosystem (Demarcq et al., 2003), and to describe the dynamic variations within the system (Demarcq et al., 2002a). Low resolution (4.5 km) SeaWiFS data has also been used to describe the temporal variation in chlorophyll concentration over 5 years (1997-2002) from 12-34°S (Demarcq et al., 2002b). High resolution (1 km) SST data has been used to investigate the effects of

environmental variability on the pelagic fish distribution in South Africa (Agenbag et al., 2003) and Namibia.

Although low-resolution SST and chlorophyll indices may be useful for investigating general patterns over large scales, the finer scale spatial and temporal variability is lacking, especially in the inshore coastal zones. High-resolution indices are therefore required to examine patterns of change in more detail, particularly in the inshore regions. A specific objective of the regional BENEFIT Programme is to utilise one kilometre resolution NOAA AVHRR and SeaWiFS ocean colour satellite data to investigate these dynamic variations, and to derive quantitative indexes to serve as a measure of the ecosystem function. The purpose here is to initiate the development of the best possible updateable products that would incorporate the best features of previous work.

Specific questions are:
1) What is the spatial and temporal variability in SST, upwelling cells and upwelling events on intra-seasonal time scales?
2) What is the spatial and temporal variability in SeaWiFS chlorophyll on intra-seasonal time scales?
3) Is there a clear relationship between SST and phytoplankton biomass?
These questions are addressed by comparing the differences in variability of upwelling and phytoplankton biomass between various biogeographic regions in the southern Benguela, namely the Cape Peninsula, Cape Columbine and Namaqua shelf upwelling cells, St Helena Bay and the western Agulhas Bank (Fig 5.1a).

2. Methodology

Southern Benguela SST and chlorophyll time series were generated by extracting data from the daily five year NOAA and SeaWiFS time series to include the region 29-36°S and 15-21°E (672 lines by 576 pixels), the cylindrical equirectangular projection having a resolution of 0.0104° of latitude and longitude. Missing data does occur on some days due to cloud, incomplete coverage of the region by the satellite, or flagged data for reasons as outlined in Chapter 2. Additionally, there are occasional days in the extracted time series (8.4% for SST, 11.7% for chlorophyll) when no high resolution data is available for this region, due to the position of the satellite zenith angle for a particular orbit swath of the day or due to problems with the satellite acquisition system. Hence, limited spatial and temporal interpolation was applied to attain the minimum of data detail loss, while simultaneously filling in missing data where possible.

For the spatial interpolation, a spatial fill was applied to each individual daily image using a mean box function to fill missing data only. All original valid ocean data values were retained. For the temporal interpolation, alternative approaches were discussed and trials run wherein different temporal weightings were applied to images over running three and five day periods (for example, $^1/_7$, $^5/_7$, $^1/_7$, and $^1/_{24}$, $^3/_{24}$, $^{16}/_{24}$ $^3/_{24}$, $^1/_{24}$). The trials tested both interpolations (a) of missing data only and (b) of all ocean data. The interpolated time series were assessed, both by image-to-image comparison and by animating alongside the original non-interpolated data series, to ultimately select the result that most closely represents the expected value while optimally filling missing values. It was necessary to take into account both the rapid variation in physical dynamics and the associated phytoplankton response, particularly during periods of active upwelling. At such times, a temporal mean over the shortest time period appeared obviously preferable. Due, in particular, to the patchiness of the resultant high phytoplankton biomass, it was determined that a temporal interpolation over no longer than three days and for all the ocean data, was optimal. The evaluation determined that optimal results were obtained by applying, to the original daily images:

(i) a spatial fill per image for missing ocean data using a mean box function of size 7x7 pixels, requiring a minimum of 50% good valid pixels. All original valid ocean data values were retained, and then

(ii) a three day temporal interpolation on all ocean data using a $^1/_7$, $^5/_7$, $^1/_7$ weighting.

Thereafter, three and five day arithmetic means were generated from the daily, interpolated time series. There were two periods during which a number of daily images were missing, namely SST for 16-21 November 1998 and chlorophyll for 14-21 September 1998, and hence consecutive means could not be generated for these periods. Subsequent results obtained from these periods should therefore be considered with caution. Monthly, annual and five year means were also generated. However, original non-interpolated data were used for the generation of these longer period means. The implication of the three day sampling is such that the shortest period that can be adequately resolved is of the order of 10 days or more (Emery & Thomson, 2001). Synoptic-scale three to seven day events are excluded and hence caution must be applied in interpreting the processes giving rise to any one signal. For the purpose of this thesis, therefore, the event scale refers to short-term intra-seasonal events.

Since, primary to this study is the exploitation of high spatial and temporal resolution NOAA and SeaWiFS data, further work discussed in this thesis focuses on using the three day mean images. The

relevant five year time series, extending from July 1998 to June 2003, comprises a total of 610 three day mean files for each of the SST and chlorophyll parameters.

3. Results

The upwelling processes in the southern Benguela are influenced to a large degree by bottom topography – this is clearly illustrated by comparison of the bathymetry of the region (Fig. 5.1a) with the five year mean (July 1998-June 2003) SST and chlorophyll images (Figs. 5.1b and 5.1c). Hence, a first assessment of the dynamic variations in SST and chlorophyll in this region was undertaken by examination of these parameters over different depths of the continental shelf. Hovmöller (1949) shelf width-averaged plots (Section 3A) were generated for the inner, mid- and outer continental shelves of the southern Benguela comprising latitudinal mean shelf width values of the parameters over time.

However, the shelf widths vary considerably alongshore, and the offshore extent of SST and chlorophyll variability may not be adequately resolved. In Section (3B), therefore, a number of key latitudinal lines were selected and Hovmöller latitudinal plots were generated to show the variation of the offshore extent of SST and chlorophyll. In Chapter 6, a number of key inshore locations were selected in order to examine the variation of SST and chlorophyll over the five year study period, to generate upwelling indices, and to explore the relationship between these parameters.

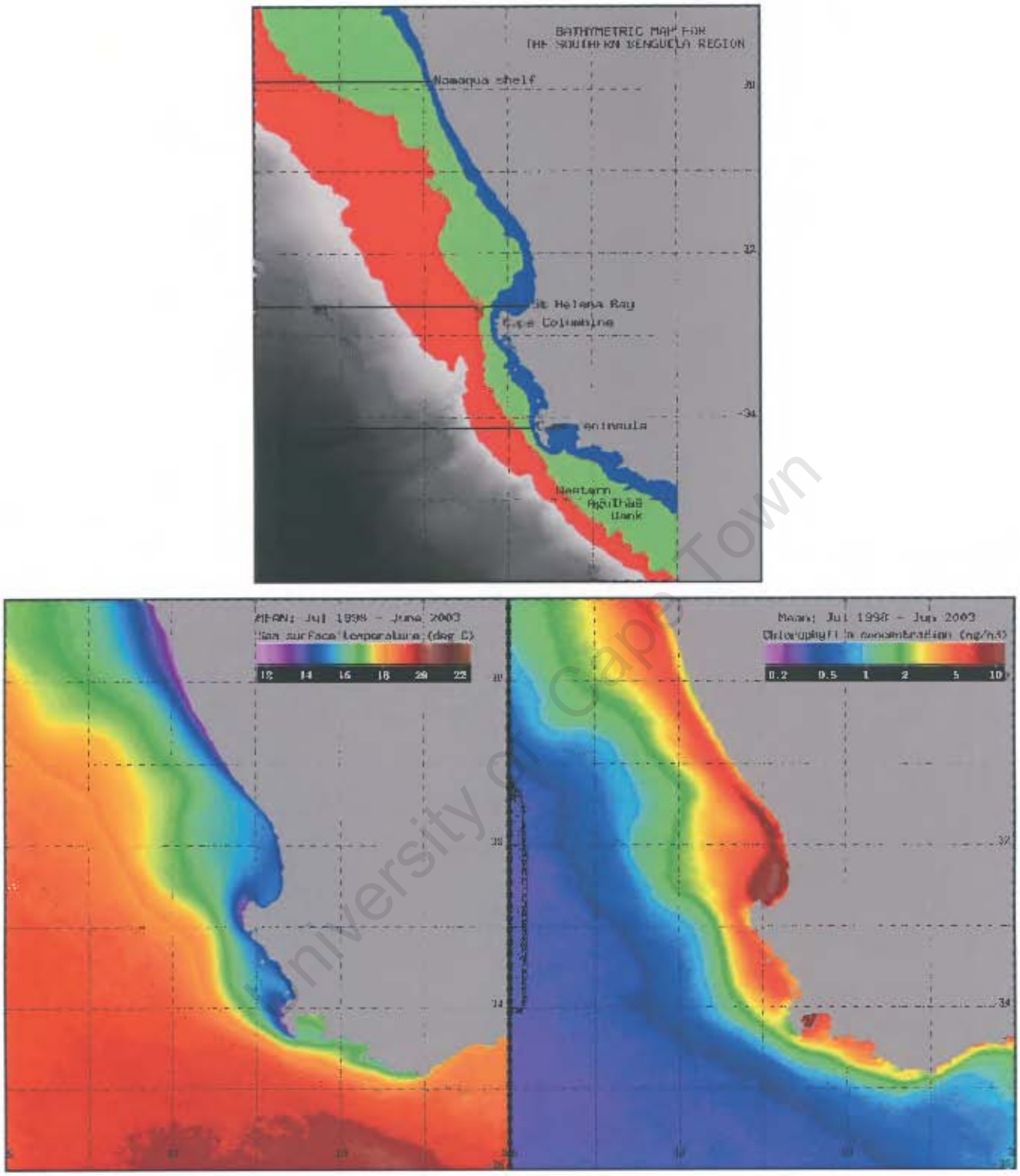

Figure 5.1. (a) Southern Benguela bathymetry: inner shelf: 0-100m (blue), mid-shelf: 0-200m (green), and outer shelf: 200m-500m (red); (b) mean SST for July 1998-June 2003; (c) mean chlorophyll for July 1998-June 2003. The three key latitudinal lines, for which Hovmöller latitudinal plots are generated, are overlain on the bathymetry map.

3A. Bathymetric influence

Hovmöller shelf width-averaged plots

The bathymetric file for the region of interest (Fig. 5.1a) was generated from ETOPO2 data (http://www. ngdc.noaa.gov/mgg/fliers/01mgg04.html) at a two nautical mile resolution, and projected to a cylindrical equirectangular projection so as to exactly coincide with that of the SST and chlorophyll time series (Chapter 2). A high resolution (1km) continental outline (CIA Database, http://seadas.gsfc.nasa.gov/doc/ seadisp/coast.html) was overlain and the data manually corrected so as to accurately reflect the landmass outline. Coastal bays and islands were masked to exclude them from any computation. Similarly, data eastwards of 20E°S were excluded from the analysis. The 100m and 200m contours were then smoothed according to detailed local surveys (Marine and Coastal Management, Cape Town). The inner continental shelf was defined as the area with water depth at or less than 100m (blue), the mid-shelf for depths of 100m to 200m (green), and the outer shelf for depths of 200m to 500m (red).

Latitudinal and temporal patterns of SST and chlorophyll variability for the inner, mid- and outer continental shelves are illustrated in Figure (5.2). These Hovmöller plots (hereafter referred to as shelf width plots), were generated from the three day mean time series to include data from 29.00°S in the north to 35.18°S, the latter being the southern tip of the 100m isobath. Note that each value in a shelf width plot represents the latitudinal mean of the particular shelf width for a three day mean image in the five year period. Missing values were minimal (< 2%), being mostly on the inner continental shelf during winter months. The missing values were interpolated by means of the Delaunay Triangulate procedure and a Trigrid function (IDL Reference Guide, 2003).

The inner continental shelf (0-100m depth)

Sea surface temperature

The SST shelf width plot for the inner shelf (Fig. 5.2a) shows two distinct bands of cold (9–13°C) water from approximately 32.7°S to 33.0°S and from 33.9°S to 34.3°S, representing the upwelling cells of Cape Columbine and the Cape Peninsula, respectively. These cold water bands appear synchronous in nature and generally more intense in the spring /summer months, being most intense during summer 2000 (Feb-Apr) and spring/summer 2000/2001 (Nov -Apr). The pulsating nature of the cold upwelling events is evident, particularly when most intense, at which times cold upwelled water is also apparent along the length of the inner shelf between these Capes. The intense upwelling

of summer 2000 (Fig. 5.2a; Roy et al., 2001) occurred following a distinct warm event in December 1999, at which time a band of warm (20–22°C) water extended the length of the inner shelf of the southern Benguela. A second, but less intense warm event is seen in February 2002.

In the north, cold water off the Namaqua upwelling cell extends over a much broader latitudinal range, from the northward extent of the analysis region (29.0°S) southward to, on average, 30.7°S, and appears more perennial in nature. Southward of this, and towards the broad inner shelf of St Helena Bay, sea surface temperatures largely reflect a seasonal insolation pattern. In the Cape Peninsula area, an abrupt change in SST pattern is notable at 34.35°S due to the combined affects of (a) this being the southern limit of the Cape Peninsula upwelling cell and (b) the sudden broadening of the inner shelf immediately to the south of the Peninsula (Fig. 5.1a). A strong seasonal signal is evident in the waters to the south thereof, on the western Agulhas Bank, due to both insolation and the influence of warmer waters of Agulhas Current origin. However, intense upwelling events are seen to also manifest on the western Agulhas Bank (Feb-Apr 1999, Feb-Apr 2000, Feb-Apr 2001), as far south as Cape Agulhas (35°S).

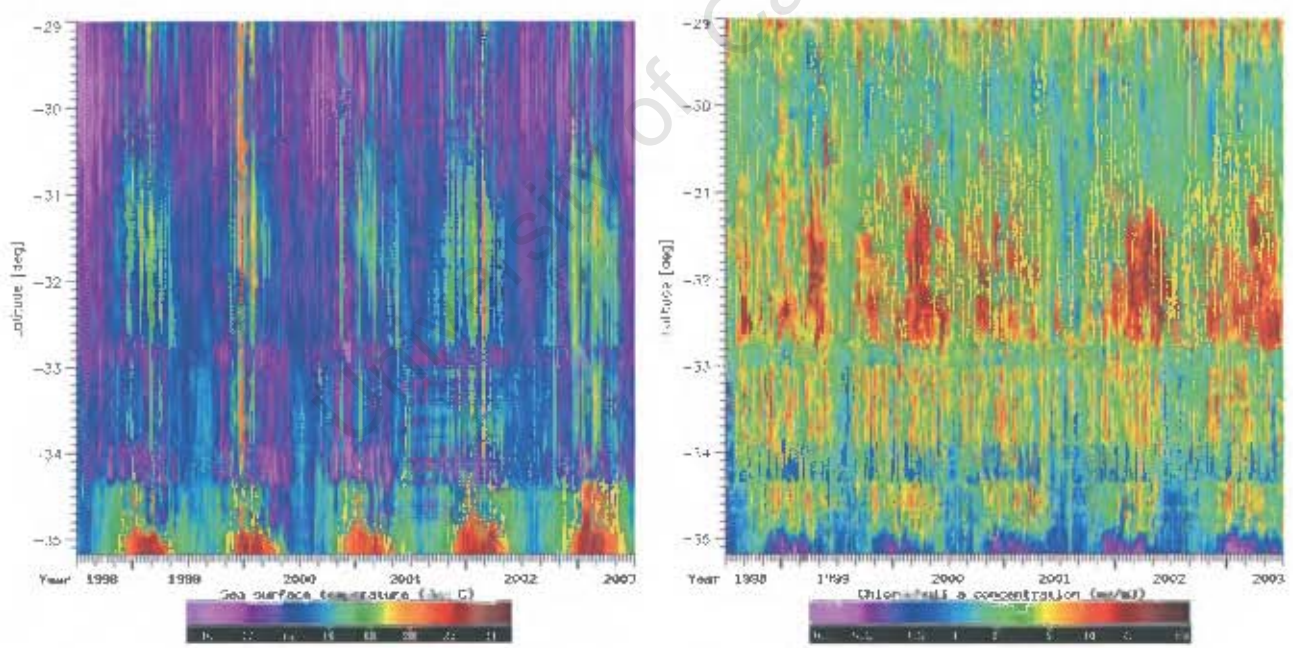

Figure 5.2. Hovmöller shelf width-averaged plots for the Southern Benguela inner shelf (0-100m) from 29.00°S to 35.18°S; (a) SST for July 1998-June 2003; and (b) chlorophyll a concentration for July 1998-June 2003.

Chlorophyll a concentration

Chlorophyll concentration on the inner shelf of the southern Benguela (Fig. 5.2b) to a large degree mirrors the pattern of SST variability (Fig. 5.2a), similarly dominated by the event scale processes.

Two distinct bands of lower chlorophyll (< 3mg m^{-3}) water are seen to coincide with the cold water bands described above, at the locations of the Cape Columbine and Cape Peninsula upwelling cells, chlorophyll in the latter being even lower that that on the Cape Columbine inner shelf. The pulsation of the event scale is particularly evident in the Cape Peninsula band, where pulses of very low chlorophyll (< 1mg m^{-3}) appear to correspond with very cold water (9–12°C) events. Highest chlorophyll concentrations are apparent in St Helena Bay and the inner shelf extending to the north thereof, with very high chlorophyll concentrations (> 10mg m^{-3}) sustained during the late summer months (generally Feb-early May), with the exception of summer 2001. Comparison with the SST for this area (Fig. 5.2a) reveals a relatively cool summer 2001 with typical warmer summer SSTs (> 19°C) not experienced in the St. Helena Bay area.

No clear seasonal chlorophyll signal is generally apparent along the inner shelf of the southern Benguela (Fig. 5.2b), although lower biomass is somewhat evident in the July -August winter months. Along the Namaqua inner shelf, though, the more perennial nature of upwelling appears to result in a corresponding biological response. In the south, an abrupt change in chlorophyll at 34.35°S again mirrors that of the SST pattern noted above. A seasonal chlorophyll signal is evident in the waters of the western Agulhas Bank, with warmer waters of Agulhas Current origin (Fig. 5.2a) showing very low chlorophyll concentrations (Fig. 5.2b).

Mid-continental shelf (100-200m depth)

Sea surface temperature

The marked Cape Columbine and Cape Peninsula cold water bands shown for the inner shelf (Fig. 5.2a) are still clearly visible over the mid-shelf (Fig. 5.2c), albeit less distinctly. The offshore extension onto the mid-shelf of cold upwelling events at these Capes is less pronounced in the spring/summer months of 2001/2002 and 2002/2003 than in the previous 3 years. Most distinguishable is the very intense cold event of summer 2000 (Feb-Apr), the upwelled waters again clearly evident off Cape Columbine and Cape Peninsula and sustained along the length of the mid-shelf between these Capes. This is preceded by the intense warm event of December 1999 extending the length of the mid-shelf of the southern Benguela. Cold upwelled water is also clearly reflected on the mid-shelf in spring/summer 2000/2001 and 1998/1999, at times extending southwards towards Cape Agulhas. A second less intense warm event is noted north of Cape Columbine at the end of January 2000, with further warm events (>19°C) on the mid-shelf at the end of January and of February 2002, while, in 2003, warm water was fairly persistent from mid-February to early March.

Since each value in the shelf width plots represents the latitudinal mean of the shelf width, sea surface temperatures northwards of the Cape Columbine plume reflect a broader mid-shelf mean and hence generally portray seasonal insolation. As such, Namaqua cell upwelling extending onto the broad mid-shelf may therefore be masked. (The line breaks visible at 30.3°S and 30.7°S are a function of a rapid change in bathymetric contour orientation.) On the western Agulhas Bank, a strong seasonal signal is again evident due to insolation and the influence of warmer waters of Agulhas Current origin. A warm water intrusion from the south is apparent in June 2001, extending northwards almost as far as Cape Columbine. This is clearly visible in SST imagery (Fig. 5.3a) following the shedding of an anticyclonic ring from the Agulhas Current, and confirmed in Topex Poseidon/ERS2 altimeter data (not shown).

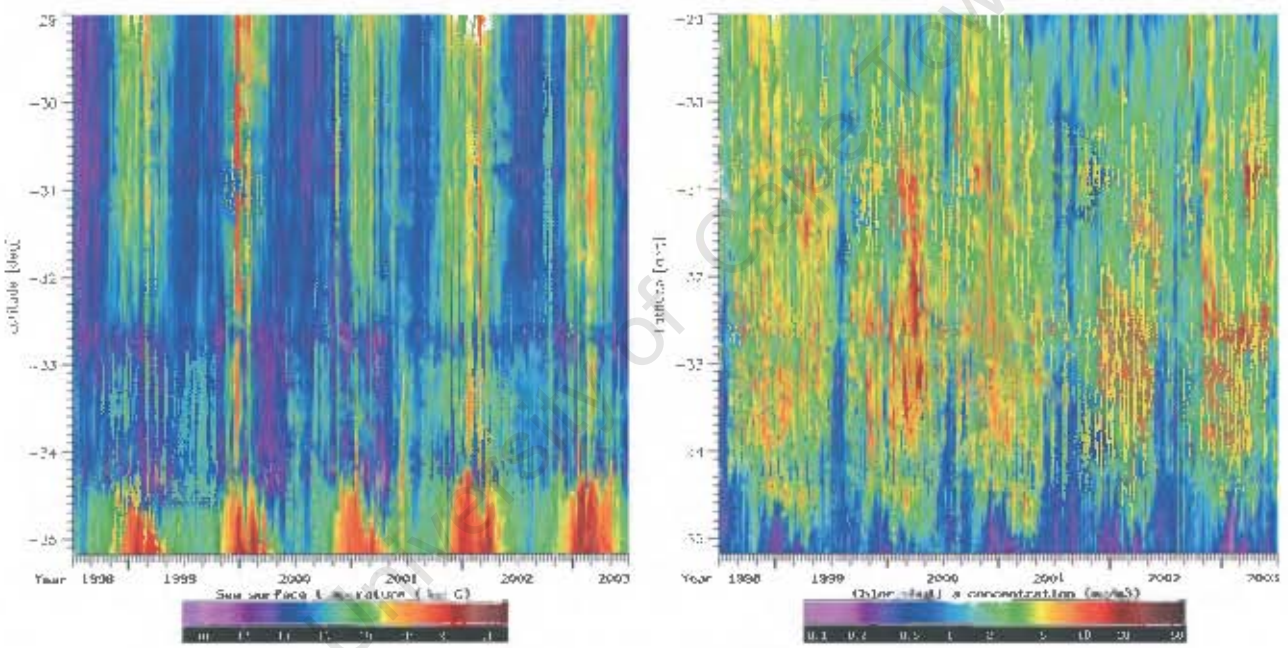

Figure 5.2. Hovmöller shelf width-averaged plots for the Southern Benguela mid-shelf (100-200m) from 29.00°S to 35.18°S; (c) SST for July 1998-June 2003; and (d) chlorophyll *a* concentration for July 1998-June 2003.

Chlorophyll a concentration

Different to the SST, chlorophyll distribution over the mid-shelf (Fig. 5.2d) is more uniform from the Cape Peninsula northwards to the Namaqua shelf. No lower chlorophyll band (< 3 mg m^{-3}) is obvious off Cape Columbine. The change in orientation of the 200m bathymetric contour (Fig. 5.1a) just north of Cape Columbine does lead to some discontinuity, and also further to the north at 30.3 °S and 30.7°S. While not distinct, a somewhat lower chlorophyll band is discernable off the Cape

Peninsula. In general, the pattern is of higher chlorophyll (> 2mg m^{-3}) throughout, although chlorophylls of less than 1mg m^{-3} are observed along the mid-shelf during most winter months (Jun-Aug). The overall pattern of variability over the mid-shelf also manifests high chlorophyll (> 10mg m^{-3}) on the event scale, being highest in summer 2000 (Feb-Apr) from north of the Cape Peninsula to about 30.3°S. High chlorophyll events also appear more evident in the spring/summer months of 2002/2003.

Very low chlorophyll (< 0.5mg m^{-3}) is observed in the warmer Agulhas-conditioned waters on the western Agulhas Bank mid-shelf during summer months. The latter is particularly low (< 0.2mg m^{-3}) during January - March 2003, coincident with very warm waters (> 23°C) over the western Agulhas Bank mid-shelf (Fig. 5.2c). Very low chlorophyll is also noted here in June 2001 coincident with the previously noted warm water intrusion from the south.

Outer continental shelf (200-500m depth)

Sea surface temperature

The dominant pattern of SST variability along the outer shelf (Fig. 5.2e) is seasonal. Interannual variation is apparent, with comparatively cooler SST in spring/summer 2000/2001. However, north of 30.4°S, the averaged values are not representative of the mean outer shelf due to the western boundary limit of the study area (Fig. 5.1a). The intense upwelling signal of summer 2000 is seen to have extended even onto the outer shelf where cool waters (12-14°C) are evident from Cape Peninsula to Cape Columbine. The slight decrease in cool water signal at 33.3°S is due to the rapid change in orientation and broadening of the outer shelf at this location (Fig. 5.1a). Similarly, pulses of cold upwelled water onto the outer shelf are evident during spring/summer 2000/2001, while that of summer 1998/1999 is less clear. The warm event of December 1999 is prominent even along the length of the outer shelf. Warmest waters are seen on the western Agulhas Bank where the influence of the Agulhas Current is apparent, being more pronounced during the summers of 2002 and 2003. The warm intrusion from the south in June 2001 (Fig. 5.3a) is seen to have extended over the outer shelf as far north as Cape Columbine.

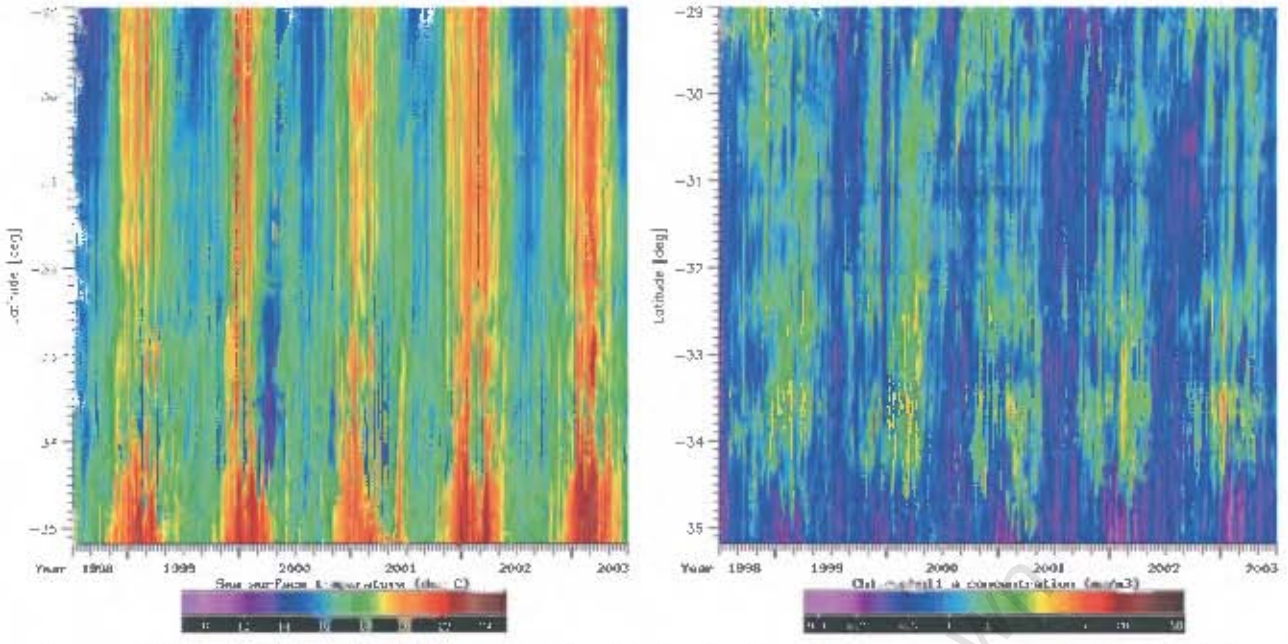

Figure 5.2. Hovmöller shelf width-averaged plots for the Southern Benguela outer shelf (200-500m) from 29.00°S to 35.18°S; (e) SST for July 1998-June 2003; and (f) chlorophyll *a* concentration for July 1998-June 2003.

Chlorophyll a concentration

Chlorophyll concentration over the outer shelf of the southern Benguela (Fig. 5.2f) is generally low (< 3mg m^{-3}) although a seasonal signal is evident. Somewhat higher chlorophyll is shown during spring/summer months, particularly south of approximately 32°S. Here, higher chlorophylls (> 5mg m^{-3}) are seen to extend onto the outer shelf, generally coincident with cool water extended onto the outer shelf (Fig. 5.2e). On the western Agulhas Bank, chlorophyll remained very low (< 0.5mg m^{-3}), especially during the summers of 2002 and 2003, coincident with warm Agulhas-modified waters at that time.

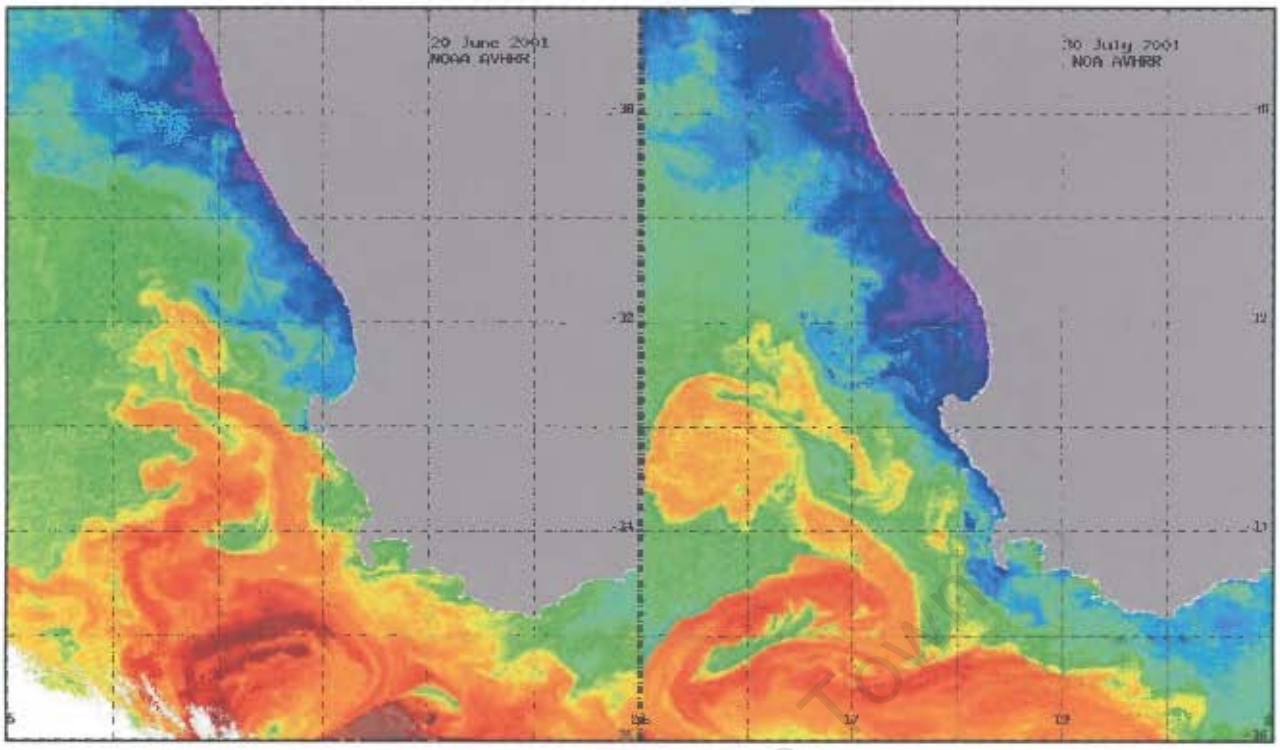

Figure 5.3. (a) SST image for 20 June 2001 showing the warm water intrusion following the shedding of an anticyclonic ring from the Agulhas Current; (b) SST image for 30 July 2001 showing enhanced offshore SST due to the offshore location of the shed Agulhas ring.

3B. Offshore extent

Hovmöller latitudinal plots

The Hovmöller shelf width plots generated above for the inner, mid- and outer continental shelves of the southern Benguela (Figs. 5.2a - 5.2f) provide a first evaluation of the dynamic variations in SST and phytoplankton biomass in this region. In order to better resolve the offshore extent of this variability along the varying shelf widths, a number of key latitudinal lines were next selected (Fig. 5.1a) for which Hovmöller latitudinal plots (hereafter referred to as latitudinal plots) were generated.

The latitudinal plots were generated from the five year SST and chlorophyll three day mean time series. Each line in a plot represents an average of five image data lines centred at the particular key latitude and extending 300 pixels (288km) offshore, after allowing for a landbuffer of 2 pixels (which are not included). For the purpose of this thesis, latitudinal plots of only three key latitudes are shown, namely the Cape Peninsula, St Helena Bay and the Namaqua shelf (Fig. 5.1a). These latitudinal lines represent varying widths of the inner, mid- and outer shelves. Due to the western boundary of the study region (15E), the Namaqua latitudinal plots are unfortunately limited to extend

only 200 pixels (192km) offshore, after the 2 pixel landbuffer, and thus only partially include the outer shelf data values. As for the shelf width plots, missing values were interpolated by means of the Delaunay Triangulate procedure and a Trigrid function (IDL Reference Guide, 2003).

The Cape Peninsula latitudinal line

Sea surface temperature

The C Peninsula latitudinal line (Fig. 5.1a; 34.13°S) represents a key latitude having both a narrow inner and mid-shelf, with an outer shelf of moderate width. Most dominant in the Cape Peninsula SST latitudinal plot (Fig. 5.4a) is the cooler (< 14°C) water confined primarily to a narrow band inshore with a strong seasonal signal extending over much of the offshore distance. Interannual variability is noted in the seasonal offshore signal, with the coolest spring/summer occurring in 2000/2001. Event scale pulses of cold (9–13°C) water are seen extending offshore beyond the narrow inner shelf, being most intense during the spring/summers of 1999/2000 and 2000/2001, during which times cold water extended up to 100km offshore. Less intense cold water pulses are also evident at other times through the five year time series.

The onshore movement of warm (19–21°C) water in December 1999 is apparent but, although not reaching the coast, warm onshore movement is also evident each summer (Dec-Mar), interspersed between cold events. Interestingly, the most sustained warm event at this latitude is seen to have occurred during winter 2001 (May/Jun) following the shedding of the above-mentioned anticyclonic ring from the Agulhas Current (Fig. 5.3a). The subsequent anticyclonic entrainment of warm Agulhas waters was felt even on the Peninsula inner shelf, as the Agulhas ring moved in a northwesterly direction, closely approaching the shore. Another such pronounced Agulhas ring passed further offshore during October 2002, the warm (19–21°C) waters approaching only the outer Peninsula shelf. This event was preceded by an intrusion of cold water at a distance greater than 200km offshore (Fig. 5.4a).

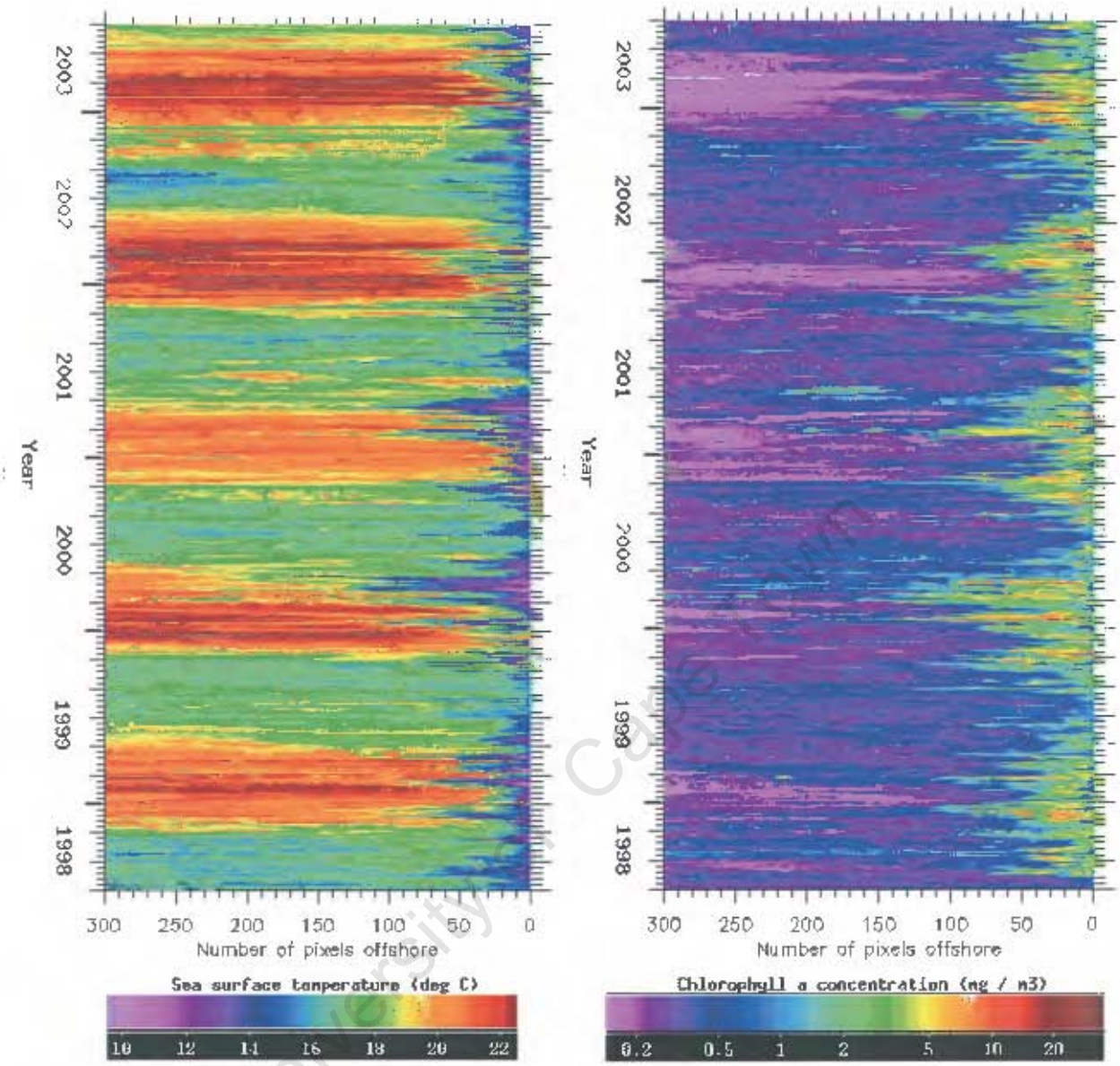

Figure 5.4. Hovmöller latitudinal plots for the period July 1998 to June 2003. Three day mean (a) SST and (b) chlorophyll *a* concentration for the Cape Peninsula latitudinal line, extending 300 pixels (288km) offshore

Chlorophyll a concentration

Chlorophyll concentration off the Cape Peninsula (Fig. 5.4b) shows a different pattern of variability to that of the associated SST (Fig. 5.4a). The region beyond the outer continental shelf comprises generally very low chlorophyll (< 1mg m^{-3}) with no strong seasonal signal. Inshore chlorophyll, although also relatively low in concentration (< 3mg m^{-3}), does exhibit a seasonal signal.

Highest chlorophyll events (> 5mg m^{-3}) with most offshore extension are seen primarily in spring/summer, especially when cold upwelled waters appear most intense (spring/summers of 1999/2000 and 2000/2001). At such times, the higher chlorophyll is displaced slightly offshore, low chlorophyll being coincident with freshly upwelled waters on the inner shelf. Slightly elevated chlorophyll (1-3mg m^{-3}) observed offshore at times (for example, end February and end April, 2001), is due to the presence of filaments or eddies comprising the convoluted frontal boundary.

The St Helena Bay latitudinal line

Sea surface temperature

The continental shelf along the St Helena Bay latitudinal line (Fig. 5.1a; 32.65°S) comprises a broad inner shelf, narrow mid-shelf, and broad outer shelf. The SST along this latitudinal line (Fig. 5.4c) generally shows a very different trend to that off the Cape Peninsula (Fig. 5.4a). Most notable is the strong cold water signal along the boundary of the 100m isobath, approximately 40 pixels offshore (Fig. 5.4c), where the core of the Cape Columbine upwelling plume extends northward from the Cape Columbine headland along the inner shelf boundary.

When most intense (9–13°C), the Cape Columbine plume appears to retain cold water inshore in St Helena Bay, while also limiting the onshore movement of warmer water (> 17°C). However, strong onshore warm water events are seen to occur, being particularly intense in December 1999, and in February 2002. At other times in spring/summer, warmer water is apparent inshore of a moderate plume signal, probably due to retention and seasonal warming in the Bay. Offshore extension of cold water onto the outer shelf is strongest in February - April 2000, but also frequently evident at other times as cold event scale pulses. Similar to the Cape Peninsula SST latitudinal line (Fig. 5.4a), a strong seasonal signal dominates the region offshore beyond the continental shelf, also demonstrating some interannual variability.

Chlorophyll a concentration

Chlorophyll concentration along the St Helena Bay latitudinal line (Fig. 5.4d) is appreciably higher than along the Cape Peninsula line (Fig. 5.4b). The offshore extension and distribution of higher chlorophyll (> 3mg m^{-3}) over the broader continental shelf is seen as generally double that over the narrower Cape Peninsula shelf.

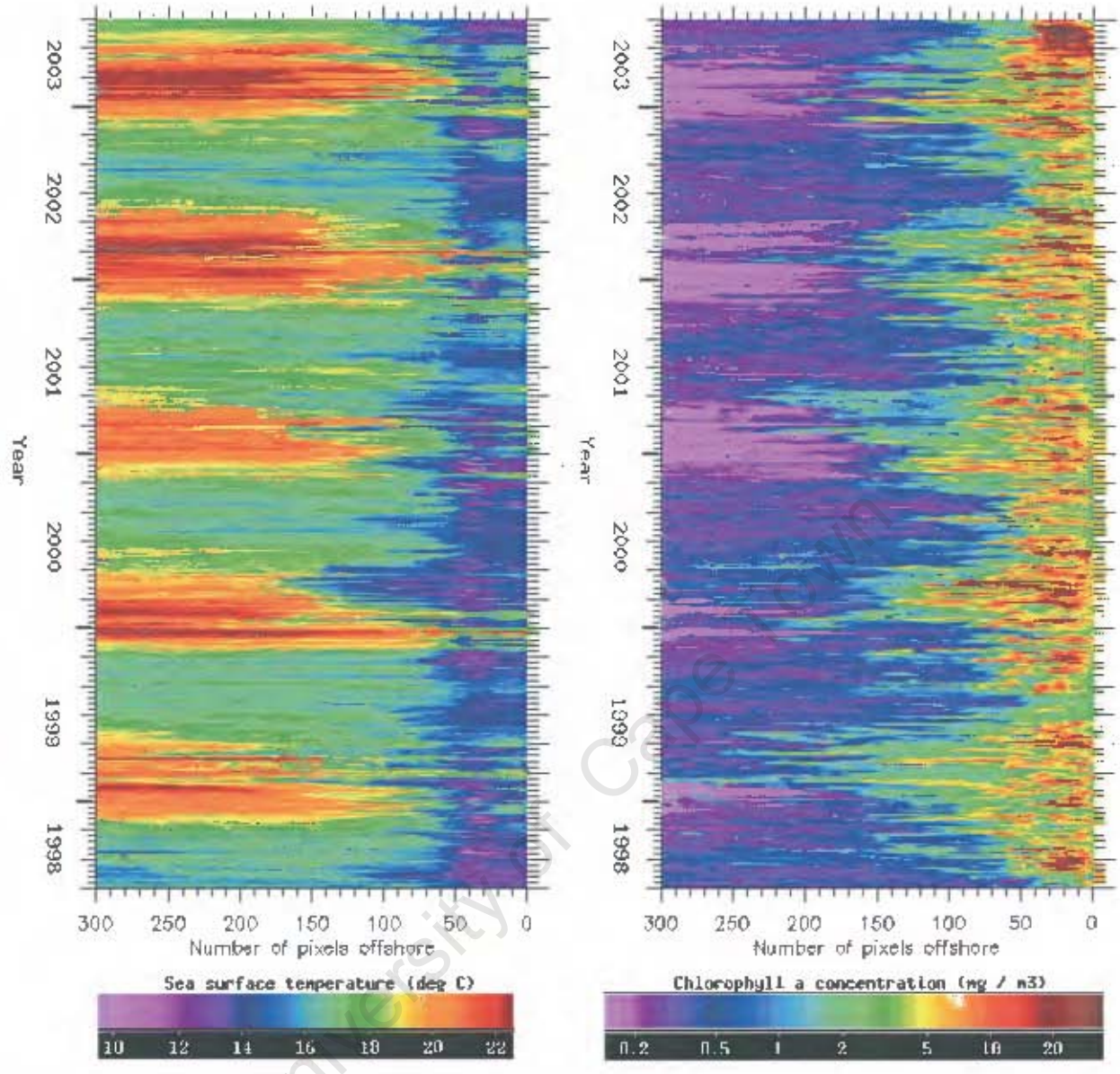

Figure 5.4. Hovmöller latitudinal plots for the period July 1998 to June 2003. Three day mean (c) SST and (d) chlorophyll *a* concentration for the St Helena Bay latitudinal line, extending 300 pixels (288km) offshore.

High chlorophyll (> 5mg m^{-3}) is apparent throughout the year but with greater offshore extension in the spring/summer months (Nov-Apr). At such times, event scale pulses of high chlorophyll appear to be associated with strong offshore cold water events. Retention of high chlorophyll concentrations on the inner shelf does seem generally apparent, with a lower chlorophyll signal visible at times along the inner shelf boundary (Fig 5.4d: 40 pixels offshore), coincident with the cold Cape Columbine plume. High chlorophyll may be visible on either side of this plume signal. Lowest chlorophyll (> 0.2mg m^{-3}) is generally noted furthest offshore, coincident with warm water (> 20°C) during the summer months.

The Namaqua shelf latitudinal line

Sea surface temperature

The third key latitudinal line to be considered in this thesis, the Namaqua shelf line (Fig. 5.1a; 29.90°S), is located in the northernmost part of study region, having a narrow inner shelf, a broad mid-shelf but only partly representing the outer shelf. In contrast to the SST for the previous two key latitudinal lines (Figs. 5.4a and 5.4c), there is a strong cold water seasonal signal extending across the width of the Namaqua line (Fig. 5.4e), being most intense during winter. Correspondingly, a strong onshore warm water seasonal signal is seen of equivalent extent, being most intense during the summer months. Cold upwelled water is still evident on the event scale during summer, but confined primarily to the narrow inner shelf. Some interannual variability is generally apparent, the warmest winter being that of 2001, following the coolest summer. The strong warm event of December 1999 is also clearly observed at this latitude, this signal thus appearing to be evident along the length of the southern Benguela.

Chlorophyll a concentration

Although less concentrated than chlorophyll along the St Helena Bay line (Fig. 5.4d), moderate to high biomass (2-10mg m^{-3}) extends along the width of the Namaqua latitudinal line (Fig. 5.4f), across the broad mid-shelf and onto the outer continental shelf. This considerable offshore extent is apparent throughout the year despite the strong seasonal signal seen in the associated SST (Fig. 5.4c).

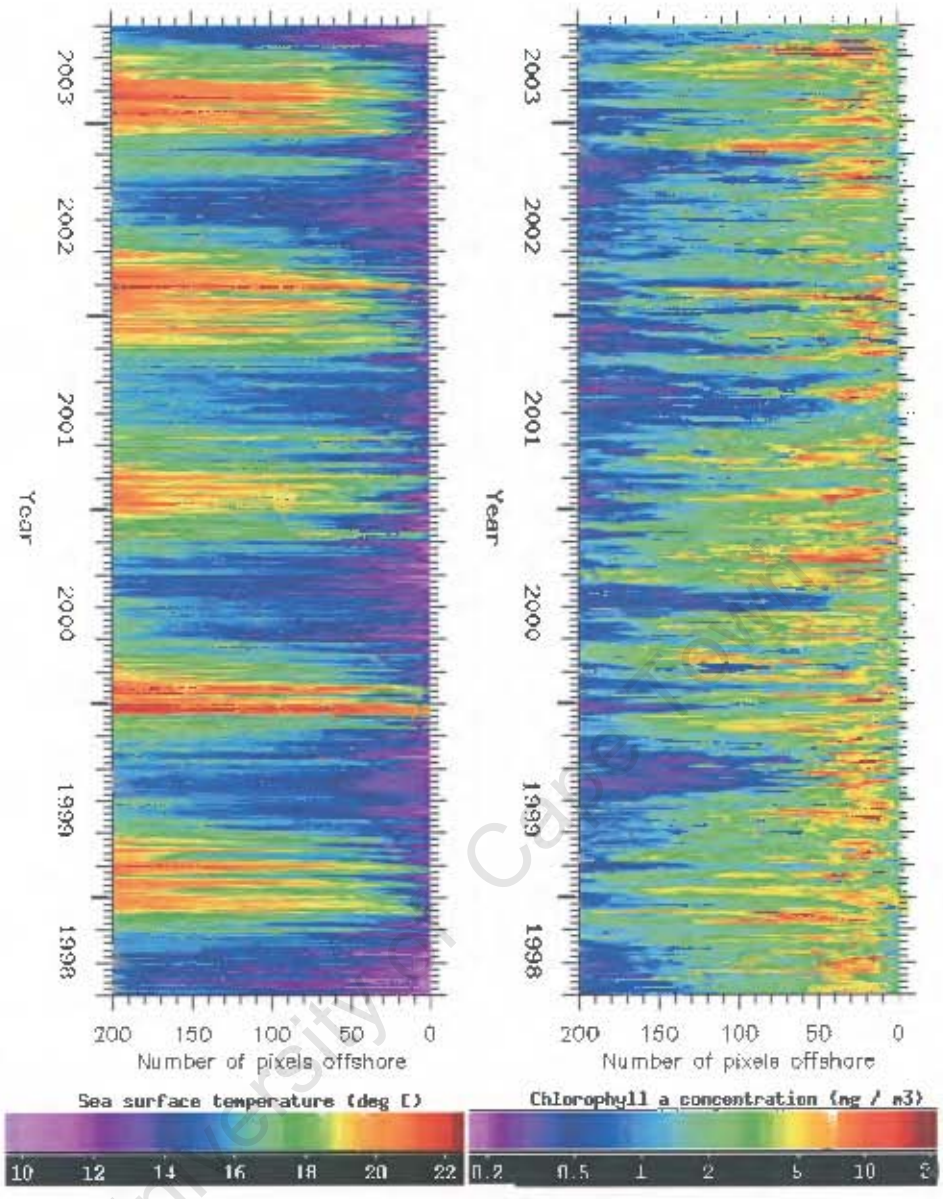

Figure 5.4. Hovmöller latitudinal plots for the period July 1998 to June 2003. Three day mean (e) SST and (f) chlorophyll a concentration for the Namaqua Shelf latitudinal line, extending 200 pixels (192km) offshore.

There appears to be no obvious correlation between the two parameters. Rather, it seems that moderate chlorophyll concentrations are generally spread across the width of the broad shelf, a slight offshore displacement coincident with very cold water (9-12°C) on the inner shelf. Pulses of higher chlorophyll (>5mg m^{-3}) are observed at intervals throughout on the event scale.

3C. Latitudinal line correlations

Sea surface temperature vs chlorophyll concentration

In order to explore the relationship between sea surface temperature and chlorophyll in Figure (5.4), a correlation analysis was performed between these two parameters for the three key latitudinal lines. Only the non-interpolated values were used, and being in byte format, the output is therefore quantised.

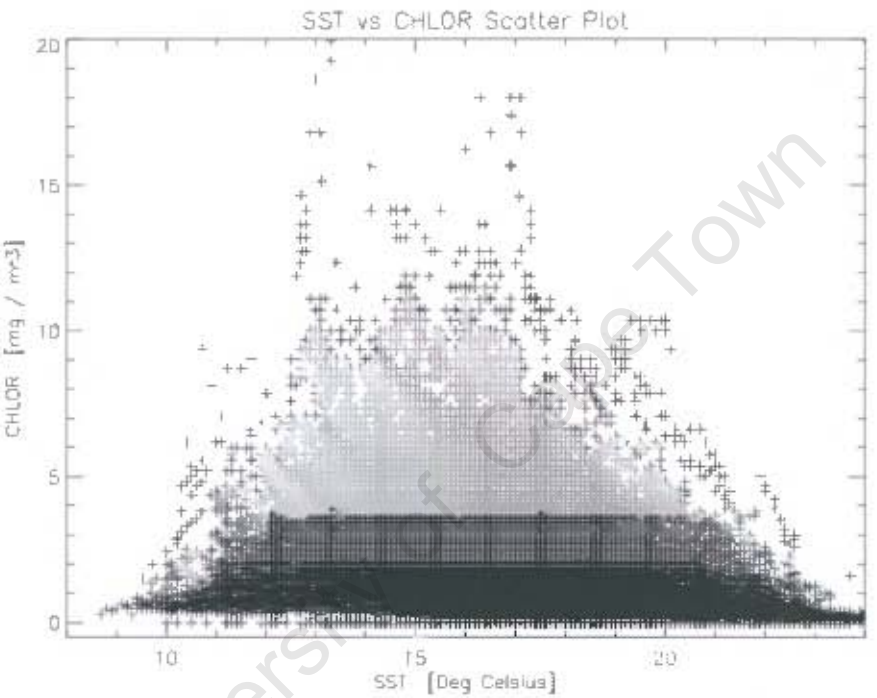

Figure 5.5. Correlation of SST and chlorophyll *a* concentration for the Cape Peninsula latitudinal line values.

No strong correlation is seen between SST and chlorophyll for the Cape Peninsula latitudinal line (Fig. 5.5). The vast majority of points represent offshore values of chlorophyll concentrations less than 2 mg m^{-3} across a range of temperature from approximately 11 - 23°C. These low chlorophyll values are also seen at the lower end of the temperature scale (< 11°C), where they represent freshly upwelled waters on the inner shelf. Higher chlorophyll concentrations tend progressively towards SSTs of about 12.5-20°C, values between about 2-7 mg m^{-3} representing phytoplankton in recently upwelled waters. Highest concentrations (> 7 mg m^{-3}) are generally coincident with temperatures of 12.5-17.5°C.

A very similar correlation (not shown) is observed for the Namaqua latitudinal line, except that chlorophyll concentrations are approximately double that of the Cape Peninsula line. Higher chlorophyll values (> 5 mg m^{-3}) relate to SSTs of 13-17°C, representing biomass across the broad mid-shelf, with concentrations of up to 40 mg m^{-3}. For the St Helena Bay latitudinal line parameters, the correlation (not shown) shows warmer offshore temperatures (> 19°C) coincident with lower chlorophyll (< 5 mg m^{-3}). Higher chlorophyll across the range of 7 – 50 mg m^{-3} is fairly evenly distributed between SSTs of 12-17°C. Generally, chlorophyll concentration along the St Helena Bay line appears almost four times higher than that of the Cape Peninsula line, and double that of the Namaqua line.

4. Summary

The extent and frequency of upwelling during the period July 1998 through June 2003 and the biological response to this physical forcing has been addressed in this chapter by focusing on specific questions outlined in the introduction. The shelf width plots (Section 3A) comprising the latitudinal mean values of the inner, mid- and outer continental shelves allow clear identification of the location and emergence of upwelling cells as well as the spatial and temporal variation in chlorophyll along the length of the southern Benguela. The Cape Columbine and Cape Peninsula upwelling cells are identified in the SST plots as two distinct bands of cold water (9–13°C) on the inner shelf, the upwelling synchronous in nature and, when intense, sustained along the length of the inner shelf between the Capes. These cold water bands are still visible over the mid-shelf. Upwelling is generally more intense at these locations in the spring /summer months. The Namaqua upwelling cell is identified on the inner shelf SST in the north as extending over a much broader latitudinal range, and more perennial in nature. Most remarkable in the SST inner and mid-shelf plots is the rapidly pulsating nature of upwelling in the southern Benguela, with intense warm/cold events clearly distinguished. Conversely, the dominant pattern of SST over the outer shelf is that of seasonal insolation, although particularly intense upwelling events are seen to extend to this part of the shelf. In the south, both the seasonal and event scale influence of warmer waters (>20°C) of Agulhas Current origin are clearly identified in the inner, mid- and outer shelf SST plots.

Chlorophyll concentration on the inner shelf to a large degree mirrors the pattern of SST variability, similarly dominated by the event scale processes. Two distinct bands of lower chlorophyll (< 3mg m^{-3}) coincide with the locations of the Cape Columbine and Cape Peninsula upwelling cells, event scale pulses of very low chlorophyll (< 1mg m^{-3}) appearing to correspond with intense upwelling events,

especially in the Cape Peninsula upwelling cell. Highest chlorophyll concentrations are apparent in St Helena Bay and the inner shelf extending to the north thereof, with very high chlorophyll concentrations (> 10mg m^{-3}) being most sustained during the late summer months. In comparison to the SST, chlorophyll over the mid-shelf is more uniform from the Cape Peninsula to the Namaqua shelf, although still manifesting the event scale. In general, the pattern is of higher chlorophyll throughout all seasons, although low biomass is observed during most winters. In the south, as for SST, a clear seasonal signal is apparent in all three shelf width plots, with the seasonal and event scale intrusions of warmer Agulhas-conditioned waters yielding particularly low chlorophyll. Chlorophyll concentration over the outer shelf is generally low (< 3mg m^{-3}).

The Hoffmueller latitudinal plots (Section B) show the offshore extent of SST and chlorophyll at selected key latitudes allowing investigation of this variability at locations of differing shelf width. The Cape Peninsula line comprises both a narrow inner and mid-shelf, with outer shelf of moderate width, the St Helena line a broad inner, narrow mid-, and broad outer shelf and the Namaqua line a narrow inner and broad mid-shelf, the outer shelf being only partly represented by the study region.

The most dominant feature in the Cape Peninsula SST latitudinal plot is the cooler water (<14°C) confined primarily to the narrow inner shelf. Event scale pulses of this cold upwelled water are seen to extend beyond the narrow inner shelf up to 100km offshore when most intense. Offshore, a strong seasonal signal dominates, with event scale onshore movement of warm water (>19°C) evident each summer between upwelling events. Agulhas Current influences may readily be seen, with entrained Agulhas-conditioned waters being observed at times on the inner shelf of the Cape Peninsula. In contrast, the strongest cold water signal (9–13°C) along the St Helena Bay line lies offshore, at the location of the Cape Columbine upwelling plume. This plume appears to cause retention of water on the inner shelf, while also limiting onshore movement of offshore water. However, offshore extension of cold water across the narrow mid-shelf and onto the broad outer shelf is frequently evident on the event scale. The Namaqua SST line in the north contrasts with the previous two latitudinal lines, primarily by way of the large offshore extent of a seasonal upwelling signal, most intense during the winter. The strong cold water signal extends across the width of the broad mid-shelf, at times even onto the outer shelf. A corresponding strong onshore warm water movement is most intense during summer, when upwelling seems diminished. Upwelling at this latitude thus appears to enhance the seasonal signal.

Chlorophyll concentration along the Cape Peninsula latitudinal line shows a clear seasonal signal with offshore extension of higher chlorophyll (> 3mg m^{-3}) onto the outer shelf, beyond that of the associated upwelling signal, occurring primarily in spring/summer. With intense upwelling, higher chlorophyll is displaced slightly offshore, low chlorophyll being coincident with freshly upwelled water on the inner shelf. Along the St Helena Bay latitudinal line, chlorophyll is significantly higher than along the Cape Peninsula line and the offshore extension over the broader continental shelf is generally double that over the narrower Cape Peninsula continental shelf. High chlorophyll (> 5mg m^{-3}) is apparent throughout the year, but with greater offshore extension in spring/summer. Retention of high chlorophyll on the inner shelf is observed, lower chlorophyll coinciding with the cold Cape Columbine plume along the inner shelf boundary. Similar to the SST, the pattern of chlorophyll along the Namaqua line contrasts with the previous two latitudinal lines by way of the large offshore extent of the distribution. Somewhat less concentrated than along the St Helena line, moderate to high biomass (2-10 mg m^{-3}) extends across the broad mid-shelf and onto the outer shelf. This is apparent throughout the year despite the strong seasonal signal seen in the associated SST. As for the Cape Peninsula line, a slight offshore displacement of biomass is coincident with very cold water (9-12°C) on the inner shelf.

No strong correlation was found between SST and chlorophyll along the three latitudinal lines, although higher chlorophyll is seen to usually occur between 13-17°C. Chlorophyll biomass along the St Helena latitudinal line is found to be generally four times higher than along the Cape Peninsula line, and double that of the Namaqua line. In the following chapter (Chapter 6), SST upwelling and chlorophyll indices are derived for the selected latitudinal lines examined in this chapter, to enable intra-seasonal variations to be more comprehensively quantified and compared.

Chapter 6

A quantitative application of satellite data - towards developing operational indices for the Benguela ecosystem. Part 2.

1. Introduction

Further to examining the dynamic variations in upwelling and phytoplankton in the southern Benguela (Chapter 5), is the development of appropriate indices to quantify these intra-seasonal variations. The following hypothesis is proposed:
By using SST indices to determine the development of upwelling cells, and chlorophyll indices to determine the development of a phytoplankton bloom, it should be possible to elucidate the response of the phytoplankton biomass in relation to thermal changes due to upwelling.

Chapter (5), Section (3A) of this thesis provides clear identification of the location and emergence of upwelling cells, as well as the variation in chlorophyll along the inner, mid- and outer continental shelves of the southern Benguela during the period July 1998 through June 2003. Section (3B) identifies the variation in intensity and offshore extent of these parameters at selected key latitudes of differing shelf width. This Chapter comprises Part 2 of the quantitative application of NOAA and SeaWiFS satellite data to the southern Benguela, and initiates the development of appropriate indices towards their application in the operational management of the ecosystem.

A number of key locations are selected along the length of the southern Benguela. The dynamic variation of SST and chlorophyll over the five year time series (July 1998 – June 2003) is examined, upwelling indices are generated and the relationship between these parameters explored. Only the key locations as per the three selected latitudinal lines in Chapter (5) are discussed in this thesis, namely the Cape Peninsula, St Helena Bay and the Namaqua shelf locations (Fig. 5.1a).

2. Methodology

The mean value of a 5x5 pixel box at an inshore location along each latitudinal line was extracted from each SST three day mean image in the time series. The fluctuation over time of SST was thus generated for each key location.

Since sea surface temperature on the shelf is a combined measure of both upwelled waters and additional processes (for example, seasonal insolation, advection), it does not provide an adequate measure of upwelling intensity. A more suitable index of upwelling strength is determined by the difference in SST between an inshore location on the inner shelf and some distance offshore, providing a measure of the temperature difference moving offshore. A positive index indicates colder water at the coast, inferring active upwelling (Carr et al., 2003). Upwelling indices were therefore generated by determining the difference in SST between an offshore reference location and the 5x5 pixel box at the inshore location of the respective latitudinal line, for each three day mean image in the time series. For the offshore reference point, the 5x5 pixel mean value at the most offshore extent (300 pixels) of the particular latitudinal line plot (Figs. 5.4) was extracted.

Chlorophyll *a* concentration *per se* serves as a measure of phytoplankton abundance, and hence may be used as an index to understand the response of phytoplankton to upwelling. Hence, as for SST, the mean value of a 5x5 pixel box at an inshore location along each latitudinal line was extracted from each chlorophyll image in the time series. The dynamic variation over time of SST, upwelling and chlorophyll concentration were thus generated for each key location. Finally, the relationship between these parameters was explored.

3. Results

The fluctuations over the five year study period of SST, and indices of upwelling and phytoplankton (chlorophyll concentration) for the Cape Peninsula, St Helena Bay and Namaqua key locations are outlined below. A low pass filter was applied to the data such that the highest frequency component of the resultant dataset was ten percent of the frequency spectrum of the original dataset. The low pass filter was used merely as a visual aid in Figure (6). All the analyses were done on the unfiltered data. The low pass filters are overlain on the graphs in Figure (6). SST and chlorophyll are also correlated with upwelling, both for the full five year period and seasonally. Chlorophyll is correlated

with SST for each of the three key locations. The latitudinal line figures (Figs 5.4) in Chapter (5) are referenced.

Since the Namaqua key location is located in the northern part of the study region (Fig 5.1a) where the western boundary (15E) limits the offshore extent to 202 pixels at this latitude (29.90°S), it was not possible to gauge the strength of upwelling using a reference point of sufficient distance offshore. Hence an upwelling index was not determined for this particular location and only the sea surface temperature and chlorophyll parameters are explored for the Namaqua shelf in this thesis.

The Cape Peninsula key location

Cape Peninsula sea surface temperature

The Cape Peninsula SST latitudinal plot (Fig. 5.4a) shows cooler upwelled water confined primarily to a narrow band inshore. Hence, the selected key location for the Cape Peninsula was sited on the narrow inner shelf (34.13°S; 18.28°E) and comprises pixels one to five (the 5x5 pixel mean) of the Cape Peninsula SST latitudinal plot.

Most notable in the fluctuation over time of SST at this location (Fig. 6.1a) are the marked temperature changes associated with the rapid pulsation of the cold/warm events, also noted in the Cape Peninsula SST latitudinal plot. Pulses of cold water (9–13°C) are again seen most frequently during the spring/summer months, the overall pattern of variation tending towards generally cooler temperatures in spring/summer, with generally warmer temperatures during autumn/winter. However, warmest events (18-21°C) are also experienced in summer (Jan 1999, Dec 1999, Jan 2001, Jan/Feb 2002, Jan 2003) interspersed between cold events, as the strong summer SST frontal boundary moves shoreward under conditions of diminished upwelling. The warm winter event (>18°C) of June 2001 (Chapter 5) is evident even on this Cape Peninsula inner shelf location, as Agulhas-entrained waters closely approached the shore. Similarly, warm waters associated with a subsequently shed Agulhas ring are also evident in September 2001.

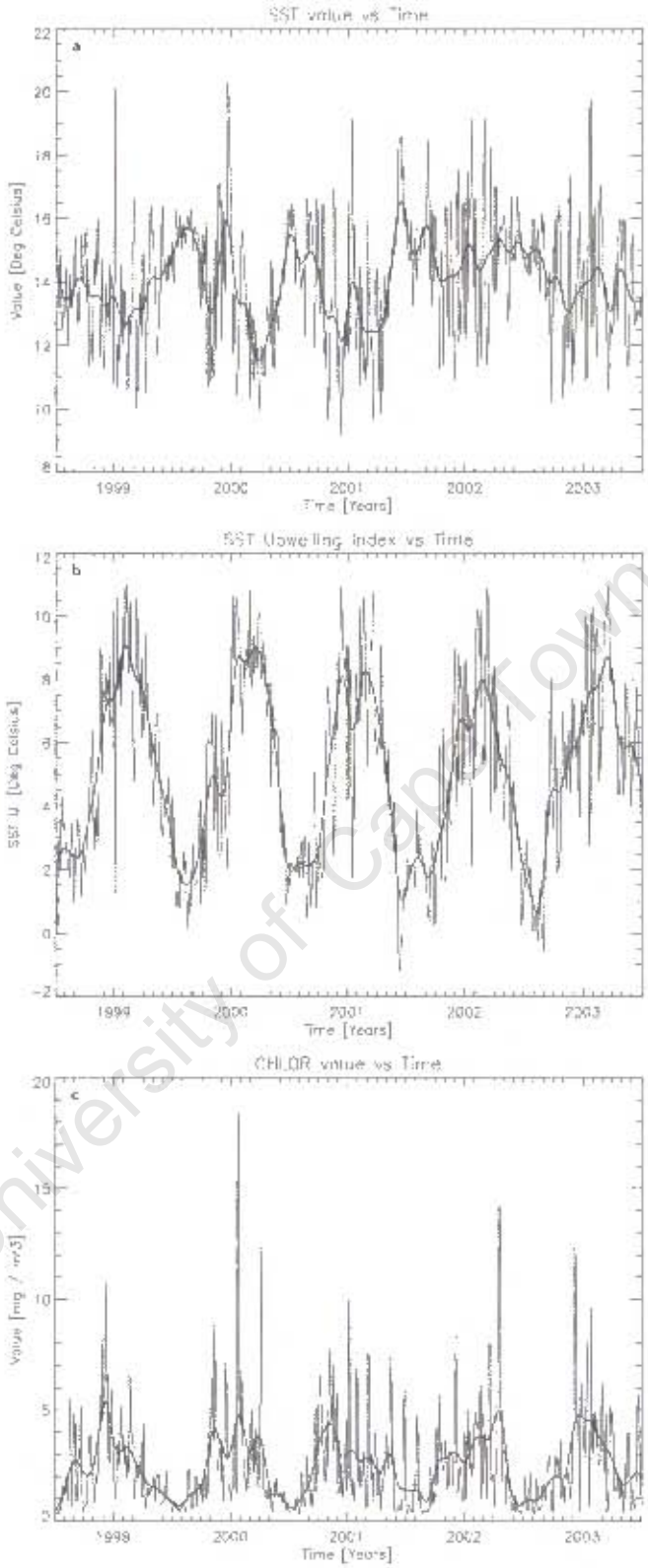

Figure 6.1. Variation of (a) SST at 18.28°E, (b) upwelling index at 18.28°E and (c) chlorophyll a at 18.10°E on the Cape Peninsula latitudinal line for July 1998-June 2003. The dark line represents the applied low pass filter.

Cape Peninsula upwelling index

A measure of the strength of Cape Peninsula upwelling, or UI, was obtained by the difference in SST (5x5 pixel mean) between the inshore key location (34.13°S; 18.28°E) SST value and a reference SST value at 300 pixels offshore (Fig. 5.4a), for each respective three day mean image.

The Cape Peninsula UI shows a strong seasonal signal (Fig. 6.1b) with most intense upwelling in spring / summer. A delta SST in excess of 10°C is attained each summer in the five year time series. The intensity of upwelling varies rapidly on the event scale, interspersed with warm SST events as demonstrated by a rapid decrease in the UI. During winter, the UI approaches zero. In fact, a negative UI (inner shelf SST exceeds that of 300 pixels offshore) is seen during June 2001 coincident with the effect of the Agulhas ring mentioned above, and again in September 2002. However, in the latter case, the negative UI is due to cooler SST at the offshore reference point as a result of the cold water intrusion noted in Chapter (5) rather than the effect of warm Agulhas-conditioned waters on the inner shelf. Interannual variation in the Cape Peninsula UI is apparent, with a decreasing trend in UI noted from 1999 to 2002.

Cape Peninsula phytoplankton index

The Cape Peninsula chlorophyll latitudinal plot (Fig. 5.4b) shows higher chlorophyll displaced slightly offshore, low chlorophyll being coincident with cold upwelled waters on the inner shelf. Hence, a location centred (5x5 pixel mean) on the 200m isobath (34.13°S; 18.10°E), being pixel 20 offshore in Figure (5.4b), was selected to gauge the biological response to upwelling along the Cape Peninsula latitudinal line.

The chlorophyll concentration in Figure (6.1c), a measure of phytoplankton response to the seasonal upwelling off the Cape Peninsula (Fig. 6.1b), demonstrates an associated seasonal signal, also varying rapidly on the event scale. Higher chlorophyll concentrations (> 5mg m^{-3}) are seen primarily in spring / summer, even though overall concentrations were relatively low. The highest chlorophyll concentration (18.5mg m^{-3}) at this location is observed in January 2000, after the pronounced warm event of 1999 (Chapter 5), followed rapidly by strong upwelling in the first half of January 2000. In contrast, the high chlorophyll (14.6mg m^{-3}) reached in April 2002 occurred during a period of quiescence. Concentrations during winter months were low (< 3mg m^{-3}), except for 2 peaks in winter 2001. The first peak (6.2mg m^{-3}) in late June 2001 followed the presence of warm Agulhas-entrained

waters on the inner shelf. The second lesser peak (4.8mg m^{-3}), in early August 2001, appears to be due to decreased upwelling (Fig. 6.1b) associated with an Agulhas filament drawn along the western edge of the Agulhas Bank.

However, it is important to consider that phytoplankton biomass is often patchy and that Figure (6.1c) represents only one location on the shelf, along the Cape Peninsula latitudinal line. In fact, the phytoplankton response to upwelling off the Cape Peninsula is generally upstream thereof and hence a better gauge would likely be a location further northward of the upwelling latitude. A first selection was a location 40 pixels directly north (33.70°S; 18.10°E), on the somewhat broader mid-shelf. The chlorophyll at this more northerly location (not shown) displayed a similar seasonal response to the Cape Peninsula upwelling, however with concentrations double that of the location on the same latitude as the upwelling (34.13°S; 18.10°E). The patchiness and upstream response of phytoplankton is examined further in 'The Cape Peninsula shelf regions' Section below.

Cape Peninsula correlations

The relationship between SST, upwelling and phytoplankton indices was compared for the Cape Peninsula key location, both over the five year time series and seasonally (Fig. 6.1d). The months of January to March are considered as summer, April to June, as autumn, July to September as winter, and October to December as spring.

As would be expected, a clear negative correlation is seen between SST and UI on the Cape Peninsula inner shelf for the five year period (Fig. 6.1d; sst= -0.458 ui + 16.374; r^2=0.477), coolest water being coincident with most intense upwelling. This negative correlation is strongest during summer (sst= -0.956 ui + 21.122; r^2=0.780) when upwelling is most intense (UI typically 4 - 12). The linear regressions for the remaining three seasons appear surprisingly similar. However, the scatter about the linear regression is most pronounced during spring (r^2=0.448). Upwelling is also notably weaker during winter (UI typically <4).

In contrast, a positive correlation (Fig. 6.1d; chl = 0.257 ui + 1.200; r^2=0.118) is generally apparent between chlorophyll concentration at the 200m isobath location (34.13°S; 18.10°E) and UI on the inner shelf (34.13°S; 18.28°E). However, no obvious linear correlation manifests seasonally, although a positive but weak relationship is seen in autumn (chl = 0.212 ui + 0.953; r^2=0.047). Lower chlorophyll concentrations are apparent in winter, coincident with the notably weaker upwelling. Most scatter is again noted during spring months (r^2=0.009).

Furthermore, chlorophyll concentration at the 200m isobath (34.13°S; 18.10°E) was compared with SST at the same location (Fig. 6.1c). No strong correlation is seen for the full five years period although higher concentrations (> 5mg m^{-3}) do tend to be related to SSTs between 12 to 17 °C. This relationship is similar to the SST-chlorophyll correlation for the complete (300 pixels) Cape Peninsula latitudinal line (Chapter 5). When examined seasonally, the most notable distinction is winter, when chlorophyll values are low (< 5mg m^{-3}) and associated with 14 to 18 °C temperatures.

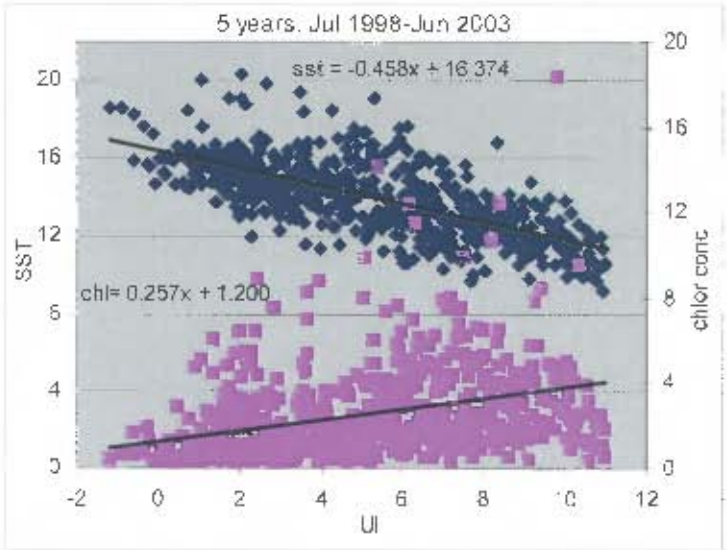

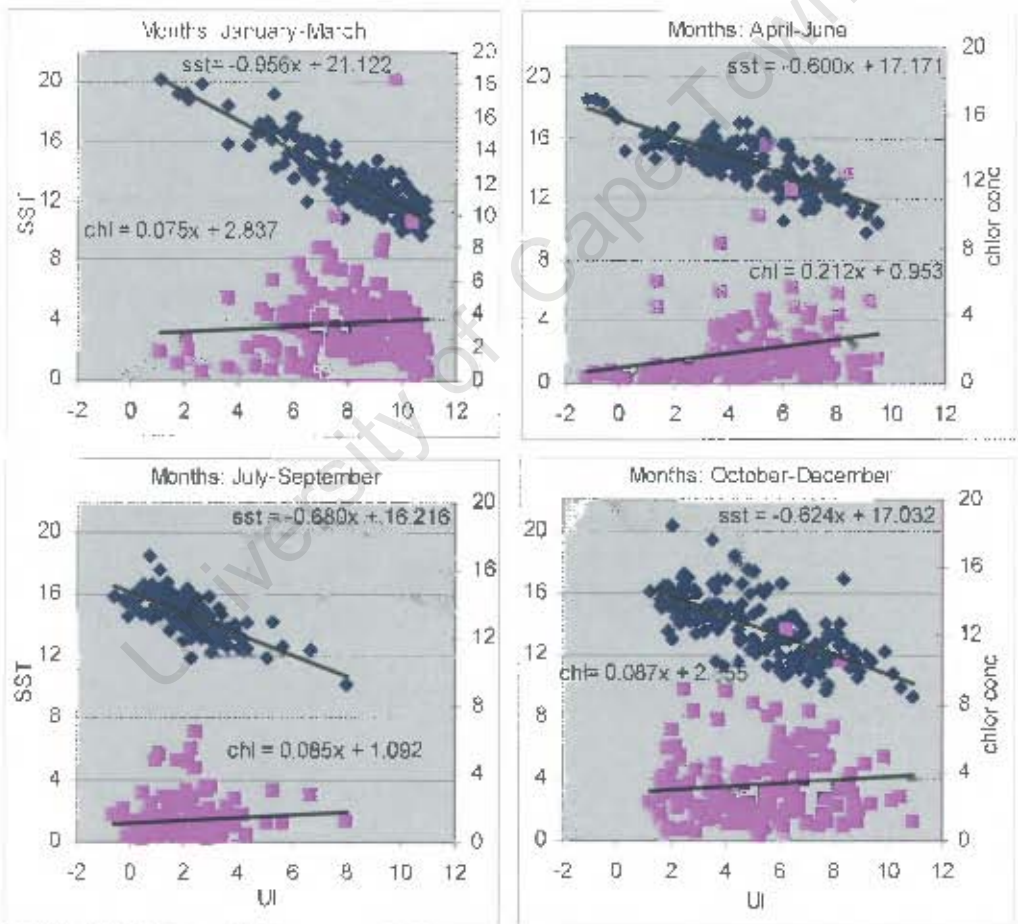

Figure 6.1d. Sea Surface Temperature at 18.28°E (blue) and chlorophyll *a* concentration at 18.10°E (pink) vs upwelling index (x-axis) on the Cape Peninsula latitudinal line.

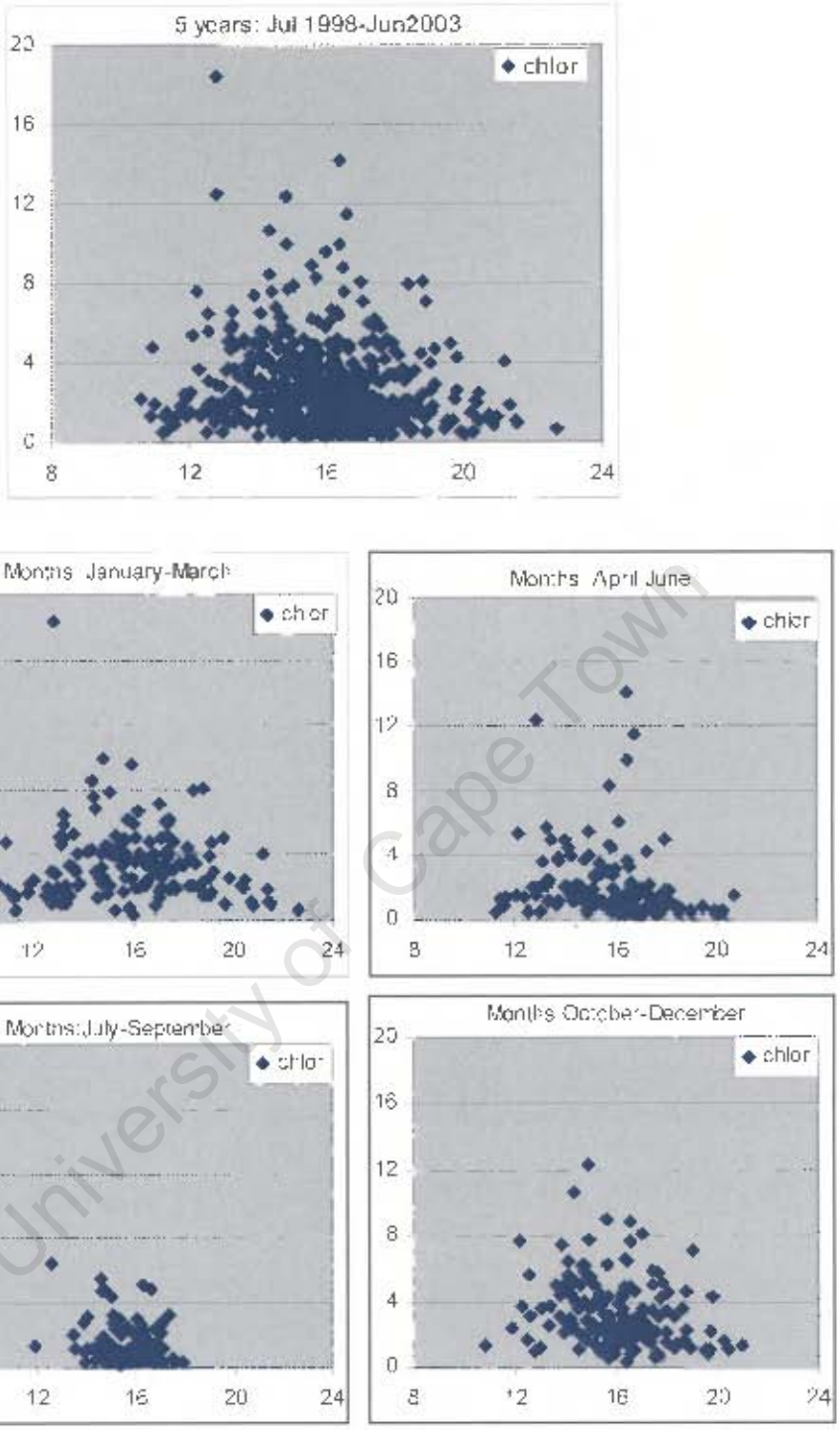

Figure 6.1e Chlorophyll a concentration (y-axis) vs Sea Surface Temperature (x-axis) on the Cape Peninsula latitudinal line at the 200m isobath (18.10°E).

The Cape Peninsula shelf regions

As noted above, phytoplankton biomass is not only often patchy and perhaps inadequately represented by one location on the shelf, but the phytoplankton response to upwelling off the Cape Peninsula is also generally upstream thereof. Therefore, mean chlorophyll concentration for the area of the mid-shelf north of the Cape Peninsula (100-200m; 33.20°S-33.90°S) was also correlated with mean SST and upwelling for the area of the Cape Peninsula inner shelf (0-100m; 33.92°S-34.32°S), as shown in Figure (6.1f).

There is no marked difference in the relationship between SST and UI for the area of the Cape Peninsula inner shelf (Fig. 6.1f) relative to that of the single inner shelf key location (Fig. 6.1d). However, a notably strengthened correlation is observed when chlorophyll for the mid-shelf area north of the Cape Peninsula is correlated with the UI of the Cape Peninsula inner shelf area. For the five year period, the latter correlation (Fig. 6.1f; chl = 0.530 ui + 1.012; r^2=0.305) is double that when chlorophyll at the 200m isobath key location is correlated with UI at the inshore location along the same latitude (Fig. 6.1d; chl = 0.257 ui + 1.200; r^2=0.118). The strengthened linear regression is most notable in spring (Fig. 6.1f; chl = 0.617 ui + 1.333) and summer (chl = 0.347 ui + 2.779), when a clear positive relationship is observed between downstream mid-shelf mean chlorophyll and the Cape Peninsula inner shelf mean UI.

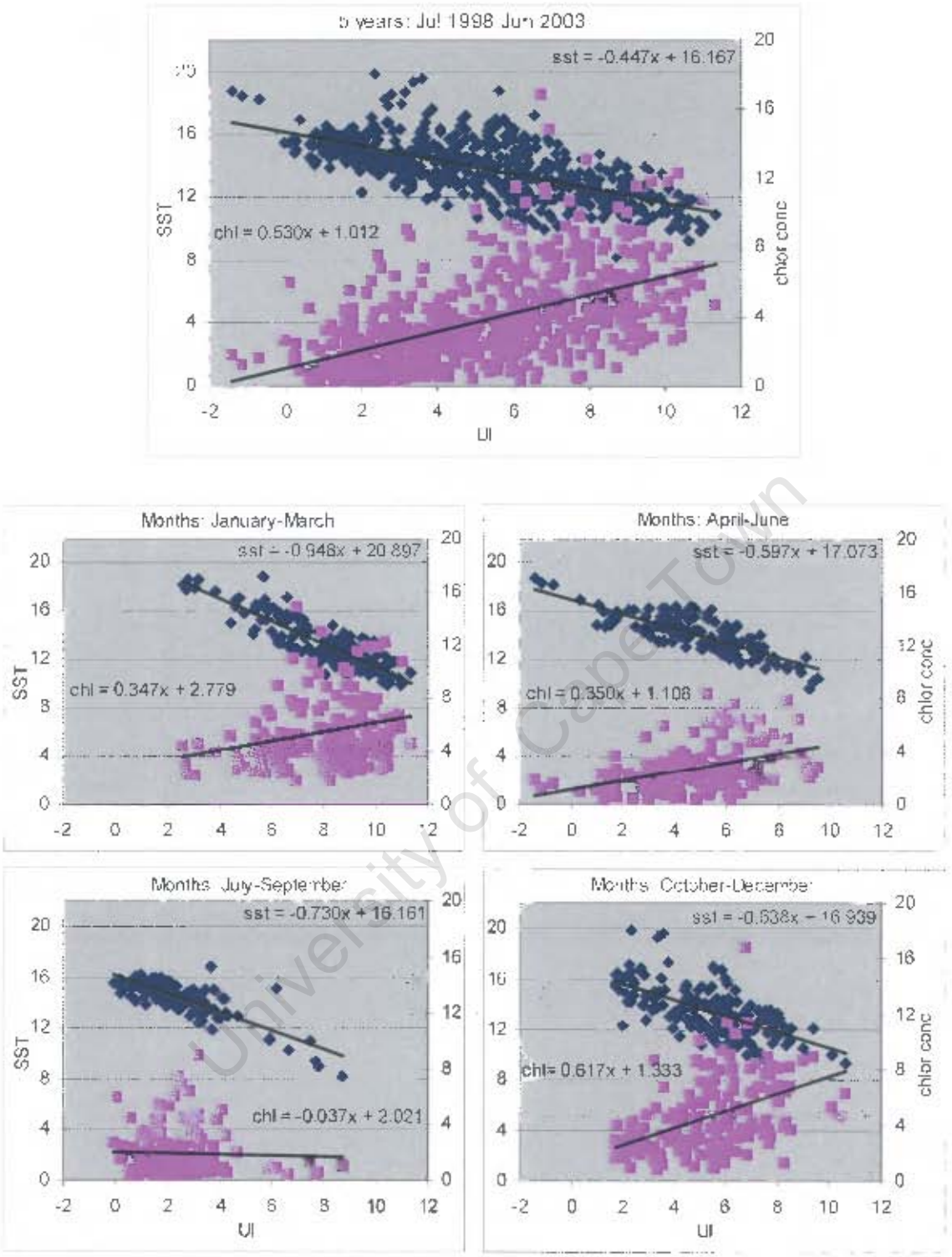

Figure 6.1f. Sea Surface Temperature vs upwelling index (blue) for the CP inner shelf (0-100m; 33.92°S-34.32°S), and chlorophyll *a* concentration (pink) for the mid-shelf north of the CP (100-200m; 33.20°S-33.90°S) vs upwelling index for the CP inner shelf.

The St Helena Bay key location

The most marked feature noted in the St Helena Bay SST latitudinal plot (Fig. 5.4c) is the strong cold water signal associated with the Cape Columbine upwelling plume. When intense, this upwelling plume appears to retain cooler water in St Helena Bay while limiting onshore movement of warmer water. Hence it may be expected that SST and phytoplankton biomass within St Helena Bay be influenced by the intensity of the Cape Columbine upwelling plume. For a measure of the relevant parameters in the St Helena Bay region therefore, the appropriate upwelling index was considered as that of the Cape Columbine upwelling plume, and is examined first in the discussions below. For a measure of the SST and phytoplankton biomass, a key location centred within St Helena Bay was selected.

Cape Columbine upwelling index

A measure of the strength of the Cape Columbine upwelling plume, or UI, was obtained by the difference in SST (5x5 pixel mean) along the boundary of the 100m isobath (32.65°S; 17.84°E; 40 pixels offshore in Fig. 5.4c) and a reference SST value at 300 pixels offshore.

The Cape Columbine UI shows a strong seasonal signal with most intense upwelling in spring/summer (Fig. 6.2a). This pattern is synchronous with upwelling off the Cape Peninsula (Fig. 6.1b), albeit it of marginally less intensity. The Cape Columbine upwelling intensity varies rapidly on the event scale, interspersed with warm events (a rapid decrease in UI). The strongest Cape Columbine upwelling index (delta SST of 11.2°C) is seen to have occurred in January 2000, immediately preceded by the warm event (delta SST of 1.9°C) of December 1999 (Chapter 5).

The "unseasonal" peak at the end of July 2001 is a not due to enhanced Cape Columbine upwelling, but rather to higher offshore SSTs, as a result of the offshore location at this latitude of the Agulhas ring (Fig. 5.3b), shed in June 2001 (Fig. 5.3a, Chapter 5). Complete cessation of upwelling off Cape Columbine seems evident during late October/ early November 2001. Together with seasonal warming, this led to the Cape Columbine UI approaching and reaching zero during this period. The almost zero UI seen in September 2002, however, appears to be due to a cooler offshore reference SST, as a result of the same cold water intrusion noted above in the Cape Peninsula UI (Fig. 6.1b).

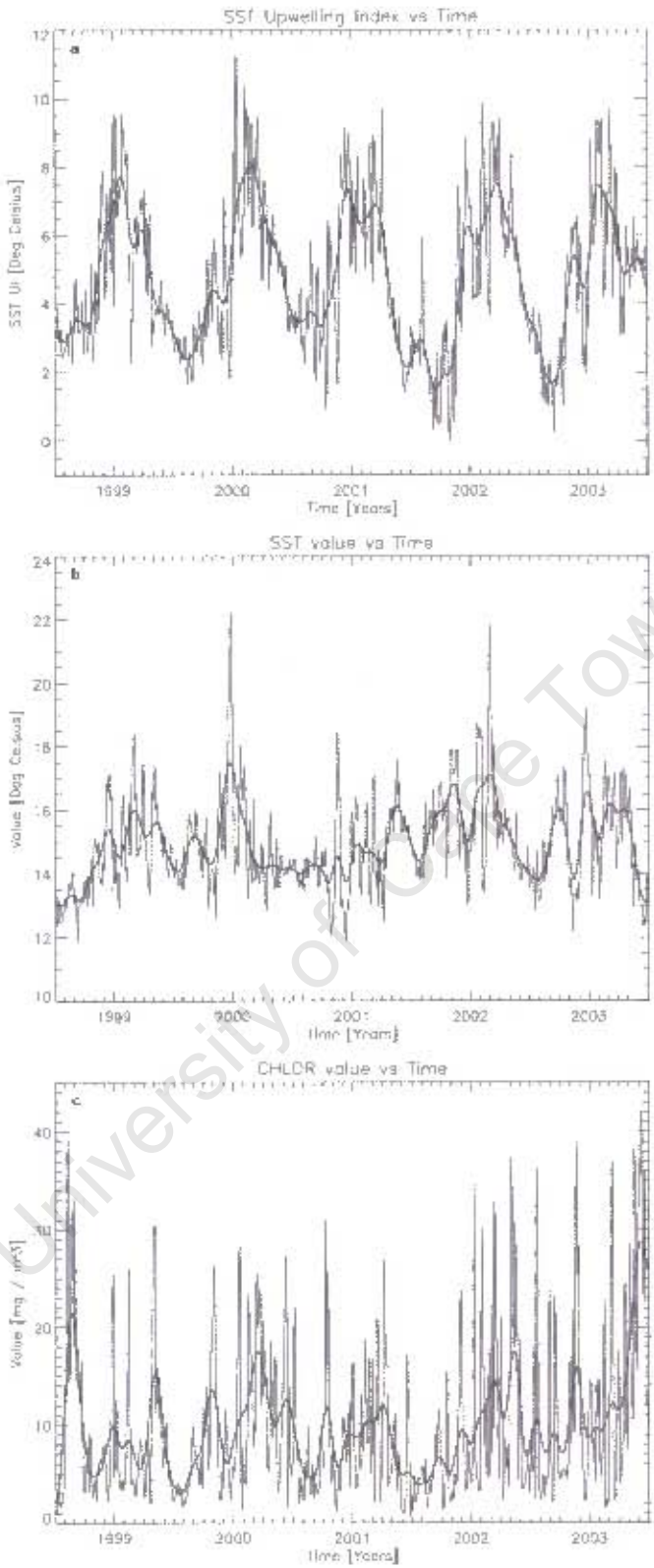

Figure 6.2. Variation of (a) upwelling index at 17.84°E, (b) SST at 18.05°E and (c) chlorophyll *a* at 18.05°E on the St Helena Bay latitudinal line for July 1998-June 2003. The dark line represents the applied low pass filter.

St Helena Bay sea surface temperature

The SST (5x5 pixel mean) for the selected location within St Helena Bay (32.65°S; 18.05°E; pixel 18 offshore in Fig. 5.4c) appears to fluctuate largely between 13-18°C (Fig. 6.2b), generally being warmer during summer months with seasonal warming of the shallower inner shelf Bay waters. This contrasts somewhat with sea surface temperatures on the Cape Peninsula inner shelf (Fig. 6.1a) where the SST variability tends towards cooler spring/summer temperatures and generally warmer autumn/winter temperatures. The warmer summer SSTs in St Helena Bay are despite the strong seasonal signal in the Cape Columbine upwelling index, with most intense upwelling in spring / summer.

Marked temperature changes are nonetheless apparent in St Helena Bay, associated with event scale occurrences. Most notable of these are the two warm events in December 1999 and February 2002 when temperatures of 22°C were experienced within the Bay (also see Fig 5.4c). In contrast, large event scale pulses are notably absent from March through October 2000.Generally, event scale pulses are significantly reduced within St Helena Bay, relative to that on the Cape Peninsula inner shelf (Fig. 6.1a), both in extent and rate of SST fluctuation.

St Helena Bay phytoplankton index

The chlorophyll concentration (5x5 pixel mean) at the same location within St Helena Bay (32.65°S; 18.05°E; pixel 18 offshore in Fig. 5.4d) was used for a measure of phytoplankton biomass for St Helena Bay. No seasonal signal is obvious in the chlorophyll concentration at this location (Fig. 6.2c), despite the strong seasonal signal in the Cape Columbine upwelling index (Fig 6.2a). Rather, chlorophyll appears to fluctuate rapidly throughout the year, from a three-day mean baseline of around 3 to 5mg m^{-3} to concentrations reaching 30 to 43 mg m^{-3}. These levels are three to fourfold greater than those observed at the Cape Peninsula key location (Fig. 6.1c).

The two highest chlorophyll peaks occurred during autumn/winter in 1998 and 2003. The reasons for this were deduced from the daily NOAA AVHRR and SeaWiFS time series (not shown). During August 1998, frontal dynamics relating to a cyclonic eddy in the lee of the 200m isobath appeared to concentrate phytoplankton biomass inshore. In June 2003, a strong frontal boundary associated with a warm water intrusion along the 100m isobath, resulted in the shoreward accumulation of phytoplankton biomass on the inner shelf. In fact, a general trend toward increased chlorophyll

concentrations is observed in 2002 and 2003. In particular, very high chlorophylls are seen from March to June 2003. Interestingly, the coccolithophore bloom documented in Chapter 4 emerged from within the core of an intense phytoplankton bloom during this period.

St Helena Bay / Cape Columbine correlations

The relationship between SST and phytoplankton biomass centred at the key location within St Helena Bay, and the Cape Columbine UI, was examined (Fig. 6.2d). A weak negative relationship is observed between SST in St Helena Bay and the UI at Cape Columbine over the five year period (sst = -0.134 ui + 15.569; r^2=0.037). This negative relationship is strongest during winter (sst = -0.635 ui + 16.092; r^2=0.387), but only over a very limited range of weak upwelling (UI < 6). Of more relevance is the negative correlation between St Helena Bay SST and Cape Columbine UI during spring (sst= -0.502 ui + 17.409; r^2=0.289) and summer (sst= -0.494 ui + 18.863; r^2=0.279).

In contrast, a positive relationship is apparent between chlorophyll concentration in St Helena Bay and the Cape Columbine UI (Fig. 6.2d), although with substantial scatter (chl = 0.969 ui + 5.401; r^2=0.067). Chlorophyll concentrations range from 0 to 43 mg m^{-3}. Surprisingly, the linear regression slope is most positive in autumn (chl = 1.775 ui + 3.954; r^2=0.073), although also strongly positive in summer (chl = 1.386 ui + 1.233; r^2=0.098) when upwelling is most intense (UI=2-12), and in spring (chl = 0.897 ui + 4.649; r^2=0.075) when upwelling is only marginally weaker (UI=0-10). However, the large degree of scatter in the data results in weak correlation coefficients, and hence, the relationship between chlorophyll concentration in St Helena Bay and the Cape Columbine UI, although positive, cannot be regarded as significant.

Phytoplankton biomass at the key location centred within St Helena Bay was also compared with SST at the same key location (Fig. 6.2e). No clear relationship is evident, either for the full five year period, or seasonally. Rather, chlorophyll concentrations ranging from 3 to 43 mg m^{-3} are seen to coincide with sea surface temperatures from 12 to 18°C. Low chlorophyll concentrations (typically < 5mg m^{-3}) are generally observed in warmer waters (>18°C).

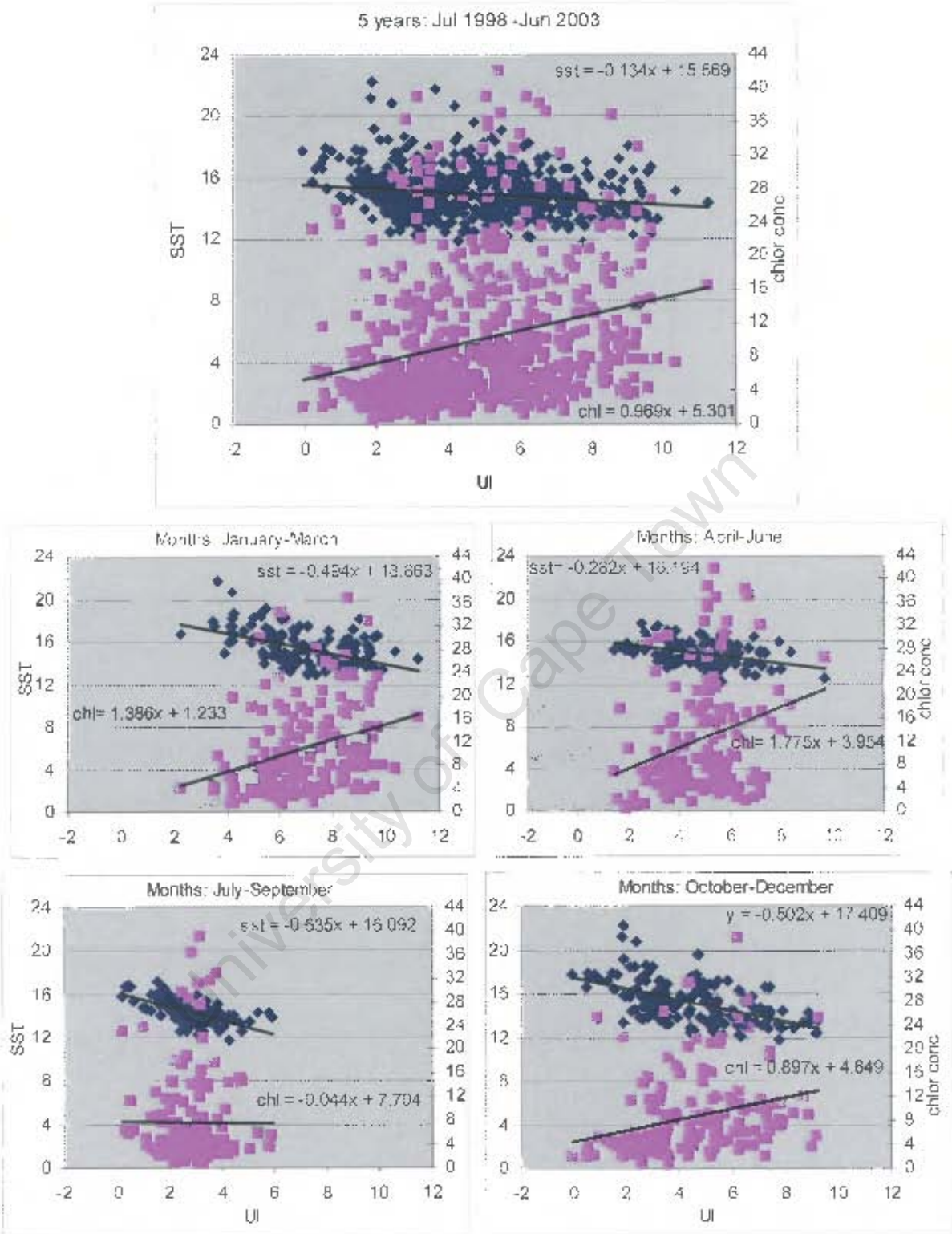

Figure 6.2d. Sea Surface Temperature in St Helena Bay (18.10°E; blue) and chlorophyll a concentration in St Helena Bay (18.10°E; pink) vs the Cape Columbine upwelling index (x-axis) on the St Helena Bay latitudinal line.

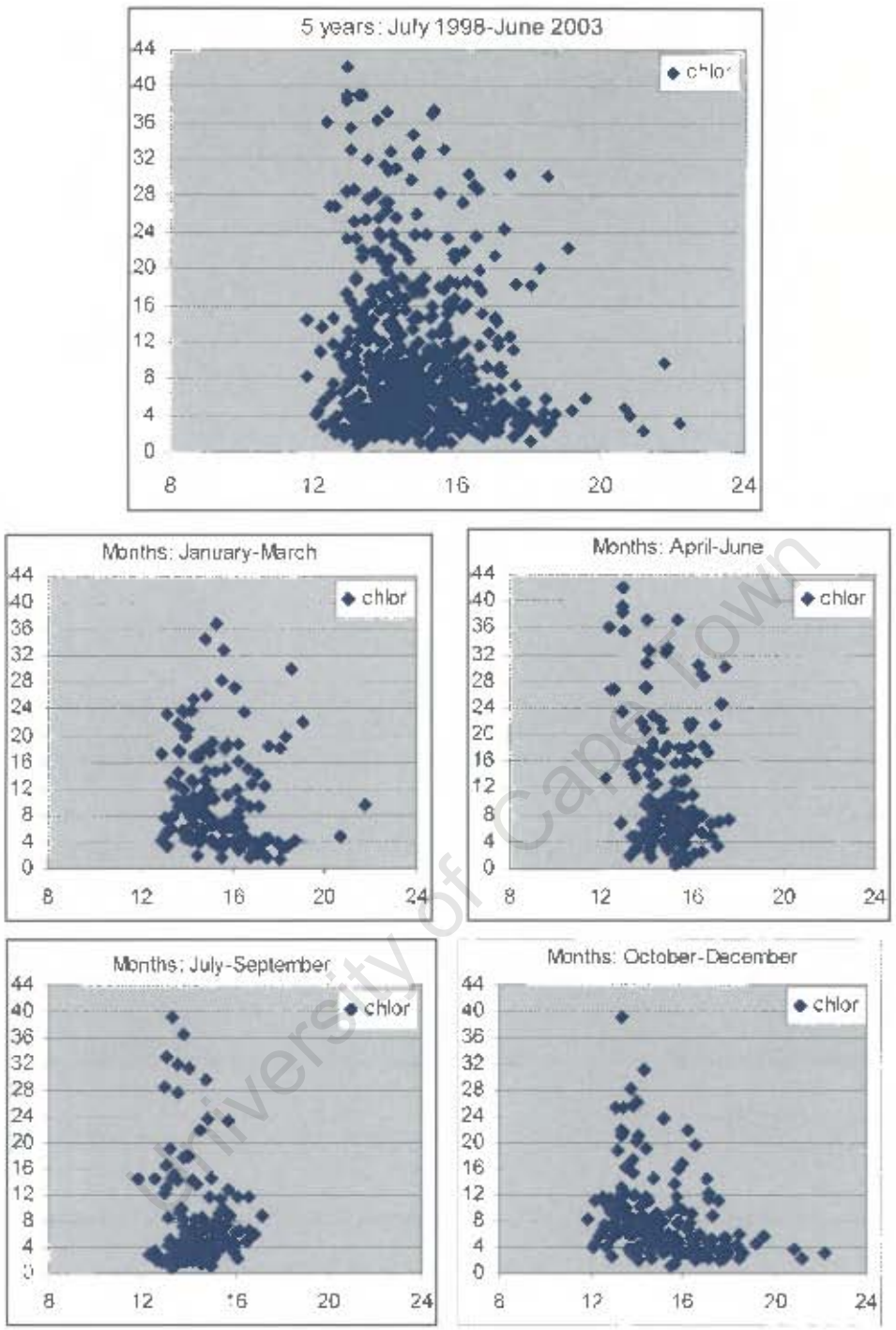

Figure 6.2e. Chlorophyll a concentration (y-axis) vs Sea Surface Temperature (x-axis) on the St Helena Bay latitudinal line at 18.10°E (middle of Bay).

The Namaqua shelf key location

Namaqua shelf sea surface temperature

The Namaqua SST latitudinal plot (Fig. 5.4e) shows coolest upwelled water primarily on the narrow inner shelf, although of far greater offshore extent, especially during winter months. Hence, the selected SST key location for the Namaqua shelf was also sited on the narrow inner shelf (29.90°S; 17.06°E) and comprises pixels one to five (the 5x5 pixel mean) of the Namaqua SST latitudinal plot.

A seasonal signal (Fig. 6.3a) is apparent in the SST data for this location on the narrow inner Namaqua shelf. Temperatures are generally warmer (13-16°C) in spring/summer with cold sea surface temperatures (9-13°C) in winter, in contrast to that on the Cape Peninsula inner shelf (Fig. 6.1a). Strong event scale pulsation of cold water is again clearly evident. The warm event of December 1999 (Chapter 5) is manifest even at this more northern latitude, with temperatures reaching 21.7°C at the time. This warm event signal noticeably affects the interannual variability. Relatively warmer temperatures are also apparent during winter 2001, inferring decreased seasonal upwelling. Since this Namaqua key location (29.90°S; 17.06°E) is located in the northern part of the study region, where the western boundary (15E) limits the offshore extent to 202 pixels at this latitude, it was not possible to determine an upwelling index using a reference point of sufficient distance offshore. Therefore, only sea surface temperature and phytoplankton biomass are examined for the Namaqua shelf in this thesis.

Namaqua shelf phytoplankton index

Similar to the Cape Peninsula (Fig. 5.4b), higher chlorophyll is displaced slightly offshore along the Namaqua line (Fig. 5.4f), low chlorophyll being coincident with cold upwelled waters on the inner shelf. Hence a location centred (5x5 pixel mean) on pixel 20 offshore (29.90°S; 16.88°E) was selected to estimate the phytoplankton response to upwelling at this latitude.

Moderate chlorophyll (2-8 mg m^{-3}) is apparent throughout the year (Fig. 6.3b), despite the seasonal SST signal at this location (Fig. 6.3a). Pulses of high (8-32 mg m^{-3}) chlorophyll are observed at intervals on the event scale. Highest chlorophyll was attained in early February 2002, due to a persistent (~10 days) patch of very high biomass (>30 mg m^{-3}) on the seaward side of the upwelling front (daily NOAA and SeaWiFS time series, not shown). Several such patches were also prevalent

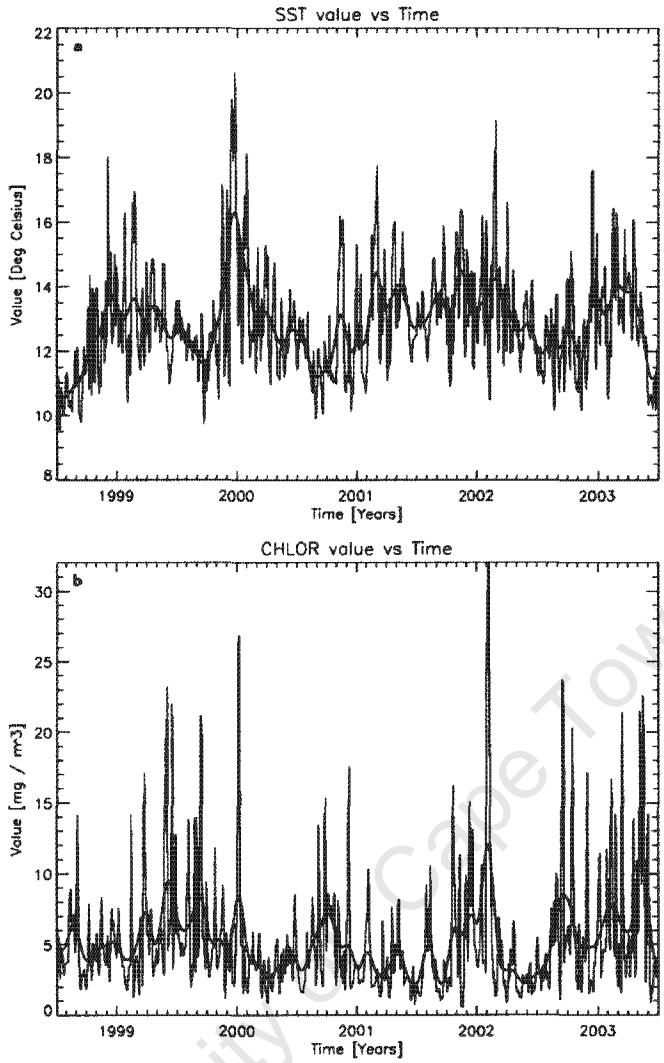

Figure 6.3. Variation of (a) SST at 17.06°E and (b) chlorophyll *a* at 16.88°E on the Namaqua Shelf latitudinal line for July 1998-June 2003. The dark line represents the applied low pass filter.

on the broad Namaqua mid-shelf in January 2002 (Fig. 5.4f), although not coinciding with the selected location. Similarly, patches of high chlorophyll are seen to have occurred at other times at this location (Fig. 6.3b), in particular, in early January 2000, autumn/winter of 1999 and during Oct 2002 to May 2003.

Namaqua shelf correlations

As mentioned above, an upwelling index was not determined for the Namaqua shelf location and only the relationship between phytoplankton biomass and SST was therefore explored (Fig. 6.3c). Chlorophyll concentration was compared with SST for the same location, centred on pixel 20 offshore (Fig. 5.4f). No clear relationship is evident, although high chlorophyll concentrations (> 8mg m^{-3}) were generally coincident with SSTs of 12 to 17°C (Fig. 6.3c). SST was less than 16.5°C in autumn/winter and increased up to 21.5°C in spring/summer.

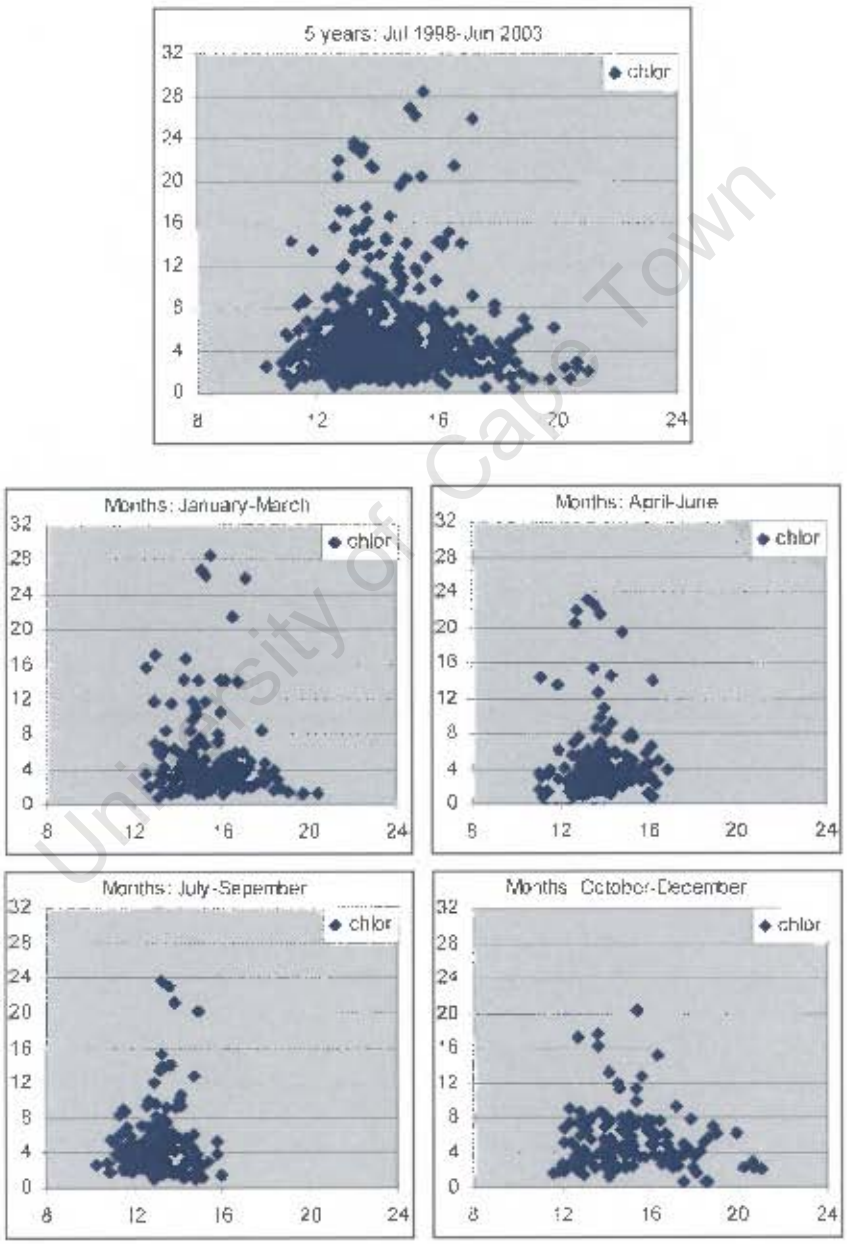

Figure 6.3c. Chlorophyll *a* concentration (y-axis) vs Sea Surface Temperature (x-axis) on the Namaqua shelf latitudinal line centred at 20km offshore (16.88°E).

4. Summary

The dynamic variation in SST, and indices of upwelling and phytoplankton over the period July 1998 to June 2003 has been outlined in this chapter for the Cape Peninsula, St Helena Bay and Namaqua shelf locations. The upwelling index (UI) was determined by the difference in SST between an offshore reference location (300 pixels) and the respective inner shelf location. An UI was not determined for the Namaqua shelf due to the offshore limit of the study region at that latitude. Chlorophyll concentration was used as a measure of phytoplankton abundance, and hence, an index of phytoplankton response to upwelling. SST and chlorophyll were correlated with UI, and chlorophyll was compared with SST, to gain further insights into these relationships.

Dynamic Variability

The Cape Peninsula UI shows a strong seasonal signal with the most intense upwelling occurring in spring/summer when a delta SST in excess of 10°C is attained each summer. The intensity of upwelling varies rapidly on the event scale, interspersed with warm events as demonstrated by a rapid decrease in UI. During winter, the UI approaches zero. Upwelling at Cape Columbine appears synchronous with that at the Cape Peninsula, the UI displaying a similar pattern of variability, albeit of a marginally less intensity.

The most notable variations in SST at all three locations are the marked temperature changes associated with rapid pulsation of event scale cold/warm events. Surprisingly, no strong seasonal signal is evident. On the Cape Peninsula inner shelf, cold pulses (9–13°C) are seen most frequently during spring/ summer, when upwelling is most intense. In contrast, SST is generally warmer (13-16°C) in spring/summer on the Namaqua inner shelf, with cold SSTs (9-13°C) observed in winter. Within St Helena Bay, SST is warmer during summer (13-22°C) due to seasonal insolation of the shallow inner shelf Bay waters. This occurs despite strong seasonal upwelling at Cape Columbine in spring/summer. Event scale cold/warm pulses are also significantly reduced within St Helena Bay relative to that on the Cape Peninsula inner shelf.

Chlorophyll concentration off the Cape Peninsula demonstrates an associated seasonal signal in response to seasonal upwelling, also varying rapidly on the event scale. Increased chlorophyll (> 5mg m^{-3}) is seen primarily in spring/summer. Particularly high chlorophyll events are distinct and may be related to the variability in UI and associated thermal changes. Upstream of the Cape

Peninsula, chlorophyll displays a similar seasonal response to Cape Peninsula upwelling, but with concentrations double that of chlorophyll at the location on the same latitude as the upwelling.

No seasonal signal is obvious in chlorophyll variability within St Helena Bay, despite a strong seasonal signal in Cape Columbine UI. Rather, chlorophyll appears to fluctuate rapidly from around 3 to 5mg m^{-3} to concentrations reaching 30 to 43 mg m^{-3} throughout the year, three to fourfold greater than levels attained at the Cape Peninsula. A general trend toward increased chlorophyll concentrations is observed in 2002 and 2003. On the Namaqua shelf, moderate chlorophyll biomass (2-8 mg m^{-3}) seems apparent throughout the year, even though a weak seasonal signal in seen in the associated SST. This may however be more a function of seasonal insolation rather than of UI (not determined for Namaqua shelf). Pulses of high chlorophyll (8-32 mg m^{-3}) are interspersed on the event scale.

Correlation of parameters

No obvious relationship is apparent between phytoplankton biomass and SST at any of the three selected locations. At the Cape Peninsula, higher chlorophyll (> 5mg m^{-3}) does however tend to be related to SSTs between 12 to 17°C. Similarly, high chlorophyll (> 8mg m^{-3}) is generally coincident with SSTs between 12 to 17°C on the Namaqua shelf. Within St Helena Bay, chlorophyll concentrations ranging from 3 to 43 mg m^{-3} coincide with sea surface temperatures from 12 to 18°C. However, when SST and chlorophyll are correlated with UI, evident relationships do emerge.

A negative correlation is seen between SST and UI on the Cape Peninsula inner shelf, being strongest during summer when upwelling is most intense. In contrast, a positive correlation is generally apparent between Cape Peninsula chlorophyll and UI. This correlation doubles when mean chlorophyll for the mid-shelf area north of the Cape Peninsula is correlated with mean UI for the Cape Peninsula inner shelf area. The greater positive correlation is most significant in spring, but is also of importance in summer.

For the five year time series, a weak negative correlation exists between SST in St Helena Bay and UI at Cape Columbine. However, when examined seasonally, this negative correlation is substantially greater during spring and summer. In contrast, a strong positive relationship is apparent between chlorophyll concentration in St Helena Bay and upwelling intensity at Cape Columbine.

However, this relationship is highly variable, and hence, although positive, cannot be regarded as significant.

In conclusion, Chapters 5 and 6 present an approach towards developing appropriate indices to quantify the intra-seasonal variations in SST, and indices of upwelling and phytoplankton in the southern Benguela. The results suggest that SST indices may be used to determine the development of upwelling cells, and chlorophyll indices to determine the development of a phytoplankton bloom, as proposed in the hypothesis. Evident relationships between these parameters have emerged which may be used to elucidate the response of phytoplankton biomass in relation to thermal changes due to upwelling, and should be explored further.

Chapter 7

Summary & concluding remarks

The objective of this thesis was to utilize high resolution satellite data (1 km), in particular from the NOAA AVHRR and the OrbView-2 SeaWiFS sensors, to investigate the upper layer dynamics of the Benguela ecosystem in more detailed space and time scales than has previously been undertaken. A consistent time series of high quality daily sea surface temperature and chlorophyll *a* concentration images, for the period July 1998 to June 2003, was therefore generated to study the mesoscale upwelling events and consequent phytoplankton response in the Benguela.

In processing the high resolution SeaWiFS data, it became apparent that the standard bio-optical algorithms and processing parameters, developed for the global dataset, are not ideal for the high productivity waters of the Benguela. A detailed investigation of the SeaWiFS bio-optical algorithms was undertaken and the processing parameters were modified for more optimal application to Benguela regional waters. Examination of the individual radiances used in the bio-optical algorithms revealed that constituents, other than chlorophyll, were at times contributing significantly to the in-water light field. Specific event scale phenomena were occurring in the Benguela ecosystem, in particular, hydrogen sulphide eruptions in northern Benguela waters. It was recognised, therefore, that no one set of processing parameters can be accurate for every individual day's data within a longterm time series. Also, within the African situation, opportunities for the quantitative calibration of event scale signals are limited. Hence, the application of SeaWiFS data to Benguela waters should be considered either as qualitative, for event scale phenomena, or quantitative, for a longterm time series study. The processing of SeaWiFS ocean colour data should be adjusted accordingly. Specific event scale qualitative applications of satellite data have been documented in this thesis, namely, hydrogen sulphide eruptions in the northern Benguela and an unusual coccolithophore bloom in the southern Benguela. A quantitative analysis of high resolution NOAA AVHRR and SeaWiFS ocean colour data for the southern Benguela ecosystem has been undertaken, and initial operational indices derived for application to the management of the ecosystem.

Qualitative applications

The conventional view has been that sulphide-laden eruptions, observed from the shore along the central coast of Namibia, are very local features with only limited ecosystem-scale consequences.

But, as has been documented in this thesis, it is now possible to identify and monitor such anoxic phenomena, using high resolution ocean colour satellite data (Weeks et al., 2002). This capability appears to have altered the conventional view, and has already revealed much that was previously unsuspected about these events. Certainly, the new view of their very large extent and high frequency of occurrence has made clear their great potential ecological importance to the northern Benguela Current marine ecosystem. And it clearly suggests that hydrogen sulphide emissions from the sediment can be held more responsible for hypoxic conditions along the Namibian coast, than advected hypoxic water of Angolan origin (Weeks et al., 2004a).

The hydrogen sulphide emissions are perhaps also very important to the Benguela marine ecosystem as a whole, in that they may be a major factor in the functional separation into northern and southern subsystems, of what would seem to be a natural integral large marine ecosystem. Only in the Benguela does an upwelling maximum zone (that near Lüderitz) so effectively separate migrating fish species into evidently separate self-contained stocks. The fish populations seem to strongly avoid passing the zone of major sulphide eruptions north of Lüderitz. In fact, the location of the point of ultimate stock separation, based on biological characteristics of the fish, is ordinarily placed not at the site of maximum upwelling at Lüderitz, but north of it (Agenbag and Shannon, 1988) in a zone that coincides with the southern extent of sulphide-enriched sediments. Biogeographical regions based on intertidal rocky shore faunal distribution show the transition from southern temperate to northern temperate zones to occur at Sylvia Hill, with species diversity dropping dramatically along the central coast (Currie, 1997). Similarly tag-and-release results of popular shore-angling fish species indicate a distributional divide at Sylvia Hill (Holtzhausen, 1999). The abundance of rock lobster decreases sharply within its range distribution north of 25^0S (Pollock and Beyers, 1981), which can almost certainly be attributed to the oxygen deficient coastal water (Beyers et al., 1994; Grobler and Noli-Peard, 1997).

In other upwelling systems, adult sardines, which are capable of filter-feeding directly on phytoplankton, generally migrate for feeding near the enriched zones of maximum upwelling (Bakun, 1996). However, in the Benguela Current region there seems less tendency to do this, with adults in each subsystem appearing to migrate in the directions opposite to the ones leading toward the area of underutilized phytoplankton production, situated downstream of the intense upwelling site near Lüderitz. Hence, in the northern Benguela, the predominant adult sardine migration seems to be northward, toward the Angola-Benguela frontal zone, while the adult sardines of the southern Benguela tend to migrate south- and eastward, around the Cape Peninsula to the Agulhas Bank and

beyond. Thus it seems that the danger to survival represented by the toxic hydrogen sulphide emissions, and the associated lingering depletion of oxygen in the water column, might have promoted an inborn adaptive avoidance of the very zone that would appear to be naturally the most beneficial feeding ground for sardines, and other important fish components of this upwelling-dominated ecosystem. This could be contributing to the fact that the Benguela system as a whole, while estimated to have as much as two times more primary production than the Peru-Humboldt system (Carr, 2002), typically has yielded very much smaller quantities of fish (by a factor of 10 to 20). Furthermore, these findings may have important connotations to atmospheric chemistry as a result of the emitted products. Methane is an important greenhouse gas, and sulphides are implicated in aerosol production, thus affecting radiative forcing of earth's climate. The existence of a credible mechanism for "atmospheric greenhouse"-related intensification of coastal upwelling (Bakun, 1990) opens the disturbing possibility that, as the accumulation of greenhouse gases in the earth's atmosphere continues, additional intense upwelling ecosystems in other regions of the world's oceans might be switched to less desirable states, similar to that currently existing off Lüderitz (Bakun and Weeks, 2004).

The ocean colour satellite observations also introduced another interesting issue. Hydrogen sulphide features separated from the coast, particularly after having existed at the sea surface for some time, tend to appear quite similar to satellite observations of very large coccolithophore blooms (Tyrrell et al., 1999). The possibility of some degree of involvement of coccolithophores in the offshore signatures cannot be discounted at this time. If so, such a relationship of coccolithophore blooms to sulphide/anoxia is previously unreported and in itself would be of ecological significance.

Coccolithophore blooms differ optically from other blooms of non-calcifying marine phytoplankton, largely due to the influence of high concentrations of detached coccoliths (Ackleson et al., 1994; Balch et al., 1996a). The consequent high reflectances are visible from satellite, and, similar to hydrogen sulphide eruptions, may be distinguished using derived quasi-true colour imagery. The evolution of an unusual coccolithophore bloom in the southern Benguela, during the autumn of 2003, has been documented in this thesis, the first such extensive bloom monitored by satellite in the Benguela upwelling region (Weeks et al., 2004b). Both SeaWiFS and MODIS ocean colour data were used, the 250m – 500m MODIS resolution allowing detailed analysis not possible before. The bloom was dominated by a species not previously known to form such intense concentrations.

The coccolithophorid, *Syrachosphaera pulchra,* and a mixed assemblage of dinoflagellates dominated the phytoplankton assemblage. The close match-up (within 5 %) of SeaWiFS-derived and *in situ* normalized-water leaving radiances for the coastal sampling station provides validation of the level-1 to level-2 processing parameters selected for the Benguela coastal waters. In fact, application of the SeaWiFS default processing parameters to this data results in total masking of the coastal sampling station, precluding the attainment of any SeaWiFS-derived radiances. Sampling stations with high concentrations of *S. pulchra* all showed elevated SeaWiFS normalised water-leaving radiances, associated with the presence of highly backscattering calcite particles in surface waters. However, the optical impacts are not solely dependent on the number of coccoliths in the water. Rather, the optical impacts also vary according to how much chlorophyll is in the water (Tyrrell et al., 1999). The variable presence of a mixed dinoflagellate community, therefore, introduced an additional large source of absorbing material to the optical signal.

The high reflectivity of coccolithophorids and associated coccoliths at the sea surface, however, interferes with the SeaWiFS chlorophyll estimation. As for precipitated sulphur in surface waters, both the radiances used in the bio-optical algorithm and the radiances used in the atmospheric correction process are likely to be adversely affected by the high reflectance. The SeaWiFS bio-optical algorithm uses band-ratios with the denominator, 555nm, assumed to be relatively stable. The presence of coccoliths, or precipitated sulphur, at any one location, producing a significant contribution at 555nm, will yield erroneous estimates of chlorophyll *a*. SeaWiFS-derived chlorophyll values for stations with high concentrations of *S. pulchra* yielded substantially depressed (52%) estimates of chlorophyll, relative to measured *in situ*. Similarly, limited *in situ* chlorophyll sampling in sulphur-enriched coastal waters yielded very low chlorophyll concentrations. Generally, the SeaWiFS bio-optical algorithm becomes untrustworthy in any "Case 2" waters, where constituents other than chlorophyll contribute significantly to the in-water light field (O'Reilly et al., 2000). Hence, alternative algorithms need to be explored for estimates of chlorophyll concentration in these "Case 2" regional waters. In any case, *in situ* validation is needed to accurately calibrate the satellite sulphur signal. This would seem to require some significant supporting at-sea observational / experimental operations. The new view of the very large extent and high frequency of occurrence of the hydrogen sulphide events has made clear their great potential ecological importance to the northern Benguela Current marine ecosystem. And hence the calibration of these, and other, event scale signals in Benguela regional waters should be considered with some degree of urgency.

Quantitative applications

The quantitative analysis of high resolution NOAA SST and SeaWiFS chlorophyll data for the southern Benguela allowed identification of the extent and frequency of upwelling during the period July 1998 to June 2003, and the response of the phytoplankton community to this physical forcing. The temporal and spatial variability in SST and chlorophyll along the length of the inner, mid- and outer continental shelves of the southern Benguela allowed identification of the location and emergence of upwelling cells, and the distribution patterns of phytoplankton biomass. The offshore extent of this variability at selected latitudes of differing shelf width was identified. SST, upwelling and chlorophyll indices were derived for selected locations, and the relationship between these parameters was determined.

The Cape Columbine and Cape Peninsula upwelling cells are identified as two distinct bands of cold water (9–13°C) on the inner and mid-continental shelves. Upwelling at these locations is synchronous in nature, and generally more intense in spring/summer. The Namaqua upwelling cell extends over a much broader latitudinal range, and is more perennial in nature. Most remarkable in the inner and mid-shelf SSTs, is the rapidly pulsating nature of upwelling in the southern Benguela, with intense warm/cold events clearly distinguished. The dominant pattern of SST over the outer shelf is that of seasonal insolation. In the south, both the seasonal and event scale influences of warmer waters (>20°C) of Agulhas Current origin are clearly identified.

Chlorophyll concentration on the inner shelf largely mirrors the pattern of SST variability, similarly dominated by event scale processes. Two distinct bands of lower chlorophyll (< 3mg m^{-3}) coincide with the Cape Columbine and Cape Peninsula upwelling cells. Pulses of very low chlorophyll (< 1mg m^{-3}) correspond with intense upwelling events. Highest chlorophyll concentrations (> 10mg m^{-3}) are apparent in the St Helena Bay region, being most sustained during the late summer months. Over the mid-shelf, higher chlorophyll is observed throughout all seasons, although low biomass occurs during most winters. Chlorophyll concentrations over the outer shelf are generally low (< 3mg m^{-3}). In the south, the seasonal and event scale intrusions of warmer Agulhas-conditioned waters yield particularly low chlorophyll.

At the Cape Peninsula latitude, cooler upwelled water (<14°C) is confined primarily to the narrow inner shelf, with event scale pulses seen to extend up to 100km offshore. Offshore, a strong seasonal signal dominates, with onshore movement of warm water (>19°C) each summer, between upwelling

events. Agulhas Current influences are readily observed, even on the Cape Peninsula inner shelf. Chlorophyll concentration off the Cape Peninsula shows a clear seasonal signal, with offshore extension primarily in spring/summer. Higher chlorophyll is displaced somewhat offshore when upwelling is intense. In the St Helena Bay region, the cold Cape Columbine upwelling plume (9–13°C) causes retention of water on the inner shelf, while limiting onshore movement of offshore water. However, event scale pulses of cold water extending as far as the broad outer shelf, are frequently evident. Considerably high chlorophylls (> 5mg m^{-3}) are apparent throughout the year, with a greater offshore extension over the broader continental shelf in spring/summer, that is generally double that off the Cape Peninsula. Upwelling in the Namaqua region is dominated by a seasonal signal of large offshore extent, most intense during winter, while a corresponding onshore warm water signal dominates in summer. However, this warm water signal, across the broad Namaqua mid-shelf, may be more a reflection of seasonal insolation, rather than diminished upwelling. Moderate to high chlorophyll (2-10 mg m^{-3}) extends across the broad Namaqua mid-shelf and onto the outer shelf, being apparent throughout the year, despite the seasonal signal in the associated SST. In fact, chlorophyll concentrations vary considerably between the three selected latitudes of differing shelf width. Chlorophyll along the St Helena Bay latitude is generally four times greater than along the Cape Peninsula latitude, and double that along the Namaqua Shelf latitude.

SST, upwelling and chlorophyll indices were derived for the Cape Peninsula, St Helena Bay and Namaqua shelf locations, enabling intra-seasonal variations to be more comprehensively quantified and compared. Most notable in the SST indices at all three locations are the marked temperature changes associated with rapid pulsation of event scale cold/warm events. The cold/warm pulses are significantly reduced within St Helena Bay, relative to that on the Cape Peninsula inner shelf. Surprisingly, no strong seasonal signal is evident. This is unexpected, particularly at the Cape Peninsula, where cold pulses (9–13°C) are seen most frequently during spring/ summer. Within St Helena Bay, SST is, in fact, generally warmer during summer (13-22°C), due to seasonal insolation of the shallow inner shelf Bay waters.

Both the Cape Peninsula and Cape Columbine upwelling indices show a strong seasonal signal, with most intense upwelling occurring in spring/summer. The upwelling intensity varies rapidly on the event scale, interspersed with warm events. During winter, the UI approaches zero. The UI graphs (Fig. 6) demonstrate a quasi-monthly variability, with an average of 14 major peaks annually. There appear to be three dominant modes of periodicity in the UI signal, *viz.*, a high frequency mode, a

seasonal mode and a longer term interannual mode. Additionally, single, event scale, modes are evident, coincident with event scale phenomena, such as an Agulhas ring "intrusion". For the purpose of this thesis, however, the quantitative focus has been on the intra-seasonal event scale, and hence, only a limited analysis is included herein. There is much information to be deduced from these graphs and a more detailed analysis will be considered in the future.

Chlorophyll concentrations off the Cape Peninsula demonstrate a seasonal signal, in response to the associated seasonal upwelling, also varying rapidly on the event scale. Particularly high chlorophyll events are distinct and may be related to the variability in UI and associated thermal changes. No seasonal signal is obvious in chlorophyll variability within St Helena Bay, despite a strong seasonal signal in the Cape Columbine UI. Rather, chlorophyll appears to fluctuate rapidly throughout the year, with concentrations three to fourfold greater than levels attained at the Cape Peninsula. A general trend toward increased chlorophyll concentrations in St Helena Bay is observed in 2002 and 2003, with particularly high chlorophylls toward the end of the study period, from March to June 2003. The unusual coccolithophore bloom, documented in this thesis, emerged from within a core of intense phytoplankton biomass during this period. The coccolithophore bloom was confined to the region between the Namaqua and Cape Columbine upwelling cells, where a broadening of the shelf favours stratification of the water column, conducive to the development of flagellate dominated blooms. This region is particularly susceptible to red tide formation and its negative impacts (Pitcher and Calder 2000). The very high phytoplankton biomass, and associated conditions during this period, would appear to have been precursory to the development of the *S. pulchra* bloom, a species not previously reported to form such intense concentrations.

When chlorophyll is correlated with SST, no obvious relationship is apparent at any of the three selected locations. However, when SST and chlorophyll are correlated with UI, evident relationships do emerge. A clear negative correlation is seen between SST and UI on the Cape Peninsula inner shelf, being strongest during summer when upwelling is most intense. In contrast, a positive correlation is observed between Cape Peninsula chlorophyll and UI. This correlation doubles when mean chlorophyll for the mid-shelf region downstream of the Cape Peninsula is correlated with mean UI for the Cape Peninsula inner shelf region. The greater positive correlation is most significant in spring, but is also of importance in summer. When comparing SST in St Helena Bay with UI at Cape Columbine, only a weak negative correlation results. However, when examined seasonally, this negative correlation is substantially greater during spring and summer. Conversely, a strong positive relationship is apparent between phytoplankton biomass in St Helena Bay and the Cape Columbine

UI. However, this relationship is highly variable, and hence, although positive, cannot be regarded as significant. In summary, although no obvious relationship may be apparent between parameters over the longer term, when considered on a seasonal basis, evident relationships do emerge. A seasonal approach should therefore be included in any operational application of these indices.

In concluding the quantitative analysis of NOAA SST and SeaWiFS chlorophyll data, an approach has been presented towards developing appropriate indices to quantify the intra-seasonal variations in SST, and indices of upwelling and phytoplankton in the southern Benguela. The results suggest that SST indices may be used to determine the development of upwelling cells, and chlorophyll indices to determine the development of a phytoplankton bloom. Evident relationships between these parameters have emerged which may be used to elucidate the response of phytoplankton biomass in relation to thermal changes due to upwelling, and should be developed further. Only three locations of differing biogeographic character within the southern Benguela have been examined in detail here. Upwelling is a very dynamic, three-dimensional process with strong resultant current flows and hence, mesoscale dynamics are important. It also seems apparent from this study that phytoplankton biomass is not only often patchy and perhaps inadequately represented by one location on the shelf, but the phytoplankton response to upwelling may also be primarily downstream of the upwelling centre. Hence, a next approach may be to sub-divide the northern and southern Benguela into biogeographic provinces, and apply the indices developed here to these provinces, as useful input into the management of the ecosystem.

A key policy action within the Benguela Current Large Marine Ecosystem (BCLME) Programme is the assessment of environmental variability, ecosystem impacts and the improvement of predictability. Two cornerstones of this policy action are the development of an early warning system and the improvement of predictability of extreme events and their impacts in the BCLME. Fundamental to this is the requirement of an optimal satellite remote sensing capability within the region, and the development of ecosystem indicators that can detect and monitor ecosystem changes. The application of satellite remote sensing data to the Benguela ecosystem, as outlined in his thesis, provides a firm foundation for this policy action. The qualitative application would include the detection and monitoring of specific event scale phenomena, and their potential ecosystem impacts. The processing of satellite ocean colour data should be modified accordingly. The quantitative application would encompass the development of a routine time series of updateable ecosystem indicators, to provide a measure of the current status of the ecosystem relative to the longer-term. The ecosystem indicators would serve as a measure of ecosystem function, for comparison with

fluctuations in recruitment of exploited marine resources. However, in order to succeed in either of these approaches, *in situ* validation of the satellite data is required to accurately calibrate the event scale signals. Similarly, research and development of MODIS ocean colour data is necessary to derive credible estimates of ocean properties for regional Benguela waters. This work should be considered with some degree of importance if the objectives of the BCLME are to be met.

LITERATURE CITED

Ackleson, S.G., Balch, W.M. and P.M. Holligan, 1994: Response of water-leaving radiance to particulate calcite and chlorophyll *a* concentrations: A model for Gulf of Maine coccolithophore blooms. *J. Geophys. Res*, 99: 7483-7499.

Agenbag, J.J., Richardson, A.J., Demarq, H., Freon, P., Weeks, S.J. and F.A Shillington., 2003. Estimating environmental preferences of South African pelagic fish species using catch size and remote sensing data. *Prog. Oceanog.* 59, 275-300.

Agenbag, J. J. and L.V. Shannon, 1988. A suggested physical explanation for the existence of a biological boundary at 24°30'S in the Benguela System. *S. Afr. J. Mar. Sci*, 6, 119-132.

Austin, R.W. and T.J. Petzold, 1981. The determination of the diffuse attenuation coefficient of sea water using the coastal zone color scanner. Ed. J. F. R. Gower, *Oceanography from Space*, 239-255.

Bailey, G.W., Beyers C.J. deB., and S.R. Lipschitz, 1985. Seasonal variation of oxygen deficiency in waters off southern South West Africa in 1975 and 1976, and its relation to the catchability and distribution of the Cape rock lobster *Jasus lalandii. S. Afr. J. Mar. Sci.*, 3, 197-214.

Bakun, A. and S.J. Weeks, 2004. Greenhouse gas buildup, sardines, submarine eruptions, and the possibility of abrupt degradation of intense marine upwelling ecosystems. *Ecol. Letts.*, 7, pp 1015-1023.

Bakun, A., 1996. Patterns in the Ocean: Ocean Processes and Marine Population Dynamics. University of California Sea Grant, San Diego, California, USA, in cooperation with Centro de Investigaciones Biológicas de Noroeste, La Paz, Baja California Sur, Mexico. 323 pp.

Bakun, A., 1990. Global climate change and intensification of coastal ocean upwelling. *Science,* 247, 198–201.

Bakun, A., 1975. Daily and weekly upwelling indices, west coast of North America, 1967-73. U.S. Dept. of Commerce NOAA Technical Report *NMFS Special Scientific Report, Fisheries* #693. 114pp.

Bakun, A., 1973. Coastal upwelling indices, west coast of North America, 1946-71. U.S. Dept. of Commerce NOAA Technical Report *NMFS Special Scientific Report, Fisheries* #671. 103pp.

Balch, W. M., Kilpatrick, K. A., Holligan, P. M., Harbour, D. S. and E. Fernandez, 1996a. The 1991 coccolithophore bloom in the central North Atlantic. 2. Relating optics to coccolith concentration. *Limnol. Oceanogr.*, 41, 1684–1696.

Balch, W.M., Kilpatrick, K.A. and P.M. Holligan, 1993. Coccolith formation and detachment by *Emiliania huxleyi* (Prymnesiophyceae). *J. Phycol.*, 29: 566-575.

Barlow, R.G. 1982. Phytoplankton ecology in the southern Benguela current. I. Biochemical composition. *J. Exp. Mar. Biol. Ecol.*, 63, 209-227.

Beyers, C.J.deB, Wilke C.G, and , P.C. Goosen, 1994. The effects of oxygen deficiency on growth, intermoult period, mortality and ingestion rates of aquarium-held juvenile rock lobster *Jasus lalandii. S. Afr J. Mar. Sci.*, 14, 79-87.

Boyer, D., 1996. Stock dynamics and ecology of pilchard in the northern Benguela. In: O'Toole, M.J., (Ed.), The Benguela Current and comparable eastern boundary upwelling ecosystems Deutsche Gesellschaft für Techhnische Zusammenarbeit (GTZ) GmbH. Eschborn, Germany, pp. 79-82.

Brown, C.W., 1995. Classification of coccolithophore blooms in ocean color imagery. In: McClain, C.R., W.E. Esaias, M. Darzi, F.S. Patt, R.H. Evans, J.W. Brown, K.R. Arrigo, C.W. Brown, R.A. Barnes, and L. Kumar, 1995: Case Studies for SeaWiFS Calibration and Validation, Part 4. *NASA Tech. Memo. 104566*, Vol. 28, S.B. Hooker, E.R. Firestone, and J.G. Acker, Eds., NASA Goddard Space Flight Center, Greenbelt, Maryland, 13-19.

Brown, C.W. and J.A. Yoder, 1994. Coccolithophorid blooms in the global ocean. *J. Geophys. Res.*, 99(C): 7467-7482.

Bubnov, V.A., 1972. Structure and characteristics of the oxygen minimum layer in the Southeastern Atlantic. *Oceanology*, 12, 193-201.

Carr, M-E. and E.J. Kearns, 2003. Production regimes in four Eastern Boundary Current systems. *Deep-Sea Res.* II, 50, 3199-3221.

Carr, M-E., 2002. Estimation of potential productivity in eastern boundary currents using remote sensing. *Deep-Sea Res.* II, 49, 58-80.

Chapman, P., Shannon, L.V. 1987. Seasonality in the oxygen minimum layers at the extremities of the Benguela system. *S. Afr J. Mar. Sci.*, 5, 85-94.

Currie, B., 1997. The Intertidal Area. Proceedings Annual Research Meeting, Namibian Ministry of Fisheries and Marine Resources (Internal Report).

Cushing, D.H., 1989. A difference in structure between ecosystems in strongly stratified waters and those that are only weakly stratified. *J. Plankt. Res.* 11(1): 1-13.

Demarcq, H., Barlow, R.G. and F.A. Shillington, 2003. Climatology and variability of sea surface temperature and surface chlorophyll in the Benguela and Agulhas ecosystems as observed by satellite imagery. *Afr. J. Mar. Sc.* 25, 363-372.

Demarcq H., Weeks S. and F.A. Shillington, 2002a. Dynamics of the Benguela Coastal upwelling: 4 years of combined SST and chlorophyll measurements from space. *11th S. Afr. Mar. Sc. Symp.*, July 2002, Swakopmund, Namibia.

Demarcq, H., Mitchell-Innes, B. and R.G. Barlow, 2002b. Developing satellite derived indices of ecosystem productive capacity at scales relevant to pelagic fish. *11th S. Afr. Mar. Sc. Symp.*, July 2002, Swakopmund, Namibia.

Duncombe Rae, C.M. 1991. Agulhas retroflection rings in the South Atlantic: an overview. *S. Afr. J. mar. Sci.*, 11, 327-344.

Emeis, K.-C., Brüchert, V., Currie, B., Endler, R., Ferdelman, Kiessling, A., Leipe, Noli-Peard, K., Struck, U. and Vogt, T., 2004. Shallow gas in shelf sediments of the Namibian coastal upwelling ecosystem. *Cont. Shelf. Res.*, 24, 627–642.

Emeis, K.-C., Bening, G., Berger, J., Brüchert, V., Currie, B., Endler, R., Ferdelman, T., Finke, N., Graco, M., Haferburg, G., Heyn, T., Kiessling, A., Lage, S., Leipe, T., Mollenhauer, G., Neumann, K., Nickel, G., Noli, K., Riechmann, D., Schippers, A., Schneider, R., Schulz, H., Shidjuu, A., Sonnabend, H., Stregel, S., Struck, U., Treppke, U., Vogt, T., Zemskaya, T., 2002. Cruise Report of Expedition METEOR 48-2, FB Geowissenschaften, Bremen.

Emery W.J. and R. E. Thomson, 2001. Data Analysis Methods in Physical Oceanography. Elsevier, Amsterdam, 2nd ed.

Garzoli, S.L., P.L. Richardson, C.M. Duncombe Rae, D.M. Fratantoni, G.J. Goni and A.J. Roubicek, 1999. Three Agulhas rings observed during the Benguela Current Experiment. *J. Geophys. Res.*, 104, 20971-20985.

Giraudeau J. and G.W. Bailey, 1995. Spatial dynamics of coccolithophore communities during an upwelling event in the Southern Benguela system. *Cont. Shelf. Res.*, 15, 1825-1852.

Grobler, C.A.F. and , K.R. Noli-Peard, 1997. *Jasus lalandii* fishery in post-independence Namibia: monitoring population trends and stock recovery in relation to a variable environment. *Mar. Freshwater Res.*, 48, 1015-1022.

Groom, S. B. and P. M. Holligan, 1987. Remote sensing of coccolithophore blooms. *Adv. Space Res.*, 7, 73-78.

Hamukuaya, H., O'Toole M.J. and P.M.J. Woodhead, 1998. Observations of severe hypoxia and offshore displacements of Cape Hake over the Namibian Shelf in 1994. *S. Afr. J. mar. Sci.*, 19, 57-59.

Hamukuaya, H. and M.J. O'Toole, 1994. Survey of juvenile hake in the central Namibian region, March 1994. Report of Ministry of Fisheries and Marine Resources, Namibia, 23pp.

Holden, C.J., 1985. Currents in St Helena Bay inferred from radio-tracked drifters. *The South African Ocean Colour and Upwelling Experiment.* Shannon, L.V. (Ed.). Cape Town; Sea Fisheries Research Institute, 97-109.

Holligan, P.M., Fernandez, E., Aiken, J., Balch, W.M., Boyd, P., Burkhill, P.H., Finch, M., Groom, S.B., Malin, G., Muller, K., Purdie, D.A., Robinson, C., Trees, C.C., Turner, S.M. and P. van der Wal, 1993. A biogeochemical study of the coccolithophore *Emiliania huxleyi* in the north Atlantic. *Global Biogeochem. Cycles*, 7: 879-900.

Holligan, P.M., Viollier, M., Harbour, D.S., Camus, P. and M. Champagne-Philippe, 1983. Satellite and ship studies of coccolithophore production along a continental shelf edge. *Nature*, 304: 339-342.

Holtzhausen, J.A. 1999. Population dynamics and life history of west coast steenbras (*Lithognathus aureti* (Sparidae)) and management options for the sustainable exploitation of the steenbras resource in Namibian waters. *Ph.D. thesis*, University of Port Elizabeth, 213 pp.

Hovmöller, E., 1949. "The Trough and Ridge Diagram," *Tellus*, Vol. 1, (2), pp. 62-66.

Hutchings, L. 1992. Fish harvesting in a variable, productive environment--searching for rules or searching for exceptions? *S. Afr. J. mar. Sci.*, 12, 297-318.

Lamberth, R. and G. Nelson, 1987. Field and analytical drogue studies applicable to the St Helena Bay area off South Africa's west coast. In: The Benguela and Comparable Ecosystems. Payne, A.I.L., Gulland, J.A. and K.H. Brink (Eds) *S. Afr. J. mar. Sci.* 5: 163-169.

McClain, E.P., Pichel, W.G. and C.C. Walton, 1985. Comparative performance of AVHRR-based multichannel sea surface temperatures. *J. Geophys. Res.* 90, 11587-11601.

Mitchell-Innes, B.A. and A. Winter, 1987. Coccolithophores: a major phytoplankton component in mature upwelled waters off the Cape Peninsula, South Africa in March 1983. *Mar. Biol.*, 95, 25-30.

Morel, A., 1988. Optical modeling of the upper ocean in relation to its biogenous matter content (Case I waters). *J. Geophys. Res.*, 93(C9), 10749-10768.

Mueller, J.M. et. al., 2003: Ocean Optics Protocols For Satellite Ocean Color Sensor

Validation, Revision 4, Volume III: Radiometric Measurements and Data Analysis Protocols, *NASA/TM-2003-21621/Rev-Vol III.*

Nelson, G., A.J. Boyd, J.J. Agenbag and Duncombe Rae, C.M. 1998. An upwelling filament north-west of Cape Town, South Africa. *S. Afr. J. mar. Sci.*, 19, 75-88.

Nelson, G. and L. Hutchings, 1983. The Benguela upwelling area. *Prog. Oceanogr.*, 12, 333-356.

Nykjaer, L. and L. van Camp, 1994. Seasonal and interannual variability of coastal upwelling along northwest Africa and Portugal from 1981 to 1991, *J. Geophys. Res.*, 99(C7), 14197-14208.

O'Reilly, J. E., Maritorena, S., Siegel, D., O'Brien, M.C., Toole, D., Mitchell, B.G., Kahru, M., Chavez, F.P., Strutton, P., Cota, G., Hooker, S.B., McClain, C.R., Carder, K.L., Muller-Karger, F., Harding, L., Magnuson, A., Phinney, D., Moore, G.F., Aiken, J., Arrigo, K.R., Letelier, R., Culver, M., 2000. Ocean color chlorophyll *a* algorithms for SeaWiFS, OC2, and OC4: Version 4. In: Hooker, S.B., Firestone, E.R., (Eds.), SeaWiFS Postlaunch Calibration and Validation Analyses, Part 3. *SeaWiFS Postlaunch Technical Report Series*, 11, NASA, Goddard Space Flight Center, Greenbelt, Maryland, pp. 9-23.

Parrish, R.H., Bakun, A., Husby, D.M. and C.S. Nelson, 1983. Comparative climatology of selected environmental processes in relation to eastern boundary current pelagic fish reproduction. In: G.D. Sharp and J. Csirke (eds.) Proceedings of the Expert Consultation to Examine Changes in Abundance and Species Composition of Neritic Fish Resources (pp.). FAO Fisheries Report, 291(2,3), 731-778.

Pitcher, G., Monteiro, P. and A. Kemp, 2004. The potential use of a hydrodynamic model in the prediction of harmful algal blooms in the southern Benguela. In: Harmful and Toxic Algal Blooms, Steidinger K. (Ed.), *IOC of UNESCO*, in press.

Pitcher, G.C. and D. Calder, 2000. Harmful algal blooms of the southern Benguela current: a review and appraisal of monitoring from 1989 to 1997. *S. Afr. J. mar. Sci.* 22, 255-271.

Pitcher, G.C., Boyd, A.J., Horstman, D.A., and B.A. Mitchell-Innes, 1998. Subsurface dinoflagellate populations, frontal blooms and the formation of red tides in the southern Benguela upwelling system. *Mar. Ecol. Prog. Ser.* 172: 253-264.

Pitcher, G.C. 1998. Harmful Algal Blooms of the Benguela Current. IRDB (World Bank) & IOC; National Book Printers, Cape Town. 20pp.

Pollock, D.E. and C.J. Beyers, 1981. Environment, distribution and growth rates of West Coast rock lobster *Jasus lalandii* (F. Milne Edawards). Transactions of the Royal Society of South Africa, 44, 3, 379-400.

Probyn, T.A., Pitcher, G.C., Monteiro, P.M.S., Boyd, A.J., and G. Nelson, 2000. Physical processes contributing to harmful algal blooms in Saldanha Bay. *S. Afr. J. mar. Sci.* 22: 285-297.

Robinson, W.D. B.A. Franz, Patt, F.S., S.W. Bailey and P.J. Werdell, 2003. Masks and Flags Updates, In: Patt, F.S., R.A. Barnes, R.E. Eplee, Jr., B.A. Franz, W.D. Robinson, G.C. Feldman, S.W. Bailey, J. Gales, P.J. Werdell, M. Wang, R. Frouin, R.P. Stumpf, R.A. Arnone, R.W. Gould, Jr., P.M. Martinolich, V. Ransibrahmanakul, J.E. O'Reilly, and J.A. Yoder; Algorithm Updates for the Fourth SeaWiFS Data Reprocessing, NASA Tech. Memo. 2003--206892, Vol. 22, S.B. Hooker and E.R. Firestone, Eds., NASA Goddard Space Flight Center, Greenbelt, Maryland, 74 pp.

Roy C., Weeks S., Rouault M., Nelson G., Barlow R. and C. van der Lingen. 2001. Extreme oceanographic events recorded in the Southern Benguela during the summer 1999-2000 summer season. *S. Afr. J. Sci.*, 97: 1-7.

Schulz, H.N., Brinkhoff, T., Ferdelman, T.G., Hernández Mariné, M., Teske, A. and B.B. Jørgensen, 1999. Dense populations of a giant sulfur bacterium in Namibian shelf sediments. *Science*, 284, 493-495.

Shannon, L.V. and Nelson, G. 1996. The Benguela: Large scale features and processes and system variability. In: The South Atlantic: Present and Past Circulation. G. Wefer, W.H. Berger, G. Siedler and D.J. Webb, Eds, Springer, Berlin, 163-210.

Shannon, L.V and L.C. Pillar, 1986. The Benguela ecosystem Part III. Plankton. *Oceanogr. Mar. Biol. Ann. Rev.*, 24, 65-170.

Shannon, L.V. 1985. The Benguela ecosystem. Part I. Evolution of the Benguela, physical features and processes. *Oceanogr. Mar. Biol. Ann. Rev.*, 23, 105-182.

Sherman, K. 1999. Large marine ecosystems: assessment and management. In: Sherman, K., Tang, Q. (Eds.), Large Marine Ecosystems of the Pacific Rim: Assessment, Sustainability and Management. Blackwell Science Inc. Malden, Massachusetts, pp. 442-456.

Siegel, D. A., M. Wang, S. Maritorena, and W. Robinson, 2000. Atmospheric Correction of satellite ocean color imagery: the black pixel assumption, *Appl.Opt.*, 39, 3582-3591.

Tyrrell, T., Holligan, P.M. and C.D. Mobley, 1999. Optical impacts of oceanic coccolithophore blooms. *J. Geophys. Res.*, 104 (C2), 3223-3241.

Vermote, E. and D. Tanre, 1992. Analytical expressions for radiative properties of planar Rayleigh scattering media, including polarization contributions. J. *Quant. Spectr. Rad. Transf.*, 47, (4), pp.305-314.

Voss, K.J.; Balch, W.M. and K.A. Kilpatrick, 1998. Scattering and attenuation properties of *Emiliania huxleyi* cells and their detached coccoliths. *Limnol. Oceanogr.*, 43(5), 870-876.

Weeks, S. J., Pitcher G.C. and S. Bernard, 2004b. Satellite monitoring of the evolution of a coccolithophorid bloom in the Southern Benguela upwelling system, *Oceanography*, 17-1, 83-89.

Weeks, S. J., Currie B., Bakun A. and K. Peard, 2004a. Hydrogen sulphide eruptions in the Atlantic Ocean off southern Africa: Implications of a new view based on SeaWiFS satellite imagery. *Deep-Sea Res.* I, 51, 153-172.

Weeks, S.J., Currie, B. and A. Bakun, 2002. Satellite imaging: Massive emissions of toxic gas in the Atlantic. *Nature*, 415, 493-494.

Wefer G. and G. Fischer, 1993. Seasonal patterns of vertical particle flux in equatorial and coastal upwelling areas of the eastern Atlantic. *Deep-Sea Res.*, 40, 1613-1645.

Woodhead, P.M.J., Hamukuaya, H., O'Toole, M.J., Stromme, T., Saetersdal G. and M.R. Reiss, 1998. Catastrophic loss of two billion hake recruits during widespread anoxia in the Benguela Current. Paper presented and distributed at the BENEFIT Scientific Programme Formulation Workshop, Swakopmund, Namibia, 1-4 April, 1998.

Wooster, W.S. and J.L. Reid, 1963. Eastern Boundary Currents. In: Hill, M.N. (Ed.), The Sea, Volume 2. Interscience Publications, New York pp. 253-280.

Wuethrich, B., 1999. Giant sulfur-eating microbe found. *Science*, 284, 415.

APPENDICES

Appendix 2.1. Summary of SeaWiFS Data Products.

(http://seawifs.gsfc. nasa.gov/SEAWIFS/SOFTWARE/DATA_PRODUCTS.html)

Level-1A Data Products

Level-1A products contain all the Level-0 data (raw radiance counts from all bands as well as spacecraft and instrument telemetry), appended calibration and navigation data, and instrument and selected spacecraft telemetry that are reformatted and also appended. There are Level-1A products for each of the following data types: global-area coverage (GAC), local-area coverage (LAC), lunar calibration, solar calibration, TDI check, and HRPT (High Resolution Picture Transmission) for direct- readout data.

Level-2 Data Products

Each Level-2 product is generated from a corresponding Level-1A product. The main data contents of the product are the geophysical values for each pixel, derived from the Level-1A raw radiance counts by applying the sensor calibration, atmospheric corrections, and bio-optical algorithms. Examples of geophysical values derived for each pixel are water-leaving radiances for bands 1 to 5, aerosol radiances for bands 6 and 8, chlorophyll *a*
concentration, the diffuse attenuation coefficient at band 3, the epsilon value for the aerosol correction of bands 6 and 8, and the aerosol optical thickness at band 8. In addition, 32 flags (Table 2.1) are associated with each pixel indicating if particular condition/s exist for that pixel, for example, atmospheric correction algorithm failure, sun glint, total radiance greater than the knee value, large spacecraft zenith angle, negative water-leaving radiance, stray light, coccolithophores, large solar zenith angle, high aerosol concentration, low water-leaving radiance at band 5, chlorophyll algorithm failure.

Level-3 Binned Data Products

Level-3 binned data products consist of the accumulated data for all Level-2 products corresponding to a period of for example, one day, 8 days, a month, a year. The data are stored in a representation of a regional or global, equal-area grid whose grid cells, or "bins," are determined accordingly. Each Level-3 binned data product is stored in multiple HDF files. Each multi-file product includes a main file containing all product-level metadata and data for each bin that are common to all the binned geophysical parameters. In addition, each product includes 12 subordinate files, each of which contains data of one binned geophysical parameter for all bins. Subordinate files must be read in conjunction with the associated main file.

Level-3 Standard Mapped Image Products

The Level-3 standard mapped image (SMI) products are image representations of binned data products. This image is a byte-valued, two-dimensional array of an Equidistant Cylindrical projection. Each SMI product contains one image of a geophysical parameter and is stored in one physical HDF file. A number of SMI products may be generated from each binned data product.

Near Real-Time Ancillary Data Products

Products of the meteorological data-- meridional wind, zonal wind, pressure, and relative humidity--and total ozone, used during the Level-2 operational processing, are made available by the Project. The meteorological and ozone data are referred to as ancillary data. These products are gridded, Equidistant Cylindrical images of, or derived from, data from other agencies. These data represent global "snapshots" at frequencies of at least once per day and as such are considered as near real-time (NRT) data.

Climatological Ancillary Data Products

Climatologies of the ancillary data required for Level-2 processing have been created by the SeaWiFS Project. These climatologies can be used by the Level-2 processing software in lieu of NRT data when the NRT data are unavailable or deemed to be of poor quality. Two climatological products, are used- one for four meteorological parameters and the other for ozone. For each of these five parameters, long-term monthly means were calculated using data from other agencies.

Appendix 2.2. MSI12 run-time control parameters.

(MSI12 Version 3.0 User's Guide, SeaDAS online documentation).

Keyword	Definition	Default
par	input parameter file	None
ifile	input L1b file name	None
ofile1	output L2 file #1 name	None
l2prod1	products to be included in ofile #1	nLw chl_oc2
ofile[#]	additional output L2 file names	none
l2prod[#]	products to be included in ofile[#]	none
spixl	start pixel number	1
epixl	end pixel number	the last pixel
dpixl	pixel subsampling interval	1
sline	start line number	1
eline	end line number	the last line
dline	line subsampling interval	1
ctl_pt_incr	control-point pixel increment for lon/lat arrays (0=optimize, >0=user specified)	0
proc_ocean	turn-on/off all ocean-specific processing (0=off, 1=on)	1
proc_land	turn-on/off all land-specific processing (0=off, 1=on)	0
atmocor	turn-on/off atmospheric correction processing (0=off, 1=on)	1
aer_opt	aerosol mode option 1-12: Multi-scattering with fixed model. 0: Single-scattering white aerosols (CZCS). -1: Multi-scattering with 765/865 Gordon-Wang model selection. -2: Multi-scattering with 670/865 Gordon-Wang model selection. -3: Multi-scattering with 765/865 Gordon-Wang model selection and NIR iterative NIR correction. -4: Multi-scattering with 670/865 Gordon-Wang model selection and iterative NIR correction. 100: Use tau_a_per_band for model selection and aerosol path reflectance calculations.	-3 for SeaWIFS -1 for OCTS -1 for POLDER -2 for MOS -1 for OSMI
tau_a	Input aerosol optical depth at 865 nm (or equivalent). If tau_a > 0 and aer_opt > 0, the input taua and fixed model will be used to derive aerosol reflectance at all pixels, all bands.	-1.0
tau_a_per_band	Input aerosol optical depth at each wavelength. If specified and aer_opt=100, the input aerosol optical thicknesses will be used to	[0,0,0,0,0,0,0,0]

Keyword	Definition	Default
	select the aerosol models and derive aerosol reflectance at all pixels, all bands.	
aer_iter_max	Maximum number of aerosol iterations	10 if NIR corr 2 if glint corr 1 otherwise
glint_opt	correct for residual glint radiance (1: On, 0: Off)	1
foq_opt	perform f/Q correction (1: On, 0: Off)	0
outband_opt	Out-of-band corrections (2: full correction (nLw, Lw, La, Lr), 1: partial correction (La, Lr), 0: Lr only)	0 for MOS, OSMI 2 all others
oxaband_opt	SeaWiFS/OCTS 765nm band Oxygen correction (1: On, 0:Off)	0 for MOS 1 all others
Filter_opt	filtering input data option (1: On, 0: Off)	1 for SeaWiFS 1 for OCTS 0 all others
Filter_file	data file for input filtering	$MSl12_DATA/sensor_filter.dat
demfile	digital elevation map file	$MSl12_DATA/common/digital_elevation_map.hdf
icefile	ice mask file	$MSl12_DATA/common/ice_mask.hdf
sstfile	sea surface temperature file	$MSl12_DATA/common/sst_climatology.hdf
met1	1st meteorological ancillary data file	use climatology
met2	2nd meteorological ancillary data file	None
met3	3rd meteorological ancillary data file	None
ozone1	1st ozone ancillary data file	use climatology
ozone2	2nd ozone ancillary data file	None
ozone3	3rd ozone ancillary data file	None
Land	land mask file	$MSl12_DATA/common/landmask.dat
Water	shallow water mask file	$MSl12_DATA/common/watermask.dat
calfile	system calibration file	$CAL_HDF_PATH for SeaWiFS $OSMI_CAL_PATH for OSMI
vcal_opt	vicarious calibration option controls whether gains and offsets are taken from the parameter file or sensor defaults: 0=defaults, 1=parameter gain and default offset, 2=default gain and parameter offset, 3=parameter gain and offset	0
offset	calibration offset adjustment	[0.0,0.0,0.0,0.0,0

Keyword	Definition	Default
		.0,0.0, 0.0,0.0]
gain	calibration gain multiplier	[1.0,1.0,1.0,1.0,1 .0,1.0,1.0,1.0]
albedo cloud_thresh	cloud reflectance threshold	0.027
glint glint_thresh	Sun glint threshold	0.005
absaer	Absorbing aerosol threshold on aerosol index. set < -1 to avoid the computation entirely.	0.5
sunzen	sun zenith angle threshold (deg)	75.0
satzen	satellite zenith angle threshold (deg)	60.0
epsmin	minimum epsilon to trigger atmospheric correction failure flag.	0.85
epsmax	maximum epsilon to trigger atmospheric correction failure flag.	1.35
tauamax	maximum 865 aerosol optical depth to trigger hitau flag	0.30
nlwmin	minimum nLw(555) to trigger low Lw flag.	0.15
wsmax	windspeed limit on white-cap correction.	8.0 m/s
maskland	land masking (1: On, 0: Off)	1
maskbath	shallow water masking (1: On, 0: Off)	0
maskcloud	cloud masking (1: On, 0: Off)	1
maskglint	glint masking (1: On, 0: Off)	0
masksunzen	large sun zenith angle mask option (1: On, 0: Off)	0
masksatzen	large satellite zenith angle mask option (1: On, 0: Off)	0
maskhilt	high Lt masking (1: On, 0: Off)	1
maskstlight	stray light masking (1: On, 0: Off)	1
sl_frac	SeaWiFS only: Lt 865 threshold for stray-light correction	0.25
sl_pixl	SeaWiFS only: number of LAC pixels over which stray-light correction is applied. 0=no correction, -1=program selected based on data type (default)	4 for GAC 3 for LAC

Appendix 2.3. Cruise data used for validating the Benguela processing parameters relative to the standard default processing.

Cruise	month	day	year	hh:mm	latitude	longitude	Time diff (mins)	CV	Valid pixels	filename
AMT	May	16	1998	8:30AM	-32.34	17.88	120	0.056	6	S1998136095637.L2_GAC
AMT	May	16	1998	11:30AM	-32.06	17.87	-61	0.077	7	S1998136095637.L2_GAC
AMT	May	18	1998	12:00PM	-26.71	13.96	-101	0.108	6	S1998138094714.L2_GAC
AMT	May	19	1998	9:00AM	-29.51	15.21	124	0.067	8	S1998139103201.L2_GAC
AMT	May	23	1998	9:00AM	-21.66	12.41	104	0.036	7	S1998143101412.L2_HRPT
AMT	May	23	1998	12:30PM	-21.53	12.21	-106	0.037	7	S1998143101412.L2_HRPT
AMT	May	23	1998	1:30PM	-21.4	12.1	-166	0.029	6	S1998143101412.L2_HRPT
Meteor	Oct	26	2000	8:45AM	-25.21	13.61	159	0.093	6	S2000300110155.L2_HRPT
Meteor	Oct	26	2000	9:45AM	-25.24	13.41	99	0.054	7	S2000300110155.L2_HRPT
Meteor	Oct	26	2000	10:45AM	-25.28	13.21	39	0.044	7	S2000300110155.L2_HRPT
Meteor	Oct	26	2000	11:45AM	-25.31	13.01	-21	0.07	7	S2000300110155.L2_HRPT
Meteor	Oct	27	2000	11:10AM	-25.31	13.01	-41	0.011	7	S2000301100632.L2_HRPT
Benefit	Feb	16	2002	8:39AM	-32.666	18.096	83	0.116	7	S2002047094005.L2_HRPT
Benefit	Feb	16	2002	12:30PM	-32.333	18.174	-148	0.105	7	S2002047094005.L2_HRPT
Benefit	Feb	17	2002	7:58AM	-30.474	16.971	165	0.046	7	S2002048101857.L2_HRPT
Benefit	Feb	17	2002	10:44AM	-30.1	16.886	-1	0.023	7	S2002048101857.L2_HRPT
Benefit	Feb	17	2002	1:34PM	-29.768	16.813	-171	0.022	6	S2002048101857.L2_HRPT
BenCal	Oct	7	2002	11:19AM	-32.576	18.088	-50	0.055	7	S2002280100229.L2_HRPT
BenCal	Oct	8	2002	1:46PM	-32.462	17.965	-156	0.108	6	S2002281104359.L2_HRPT
BenCal	Oct	10	2002	9:33AM	-29.434	16.678	81	0.014	7	S2002283102819.L2_HRPT
BenCal	Oct	10	2002	12:05PM	-29.494	16.683	-71	0.085	7	S2002283102819.L2_HRPT
BenCal	Oct	13	2002	12:50PM	-30.539	14.417	-91	0.032	7	S2002286105408.L2_HRPT
BenCal	Oct	14	2002	11:32AM	-29.064	16.099	-70	0.034	7	S2002287100032.L2_HRPT
BenCal	Oct	15	2002	9:01AM	-29.658	16.774	122	0.044	8	S2002288103819.L2_HRPT

SPECIFIC APPLICATIONS OF SATELLITE REMOTE SENSING TO THE BENGUELA ECOSYSTEM

SCARLA J. WEEKS